

The Prognostic Value of Perfusion MRI in Cerebral Glioma



by Dr. Muftah Manita

Thesis submitted to The University of Nottingham
for the degree of Doctor of Medicine (DM)

School of Clinical Sciences

August 2012

Dedicated to my parents, my children and my wife
for their great support and understanding

Abstract

Introduction

Cerebral glioma is the most prevalent primary brain tumour, of which the majority are high grade gliomas. High grade gliomas possess a poor prognosis, and glioblastoma patients survive less than one year after diagnosis. To date, histological grading is used as the standard technique for diagnosis and survival prediction. Previous studies using advanced techniques such as MR Perfusion have achieved a high sensitivity but a low specificity in identifying high grade gliomas. Moreover, they have failed to distinguish glioblastoma from anaplastic glioma. The purpose of the study presented here is to assess the diagnostic and prognostic value for cerebral glioma of cerebral blood volume maps derived from MR perfusion.

Methods

This retrospective study was approved by the local research ethics committee and clinical audit office. This study included 123 patients with newly diagnosed cerebral glioma, of all grades. Histological diagnosis was used as the standard reference for all potential patients. The relative tumour blood volume ($rTBV_{max}$) derived from MR perfusion was used for radiological grading of cerebral glioma. Receiver operating characteristics (ROC) were used to define the best threshold value in distinguishing the glioma grades and in determining the accuracy values (sensitivity, specificity, and positive and negative predictive values). For survival analysis, Kaplan–Meier was used to

illustrate and compare the discriminatory value of the histological and radiological classifications. A multiple Cox regression model was used to assess the prognostic value of both classifications in addition to other tested demographic and clinical variables. Finally, the influence of potential moderators was assessed using ANOVA, to assess whether the variation in $rTBV_{max}$ was only due to the difference in tumour grades.

Results

A model data set ($n = 50$) produced a 7-fold increase of TBV_{max} in tumour versus white matter and provided sensitivity and specificity of 97% and 94%, respectively, in distinguishing high versus low grade glioma. Moreover, a threshold value of 9.6 provided sensitivity and specificity of 100% and 56% in differentiating glioblastoma within the group of high grade gliomas. These threshold values were applied to the second group ($n = 73$) and provided sensitivity and specificity of 96% and 95% in distinguishing high versus low grade glioma, and 97% and 73% in differentiating, within the high grade gliomas, glioblastoma from anaplastic glioma. Using these two thresholds for a three-tier radiological classification, both the Kaplan-Meier plots and the multiple Cox regression showed that radiological classification was the most independent predictor of survival and tumour progression. The proposed radiological classification system was better than histological classification in predicting glioma patients survival especially noted in a group of moderately hyperaemic $rTBV_{max}$.

Conclusion

MR perfusion is a non-invasive and robust technique in glioma grading and survival prediction. The diagnostic value of $rTBV_{max}$ derived from MR perfusion in differentiating high versus low grade glioma is promising. It may have a role in the future in defining the appropriate treatment. However, the proposed radiological classification was inferior in differentiating anaplastic glioma from glioblastoma multiforme. In the future, a more advanced multimodal MR, such as MR spectroscopy and MR diffusion, may be studied, besides MR perfusion, in order to improve this diagnostic accuracy.

Declaration

I declare that this thesis is my own work based on research that was undertaken during my study in the Radiological and Imaging Sciences Division, School of Clinical Sciences, the University of Nottingham and Queens Medical Centre. Ethical committee approval was obtained on July 2008 under REC reference number 08/H0406/102 (Appendix D and in accordance with NHS research governance arrangements. No substantial amendments for the protocol were made during the study. The second set of recruited patients was performed with the approval of a clinical audit under reference number 1272 (Appendix E). I was responsible for recruiting and approaching the patients either via the neurosurgical departments of Queens Medical Centre, or the Neuro-oncology Department of Nottingham City Hospital. The recruiting process involved explaining the nature of the study and obtaining informed consent from the potential participants. All the post-processing and interpretation of the Perfusion MRI results, in addition to the pulling up of clinical data, were performed by me. A blind subsample analysis including drawing regions of interest within the tumour area to calculate $rTBV_{max}$ was performed by my colleague (Khalid Shah), aiming at assessing the reliability of the test.

Acknowledgements

In the name of God, the Entirely Merciful, the Especially Merciful

I would like to express my deep and sincere gratitude to my supervisor, Professor Dorothee Auer, Head of the Radiological and Imaging Science Division, for her support, constructive comments, and important guidance, which have had a remarkable influence on my entire thesis and future career in the field of magnetic resonance imaging. I wish to express my warm sincere thanks to Dr. Paul Morgan, Department of Medical Physics, Queens Medical Centre, whose personal tutorials and important guidance were supportive throughout this work. I warmly thank Professor David Walker, Paediatric Oncologist, my internal assessor, for his constructive criticism and excellent advice and comments during my first and second year of studies. I am heartily thankful to Professor James Lowe and Dr. Keith Robson for their help in providing clinical histological diagnoses throughout this project. I would like to thank Dr. Matthew Griffin and Dr. Karen Foweraker, Oncology Department, Nottingham City Hospital, and Dr. Paul Byrne, clinical lead of the Neurosurgical Multi-Disciplinary Team, Queens Medical Centre, for their great help in recruiting potential participants. I would like to thank Ms Jackie Cowley, Data Administrator, NHS Trust, for her great help and collaboration in providing the clinical information about the recruited patients. Last, but not least, I would like to thank my colleagues for their support. Without them, my time at the department would not have been as enjoyable and memorable.

Abbreviations

A	Astrocytoma
AG	Anaplastic glioma (grade III)
AUC	Area under curve
BBB	Blood brain barrier
CBF	Cerebral blood flow
CSF	Cerebrospinal fluid
CT	Computerized Tomography
2D	Two dimensions
DCE	Dynamic contrast enhanced
DSC	Dynamic susceptibility contrast enhanced
EES	Extravascular extracellular space
EPI	Echo Planar Imaging
^{18}F -FDG	Fluoro-2-deoxy-D glucose
FLAIR	Fluid attenuation inversion recovery
GBM	Glioblastoma multiforme (grade IV)
HGG	High grade glioma
HP	Histopathology
HR	Hazard ratio
IDH1	Isocitrate dehydrogenase enzyme
K^{trans}	Microvascular permeability
LGG	Low grade glioma (grade II)
MET	Methionine
MIBI	Methoxy-isobutyl-isonitrile
MPRAGE	Magnetization prepared rapid acquisition gradient echo
MRP	Magnetic resonance perfusion
MTT	Mean transit time
ODG	Oligodendroglioma
PCNSL	Primary Central Nervous System Lymphoma
PET	Positron emission tomography
Ps	Permeability surface area product
QUADAS	Quality assessment of studies of diagnostic accuracy
rCBV_{max}	Maximum relative cerebral blood volume
ROC	Receiver operator characteristic
ROI	Region of interest
rR	Relative recirculation
$\delta R2^*$	Change in tissue relaxivity
rTBV_{max}	Maximum relative tumour blood volume
SNR	Signal to noise ratio
SPECT	Single photon emission computed tomography
sROC	Summary receiver operator characteristic
T	Tesla (magnetic field strength)
^{201}Tl	Thallium
VEGF	Vascular endothelial growth factor
WHO	World Health Organization

Contents

Contents	viii
List of Figures	xii
List of Tables	xiv
1 Background	1
1.1 Introduction	2
1.2 Conventional MR imaging limitations	4
1.3 The biological relevance of neovascularisation	6
1.4 Review of MR perfusion techniques	7
1.5 Theory of cerebral blood volume calculation	20
1.6 CBV in glioma grading	22
1.7 Prediction value of MR perfusion	24
1.8 Advanced glioma imaging with non-MRI techniques	26
1.9 MR techniques in assessing brain tumour	29
1.10 MR Perfusion in tumour monitoring	31
1.11 Conclusion	33

2	Systematic review	35
2.1	Introduction and purpose	36
2.2	Methodology	38
2.3	Results	44
2.4	Discussion	50
3	General methods:	
	Dynamic susceptibility contrast MR perfusion and Dynamic contrast enhanced MR perfusion applied to cerebral gliomas	57
3.1	Introduction	58
3.2	Subject Recruitment and Patient Criteria	58
3.3	MR Imaging Protocol	62
3.4	CBV Post-Processing	65
3.5	rTBV _{max} Calculation	68
3.6	Histological Procedures	73
3.7	Statistical Analysis	73
4	Diagnostic Value of DSC in Cerebral Glioma	74
4.1	Introduction	75
4.2	Methods	78
4.3	Results	79
4.4	Discussion	85
4.5	Conclusion	90
5	Diagnostic value of DCE-T_1 in cerebral glioma	92
5.1	Introduction	93

5.2	Methods	94
5.3	Results	98
5.4	Discussion	100
5.5	Conclusion	101
6	Prognostic value of MR perfusion in brain glioma	102
6.1	Introduction	103
6.2	Methods	106
6.3	Results	110
6.4	Discussion	131
6.5	Conclusion	137
7	Testing $T2^*$MR Perfusion robustness	138
7.1	Introduction	139
7.2	Methods	140
7.3	Results	142
7.4	Discussion	147
7.5	Conclusion	152
8	General conclusions and future outlook	153
8.1	Conclusions	154
8.2	Clinical impact	159
8.3	Future outlook	162
A	Research Protocol	164
A.1	Study objectives and purpose	165
A.2	Study design	166

A.3	Statistics	173
A.4	Adverse events	175
A.5	Ethical and regulatory aspects	175
A.6	Quality assurance and audit	179
A.7	Publication and dissemination policy	181
A.8	Study finances	182
B	Consent form	183
C	Patient information sheet	185
D	Ethical Approval	188
E	Clinical Audit Approval	192
F	Demographic and Clinical Data	195
G	Ethical Amendment	200
H	QUADAS Items	203
	Bibliography	205

List of Figures

1.1	Diagram of K^{trans}	20
1.2	Signal intensity curve	22
2.1	Flow chart of search strategy	40
2.2	Literature search flow diagram	41
2.3	Forest plot-Sensitivity	49
2.4	Forest plot-Specificity	50
2.5	Diagnostic OR	51
2.6	symmetric ROC	52
3.1	Flow chart of patient recruitment	63
3.2	Perfusion raw image	68
3.3	Signal intensity curve	69
3.4	Signal intensity curve	69
3.5	Low grade images	71
3.6	Anaplastic glioma images	72
3.7	GBM images	72
4.1	Accuracy ROC	82

4.2	ROC high versus low glioma	83
4.3	ROC low grade versus anaplastic glioma	84
4.4	ROC among high grade	85
5.1	Raw images of T_1 perfusion	95
5.2	Signal intensity curve of T_1 perfusion	96
5.3	Conventional images and CBV map of DCE-MR perfusion	97
5.4	ROC comparison of MR perfusion techniques	99
6.1	Kaplan–Meier survival of histological grade	115
6.2	Kaplan–Meier time to progression of histological grade	116
6.3	Kaplan–Meier survival of radiological classification	117
6.4	Kaplan–Meier time to progression of radiological classification	117
6.5	Kaplan–Meier of survival of GBM	118
6.6	Kaplan–Meier of TTP of GBM	118
7.1	Scatter plot correlation of MRP perfusion	143
F.1	Demographic and clinical data of glioma patients	199

List of Tables

2.1	Inclusion and exclusion criteria	39
2.2	included studies	45
2.3	QUADAS criteria	46
2.4	Descriptive statistics	47
2.5	Diagnostic threshold analysis	48
2.6	Summary diagnostic odds ratio	53
4.1	Reliability test	79
4.2	Interclass correlation	80
4.3	Accuracy values of training set	81
4.4	Re-testing accuracy measure	81
4.5	Accuracy of low versus high grade	83
4.6	Accuracy of low versus anaplastic glioma	84
4.7	Accuracy among high grade glioma	85
5.1	Accuracy measures of T_1 MR perfusion	98
5.2	Accuracy T_2^* MR perfusion without pre-load dose	98
5.3	Accuracy T_2^* MR perfusion with pre-load dose	98

6.1	Karnofsky scale	109
6.2	Survival descriptive analysis	111
6.3	Survival descriptive analysis for high grade	112
6.4	Descriptive analysis of survival for glioblastoma	113
6.5	Univariate survival Cox regression	120
6.6	Multivariate survival Cox regression	121
6.7	Multivariate survival Cox regression	121
6.8	Univariate survival Cox regression of tumour progression . . .	122
6.9	Multivariate survival Cox regression of tumour progression . .	122
6.10	Multivariate survival Cox regression of tumour progression . .	123
6.11	Univariate Cox regression of survival of high grade	124
6.12	Multivariate Cox regression of survival of high grade	125
6.13	Multivariate Cox regression of survival of high grade	125
6.14	Univariate Cox regression of tumour progression of high grade	126
6.15	Multivariate Cox regression of tumour progression of high grade	126
6.16	Multivariate Cox regression of tumour progression of high grade	127
6.17	Univariate Cox regression of survival of glioblastoma	129
6.18	Multivariate Cox regression of survival of glioblastoma	129
6.19	Univariate Cox regression of tumour progression of glioblastoma	130
6.20	Multivariate Cox regression of tumour progression of glioblas- toma	130
7.1	Two perfusion methods analysis	141
7.2	Analysis of the differences between the three MRP methods .	143
7.3	Distribution of patients within covariates	144

7.4	Means and SDs for $rTBV_{max}$	144
7.5	ANOVA analysis of steroid effect	146
7.6	ANOVA analysis of pre-load dose effect	146
7.7	ANOVA analysis of cell line effect	147
7.8	ANOVA analysis of all variables	148
H.1	QUADAS Items	204

Chapter 1

Background: Issues in the diagnoses of cerebral brain tumours

1.1 Introduction

Primary brain tumours are the most prevalent (75%) type of brain tumour (Principi et al., 2003), of which the majority (65%) are high grade gliomas (Daumas-Duport et al., 1988). In general, brain tumours are classified according to their aggressiveness, i.e., benign or malignant; or to their origin, i.e., primary or secondary metastatic lesions; or to their tissue of origin (gliomas, lymphoma, etc.); or to their location, i.e., supra or infratentorial. Gliomas are classified by tissue of origin as pure astrocytoma, oligodendrogliomas, or the mixed type of oligoastrocytoma (Louis et al., 2007).

Gliomas are classified histologically according to the WHO classification system, which has been modified in the last two decades. The classification of astrocytic and oligodendrocytic tumours started in 1979 when two main categories were identified, astrocytomas and anaplastic astrocytomas (Kleihues and Ohgaki, 2000). In addition, oligoastrocytoma and mixed gliomas were classified in the same year but no anaplastic form recognised (Scheithauer, 2008). In 1993, glioblastoma was classified as an astrocytic tumour, and anaplastic oligodendroglioma was classified under the grade three World Health Organization (WHO) classification (Louis et al., 2007). In 2007, the very high oligodendroglial component with necrosis was classified as a component of glioblastoma. Currently, the histological characteristics of glioma based on the WHO classification are as follows: diffuse infiltrative glioma (grade II) may have cytological atypia; anaplastic glioma (grade III) is characterised by mitotic activity and cellular anaplasia; grade IV (glioblastoma multiforme) is where additional microvascular proliferation and necrosis is

present (Louis et al., 2007). Diffuse oligodendroglioma and oligoastrocytoma were classified as a grade II tumour, while anaplastic oligodendroglioma and anaplastic oligoastrocytoma were classified as a grade III tumour. The classification also codes pilomyxoid astrocytoma and pleomorphic xanthoastrocytoma under the grade II group (Louis et al., 2007). Glioblastoma with oligodendroglioma component was recommended to be classified as grade IV (Louis et al., 2007).

Despite having this refined outlined histological diagnosis as the gold standard for grading and treatment planning, a few but vital limitations have been encountered. Sampling error may result from a wrong biopsy target's leading to histological under-grading. Moreover, there is the risk of non-diagnostic biopsy of up to 17% (Teixeira et al., 2009) and post-operative neurological morbidity and mortality of about 6% (Teixeira et al., 2009; Dammers et al., 2010) of adverse events such as haematoma. Therefore, in certain situations, tumour grades could not be accurately identified based on histopathological findings alone.

In this chapter, the relevant background is presented for defining and evaluating non-invasive diagnostic tests based on perfusion scans. This includes a review of the pathophysiological processes of glioma, the role of angiogenesis, and potential issues of dynamic MR perfusion. In addition, I will discuss the MR perfusion parameters and their potential for clinical diagnostic.

1.2 Limitations of conventional MR imaging in grading gliomas

Conventional MR imaging has been used to define the tumour extension and the enhanced areas within the tumour, by exploiting both T_1 and T_2 in order to visualize the solid portion of the tumour and peri-tumoural areas. Nevertheless, oedema and/or microinfiltration into the adjacent brain tissue make defining the tumour a difficult task (Strugar et al., 1995). Contrast enhancement itself is not an accurate tool in tumour grading, as only about 60% of grade IV gliomas showed maximum signal peak height in the contrast-enhanced tumoural area, while the rest showed only slight changes in signal intensity (Lupo et al., 2005). On the other hand, low grade gliomas may be presented with high vascular permeability and strong contrast enhancement (Aronen et al., 1994). In addition, contrast enhancement is not specific to brain tumours (Lupo et al., 2005), but may be manifested in inflammatory brain diseases and post-radiation changes (Chang et al., 1995). It is not clear, based on conventional MR images, whether the contrast enhancement in the tumour area is due to tumour activity or BBB leak (Abbott et al., 1999). Therefore, measuring the change in signal recovery in the enhanced area may provide a clue to the nature of the enhancement (Lupo et al., 2005). Brain tissue that has contrast enhancement but a decrease in percentage of signal recovery is indicative of blood brain barrier (BBB) breakdown, while normal signal recovery is indicative of tumour activity and vasculogenesis (Lupo et al., 2005). Again the latter method has a deficiency, as the maximum peak height of signal intensity was detected in the peri-tumoural

non-contrast-enhanced area in anaplastic astrocytoma patients (Lupo et al., 2005). Conventional MR imaging with gadolinium-enhanced T_1 weighted images has shown a discordance with the degree of vessel permeability when compared with dynamic susceptibility contrast enhanced images (Cao et al., 2006).

Practically, the conventional MR technique is less sensitive (72%) in discriminating between low and high grade glioma: a large number of anaplastic astrocytoma lesions (75%) failed to enhance (Sugahara et al., 1999) while 20% of low grade gliomas showed enhanced lesion (Scott et al., 2002). The nature of glioma heterogeneity and the non-specificity of contrast enhancement on conventional MR imaging may lead to tumour misclassification. Conventional MR also failed to clearly differentiate between remnant tumour tissue or post-surgical enhancement in the surgical bed (Cho et al., 2002). Another limitation is that conventional MR imaging is less accurate (50%) in differentiating between tumour recurrence and pseudo progression (Taal et al., 2008). This is because the appearance of peri-tumoural oedema and enhancing tumour were not predictive of the outcome of glioma patients (Chow et al., 2000). These limitations may cause difficulties in patient management and monitoring.

1.3 The biological relevance of neovascularisation and blood flow in tumour grading

Vascular proliferation is a common feature associated with growing tumours due to the release of vascular endothelial growth factor (VEGF) in response to proliferation, mitosis and hypoxia (Behin et al., 2003). The expression of VEGF immune reactivity was found to be high in high grade gliomas (Maia, Jr. et al., 2005). Similarly, a significant positive correlation was seen between a high relative cerebral blood volume (rCBV) and a high VEGF in cases with anaplastic astrocytoma and also in some low rCBV glioma tumours (Maia, Jr. et al., 2005). This correlation may be attributed to the formation of new vessels and/or the adoption of existing blood vessels (vascular co-option) as a result of tumour growth (Cha et al., 2002). Both processes will lead to an increase in microvascular density and vascular leakage, which are positive indicators of tumour aggressiveness (Cao et al., 2006). Therefore, in comparison with normal brain tissue, the tumour exhibits a high blood volume as a result of the increased mitotic activity of the tumour cells and vascular proliferation. The release of VEGF is not only responsible for the formation of new blood vessels but also increases their permeability (Leung et al., 1989). An association between vascular permeability and tumour histological grade was also reported in the literature (Roberts et al., 2000; Provenzale et al., 2002). However, vascular permeability metrics were found to be very variable within the same tumour grade (McDonald and Choyke, 2003). This may be due to the influence of the degree of vascular blood volume and flow or the effect of steroids (Ostergaard et al., 1999). Few

studies have demonstrated a close association between an increase in blood flow and tumour grade (Aronen et al., 1994; Sugahara et al., 1998; Boxerman et al., 2006; Law et al., 2007a). The haemodynamic metrics hold promise for grading gliomas and for tissue characterization. In addition, it has been stated that the mapping of relative cerebral blood volume may help identify the most malignant part of the tumour as a biopsy target, thus reducing the sampling error and improving the accuracy of a stereotactic biopsy (Aronen et al., 1994; Sugahara et al., 1998; Knopp et al., 1999; Uematsu et al., 2001; Provenzale et al., 2002; Law et al., 2003; Cha et al., 2006).

1.4 Review of MR perfusion techniques

1.4.1 Introduction

Advanced MR perfusion techniques have evolved in the last two decades aiming at grading gliomas based on their vascular characteristics. The dynamic perfusion properties of tumour tissue are different from those of normal brain tissue, having an increase in blood volume, flow, and permeability (Aronen et al., 1994). This is manifested clearly in glioblastoma, where the increase in blood vessel density is driven by high mitotic cell activity (Murat et al., 2009). Previous studies have used different parameters derived from MR perfusion to distinguish between grades of cerebral glioma, parameters such as cerebral blood volume (CBV) Aronen et al. (1994); Lev and Hochberg (1998); Sugahara et al. (1998); Preul et al. (2003); Batra et al. (2004); Hakyemez et al. (2005); Boxerman et al. (2006); Catalaa et al. (2006); Chaskis et al.

(2006); Law et al. (2007b), cerebral blood flow (CBF) (Chaskis et al., 2006; Law et al., 2006c; Callot et al., 2007; Haris et al., 2008), the volume transfer constant (K^{trans}) (Law et al., 2004a; Mills et al., 2006; Haris et al., 2008), and the mean transit time (MTT) (Chaskis et al., 2006). Lastly, the peak height and the percentage of signal intensity recovery were significantly different between normal brain tissue and tumours (Cha et al., 2007). Of the MR perfusion parameters correlated to histological diagnosis, it is generally concluded that cerebral blood volume is the best metric (Law et al., 2006c). When tested to the standard WHO grading system, cerebral blood volume is found to be strongly correlated to the tumour grades (Rees et al., 1996; Law et al., 2003; Principi et al., 2003; Cha et al., 2005; Hakyemez et al., 2005; Chaskis et al., 2006). Cerebral blood volume also was highly accurate in differentiating glioma tumours from other brain tumours (Cha et al., 2002; Cho et al., 2002; Hartmann et al., 2003; Chiang et al., 2004; Bulakbasi et al., 2005; Hakyemez et al., 2006; Rollin et al., 2006; Cha et al., 2007).

1.4.2 MR perfusion techniques: The absolute cerebral blood volume

Cerebral blood volume has been adopted, among other perfusion parameters, as its value is closely correlated to tumour grades and tissue characteristics (Aronen et al., 1994; Donahue et al., 2000; Lev et al., 2004). However, biological factors such as vascular autoregulation (Tofts, 2003), age (Leenders et al., 1990), and atherosclerotic disease of the main feeding blood vessel walls (Farhoudi et al., 2011) may affect the actual value of the blood volume

and perfusion. The measurement of the absolute CBV requires accurate estimation and localization of the blood vessels solely supplying the tumour area and ensuring that the blood vessels measured are not supplying other normal brain tissue voxels (Wirestam et al., 2010). During selection of the region of interest, a sampling error may result in inadvertent inclusion of brain tissue in addition to the blood vessels (Lu et al., 2008). The absolute cerebral blood volume (CBV) values showed an overestimation with marked between-subject variation, which resulted in poor reliability (Takasawa et al., 2008).

1.4.3 MR perfusion techniques: Relative cerebral blood volume

To avoid the pitfalls in the previous technique, the value of the CBV of the tumour area was standardised to the CBV blood volume in the contralateral normal white matter, thus obtaining the *relative cerebral blood volume* (Catalaa et al., 2006). The white matter is considered to be representative of normal brain tissue as it has sufficient tissue thickness compared to grey matter (about 4 mm) (Aronen et al., 1994), thus making it less liable to sampling error or partial volume artefacts from adjacent arteries. The reason for not choosing grey matter is that its blood flow is about double (75 ml/100 gm/min) that of white matter (32 ml/100gm/min) (Brickman et al., 2009). An underestimation of the measured relative cerebral blood volume may ensue as a result of using grey matter. Few studies (Schmainda et al., 2004; Law et al., 2007b, 2008) have used either normal white or grey mat-

ter for CBV normalization. In those studies, the CBV value of tumour was normalised based on location (white or grey matter) to its counterpart brain tissue. The first two studies reported low specificity values and the last study did not calculate any accuracy measures.

Tumour grades were reportedly correlated with the degree of tumour vascularity as the main features in diagnosing glioblastoma (Aronen et al., 1994). In parallel, the $rCBV_{max}$ was reported to be higher in glioblastoma (Sugahara et al., 1998). In the same study, a comparison between anaplastic glioma and low grade glioma showed that the $rCBV_{max}$ is significantly higher in enhanced anaplastic glioma. Even among anaplastic gliomas, a difference in $rCBV_{max}$ was noted between enhanced and non enhanced lesions (Sugahara et al., 1998). The higher the tumour grade, the larger the variation in $rCBV_{max}$, which had a relatively wide range in glioblastoma multiforme (Zonari et al., 2007).

Relative CBV has been measured using different approaches. The most common method is obtaining the average value of each region of interest and then selecting the highest value of the mean rCBV ($rCBV_{max}$) (Bulakbasi et al., 2005; Arvinda et al., 2009). The second method is through obtaining the average rCBV of each region of interest and then obtaining the average of all (Barajas, Jr. et al., 2009). Others have used the 75th percentile of the rCBV within the region of interest of the tumour, aiming at avoiding averaging with normal tissue (Bian et al., 2009). However, that study did not assess glioma grading, instead it analysed genotype differences in only low grade glioma.

1.4.4 Methods of reducing or eliminating T_1 signal effect

Several methods have been adopted to reduce or eliminate T_1 effects. The most common method is by injecting a small amount of contrast agent (pre-load dose) before the MR perfusion scan (Sugahara et al., 2000; Boxerman et al., 2006). The proposed pre-load dose was about 20%–25% of the required total dose calculated as 0.1 mmol/kg of body weight (Donahue et al., 2000; Sugahara et al., 2000; Boxerman et al., 2006). A half-dose of the pre-load dose (0.05 mmol/kg) was injected twice in a stepwise protocol, which was successful in correctly differentiating treated anaplastic glioma from glioblastoma multiforme (Hu et al., 2009). Using a pre-load dose of 0.25 mmol/kg provided higher sensitivity in differentiating glioma tumour recurrence from post-treatment radiation changes (Hu et al., 2009). The technique of injecting a pre-load dose acts through saturating and setting the tissue baseline signal intensity to a new baseline level. The difference in signal change is then further optimized by subtracting the baseline signal intensity, hence avoiding any underestimation. However, it has been proposed that factors such as data acquisition, type, the dose of contrast agent (Hu et al., 2009), and steroid therapy govern T_1 signal changes as a result of change permeability (Ostergaard et al., 1999).

The second method of reducing the T_1 effect has been through using a small flip angle and a long repetition time to promote T_2^* rather than T_1 ; however, a long repetition time will reduce the signal to noise ratio and the temporal resolution (Boxerman et al., 2006). The third method in reducing

the T_1 effect depends on applying two different echo-times and performing two compartmental analyses: the intra-vascular T_2^* signal drop and extravascular T_1 signal enhancement (Uematsu et al., 2001). Though this technique improved the overall detection of glioblastoma multiforme, the effectiveness of the double echo method in other glioma grades has not been assessed.

Finally, signal changes arising from contrast extravasation can be corrected by linear fitting (Boxerman et al., 2006). This method depends on averaging the signal intensity of the whole brain after threshold background noise. Afterwards, brain pixels that showed no enhancement above a certain threshold were excluded from the analysis. Then, the effect of leakage and changes in uncontaminated relaxivity were calculated for each pixel. The data is then averaged according to whole non-enhanced pixels, assuming negligible back diffusion of contrast into the intra-vascular space. Although the study was conducted with only a small sample size ($n = 43$), it showed a significant positive correlation in corrected rCBV values (0.60) compared to uncorrected rCBV values (0.15). The study involved only a few patients with brain tumours, and the accuracy measures were not reported.

1.4.5 Tumour grades and thresholds of cerebral blood volume

A review of the literature found variations in the threshold values used in previous studies. This may be attributed to the difference in acquisition parameters and demographic characteristics of human populations. We assumed the acquisition parameter settings are the main issue in grading glioma, although

no such study has assessed the effect of different MR parameters. Technically, setting an appropriate cut-off value may assist in distinguishing high grade from low grade glioma. Setting too low a cut-off may increase the chance of false positive events within a lower grade glioma. On the other hand, setting too high a cut-off may lower the sensitivity and under-grade some high grade gliomas. However, in terms of weighing the clinical outcome, treating low grade patients of high CBV is preferred rather than missing diagnoses in high grade patients.

1.4.6 Technical aspects of using ROI to measure cerebral blood volume

High grade glioma tumours are heterogeneous tumours composed of tumour tissue, blood vessels, and necrotic cells that may present within one lesion (Roodink et al., 2010). The heterogeneity of a glioma, especially one of high grade, will create a wide range of CBVs within the tumour area (Rollin et al., 2006). From the histological point of view, grading should be based on the most malignant features (Yang et al., 2002) where cellular over-activity and vascular proliferation predominate. These features may appear in perfusion images as areas of high signal intensity.

There are no standard methods for drawing and calculating regions of interest (ROIs), which explains the variation of CBV values among studies. Previous studies identify cerebral blood volume using hot spot methods where many ROIs are drawn over the highest hyperaemic areas of the tumour (Aronen et al., 1994). An alternative strategy has been adopted by others

(Catalaa et al., 2006), in which the median value of ROI was considered, and this was significantly different between grade III and grade IV glioma in the only contrast-enhanced area. While few studies have preferred using fixed size ROI within the hot spot areas (Law et al., 2006c; Zonari et al., 2007), others have used different sizes of ROIs (Hakyemez et al., 2005) to match the size of the highest signal intensity.

ROI size and location are important for avoiding erroneous tissue sampling. For example, an inclusion of necrotic tissue within the ROI will under-rate the actual value as the total value inside ROI was averaged (Provenzale et al., 2006). On the other hand, the inclusion of blood vessels within the ROI may give false results and overestimate the CBV value. An exclusion of blood vessels showed a better correlation ($P = 0.026$) between rCBV and genetic phenotype in low grade glioma (Caseiras et al., 2008). Consequently, to avoid partial voluming and contamination from adjacent brain tissue or arteries, it is wise to select a small ROI in the hot spot areas. Despite this solution, still the problem arises when using an echo planner MR sequence to locate the hot spot area where the images experience geometric distortion (Knopp et al., 1999).

1.4.7 Histogram method in calculating cerebral blood volume

Relative cerebral blood volume (rCBV) could also be analysed using the histogram method to avoid any bias that may be generated in utilizing the hot spot method (Tofts, 2003). As the ROI is operator-dependent, there is

the chance of inaccuracy, especially when comparing two consecutive MRI sets for evaluating changes in rCBV, wherein the points in the tumour are difficult to be matched. This has been studied in detecting brain tumour infiltration into the white matter (Tofts, 2003).

The histogram method is described elsewhere (Tofts, 2003). Briefly, the first step is to perform image segmentation to deal with partial volume voxels that may contain cerebrospinal fluid (CSF). Second, to generate an absolute histogram, the bin width is selected using a reasonable number of bins. Third, the range of bins is chosen from zero to a value just higher than the highest value of the parameters which need to be studied. Fourth, the absolute histogram is corrected for the brain size, to produce the normalized histogram. To generate the rCBV value per voxel, the total value is divided by the total number of voxels.

The accuracy of the histogram method was compared to that of the hot spot method in classifying glioma grades and subtypes (Emblem et al., 2008a). In only one study the CBV derived from the histogram method possessed of a higher sensitivity (90%) than the hot spot method (74%). In another study (Emblem et al., 2008b), the histogram method had a high sensitivity (100%) and specificity (91%) in differentiating the loss of heterozygous oligodendroglioma from other glioma cell lines. The too small a number of image slices used in this study made it possible to overlook any hyperaemic lesion which may be detected by the hot spot method. In contrast, several studies have reported a higher degree of accuracy for the hot spot method (Knopp et al., 1999; Law et al., 2003; Schmainda et al., 2004; Bulakbasi et al., 2005).

The histogram method has many drawbacks. Firstly, it requires a longer time for the analysis than the hot spot method. Secondly, choosing the proper number of bins and segmentation may mask important structures or produce partial voluming in the voxels. For example, selecting too few bins may result in missing important data due to smoothing effects, while selecting too many bins will result in a decrease in the signal to noise ratio (SNR). Therefore the number of bins should be optimised (Tofts, 2003). Thirdly, segmentation does not work well between grey and white matter due to the thin tissue thickness of the former, which may result in calculation error. Finally, it is less sensitive in detecting changes in localized brain lesions such as tumours.

1.4.8 Vascular permeability methods in brain glioma

The volume transfer coefficient (K^{trans}) is a measure of the difference between the volume in the extravascular extracellular space (EES) and the vascular plasma space (Figure 1.1) (Tofts, 2003). It is equal to the product of the vascular wall permeability and its wall surface area per unit mass of tissue (Tofts, 2003). The change in contrast concentration between the intravascular and extravascular compartments is measured to indicate the degree of contrast leak and endothelial permeability (Li et al., 2003). Assessment of the transfer coefficient is undertaken during the first pass of contrast by applying a pharmacokinetic modeling algorithm (Tofts et al., 1999).

Calculating the volume transfer coefficient (K^{trans}) is carried out as part of the perfusion technique to measure the changes in vascular permeability associated with brain tumours (Tofts et al., 1999). Basically, the analysis is

based on dynamic contrast enhanced (DCE) MR by using a steady-state T_1 -weighted 3D spoiled gradient-recalled acquisition sequence after intravenous contrast injection of gadolinium (Tofts et al., 1999).

Two main methods have been used for measuring K^{trans} , taking advantage of the dynamic susceptibility contrast technique: pixel by pixel measurement or detecting the drop in signal intensity in the first pass of contrast material within the vessels (Tofts and Kermode, 1991). Pixel by pixel measurement takes a long time and has a low SNR. The second method is to calculate the maps of signal intensity drop at the first 25 seconds after contrast injection (Law et al., 2006c). Regions of interest are drawn in the areas of high signal drop. Calculation of K^{trans} follows the two compartmental theory of contrast exchange. The areas with high signal drop were reported to be strongly associated with areas of high vascular permeability (Law et al., 2004a).

The vascular permeability derived from dynamic susceptibility was assessed against the tumour grade (Law et al., 2006c). Permeabilities indexed by high values of K^{trans} were seen in high grade glioma whereas low values of K^{trans} were seen in low grade glioma (Law et al., 2004b). However, the correlation is lower than that between tumour grade and rCBV. In the same study, vascular permeability showed a weak correlation to the rCBV values obtained within the same population. In contrast, the degree of difference between glioma grades detected by K^{trans} was reported to be better ($P = 0.003$) than that for rCBV ($P = 0.03$).

Vascular permeability has been also assessed in the tumour bed after surgery (Provenzale et al., 2005). The residual tumour at the periphery of resected tumour showed high permeability, displayed in bright colours on

the look up scale (Provenzale et al., 2005). However, in situations of blood-tumour-barrier disruption such as post-radiotherapy, the vascular permeability does not differ between partial tumour resection and tumour biopsy (Cao et al., 2005). The increase in the degree of enhancement after radiotherapy has been shown to be the same for both initial contrast and non-contrast enhancing lesions, which indicates vascular leakage (Cao et al., 2005). Another factor affecting vascular permeability is treatment with steroids, which is expected to reduce vascular permeation to contrast agents (Tjuvajev et al., 1996) and hence alter the value of K^{trans} . The factors affecting the volume transfer coefficient were vascular permeability, vascular surface area, and blood flow (Padhani, 2003). Moreover, osmotic gradients across the endothelial surface and the hydrostatic blood volume within the lesion may also contribute to the leakiness of contrast (Law et al., 2006c).

Vascular permeability (K^{trans}) has been used for survival prediction in glioma patients (Sorensen et al., 2009). The decrease in K^{trans} after doses of anti-angiogenic therapy was correlated with prolonged overall survival and progression free survival in patients with recurrent glioblastoma (Sorensen et al., 2009). K^{trans} had a positive correlation with glioma tumour grades though it had an inferior sensitivity and specificity compared to relative cerebral blood volume (Law et al., 2006c). The main issue in measuring K^{trans} in treated tumours is that the gradient between the two compartment becomes less as a result of treatment (Larsson et al., 2009).

The second method used in measuring microvascular permeability is based on T_1 sequence (K^{ps}) instead of T_2^* sequence (Roberts et al., 2000). Assessing K^{ps} is based on the cumulative effect of the contrast media, not on the

first pass of contrast. The transfer coefficient factor is measured across the vascular wall with a two-compartmental model to calculate the total permeability. Measurements take place in both intravascular and extravascular compartments to avoid underestimating the vascular permeability, especially in high grade glioma. This method has a good correlation ($r = 0.76$) with tumour grades, but accuracy measures were not reported (Roberts et al., 2000).

The third method is through calculating the relative recirculation (rR) to evaluate tumour grades (Jackson et al., 2002). It is based on measuring the signal response in the period after the first-pass contrast and the data were measured during the recirculation phase (Jackson et al., 2002). This method was used as a marker of angiogenic activity in monitoring the tumoural response to anti-angiogenic therapy (Jackson et al., 2002). The relative recirculation was generally low for both grade II and III glioma and the difference between grade III and IV was not statistically significant.

1.4.9 Measurement of signal intensity changes for tumour grading

Measuring the peak height and the percentage of signal recovery in the time-intensity curve have been recently adopted for grading glioma (Lupo et al., 2005; Cha et al., 2007). These parameters were obtained during the first pass of contrast. Regions of interest (ROIs) were drawn in the tumour area and the signal intensity of the voxels in these ROIs were measured. The height of the signal peak within the tumour is normalized to the peak of the

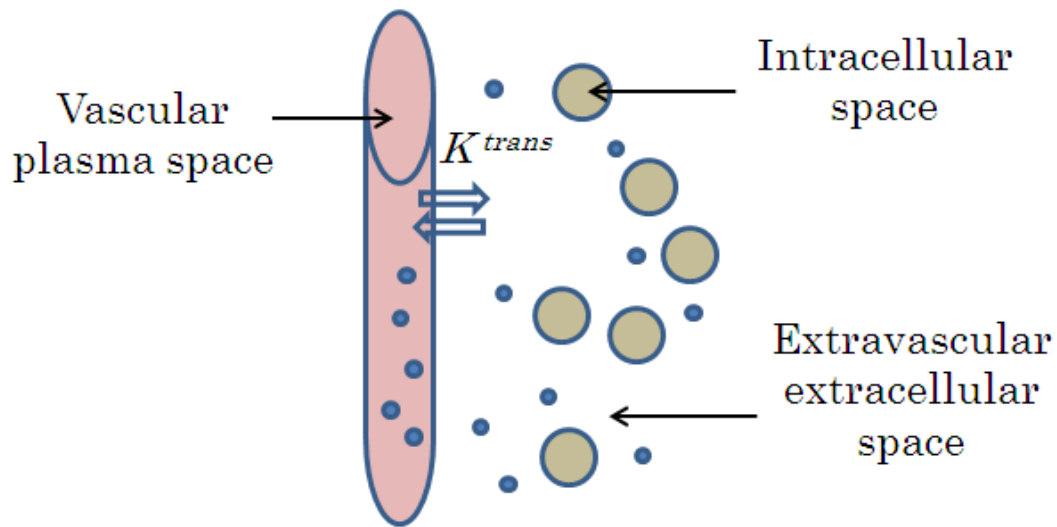


Figure 1.1: Diagram demonstrating the two main compartments in the calculation of K^{trans}

curve derived from brain tissue with a normal appearance. Voxels with a signal peak height of more than double the signal peak height in the normal curve were classified as abnormal values. The same method for generating a signal intensity curve was applied to measuring signal recovery, and values of less than 75% were considered abnormal (Lupo et al., 2005). Though signal peaks are higher for high grade glioma and metastatic lesions, the difference between the two types of lesions was not significant (Cha et al., 2007).

1.5 The theory of cerebral blood volume calculation using dynamic MR perfusion

The understanding of the kinetic properties of the brain is facilitated by the use of tracers (contrast agents). The kinetics is based on the concentra-

tion of tracer and its interaction with the environment (Tofts, 2003). The dynamic measurement of the contrast concentration in the feeding artery is an indicator of time function (Tofts, 2003). The distribution of contrast within the tissue is found by calculating the difference (mean transit time) between contrast particles that enter and exit the tissue. The injection of the contrast agent (Gadolinium) produces a shortening of the transverse relaxation time and generates a susceptibility difference across the intra-vascular and extra-vascular spaces (Tofts, 2003). The change in relaxation rate was approximately linear in the contrast concentration (Tofts, 2003).

Previous experiments assumed a linear correlation between the contrast concentration and the changes in signal intensity (Boxerman et al., 1995). The equation $\Delta R_2^* = -\ln(S(t)/S_0)/TE$ was used to calculate the cerebral blood volume, where the change in signal intensity ΔR_2^* denotes the difference in tissue relaxivity in proportion to the contrast concentration. The change in tissue relaxation (ΔR_2^*) is the reciprocal of the changes in T_2^* (ΔR_2^*) as a function of time. The time-intensity curve (Figure 1.2) produced is fitted by a gamma-variate to correct for possible contrast leak (Boxerman et al., 2006). The area under the corrected curve represent the cerebral blood volume (Knopp et al., 1999). The relative CBV is the ratio of the blood volume of the maximum hyperaemic area (hot spot area) in the tumour to that of the normal white matter. This theory is based on the assumption that the contrast agent injected is confined within the blood vessels with no contrast leak into the extravascular space and no recirculation (Knopp et al., 1999; Catalaa et al., 2006). The assumption most probably is violated in high grade glioma, in which a disruption of the blood brain barrier (BBB) may result in

a contrast leak to the extravascular compartments (Lupo et al., 2005; Boxerman et al., 2006). In this case, the gradient signal difference between the intravascular and extravascular spaces is reduced, with a decrease in the apparent relative cerebral blood volume. In fact, the contrast leakage leads to T_1 effects that diminish the drop in signal intensity of the T_2^* weighted images, and leads to an underestimation of the cerebral blood volume (Aronen et al., 1994; Henry et al., 2000).

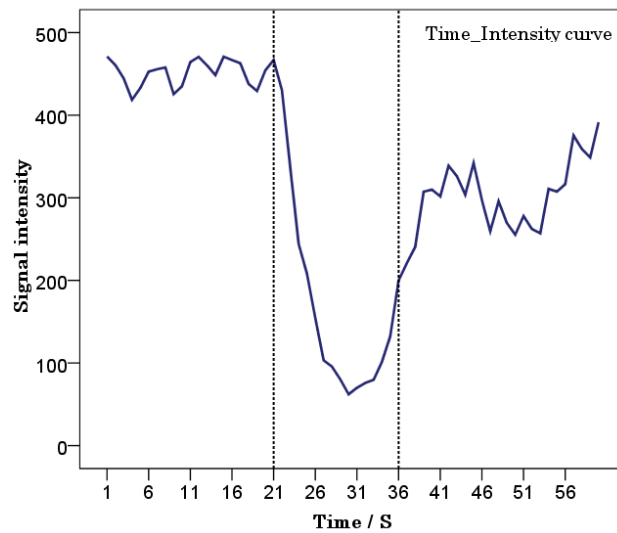


Figure 1.2: The time-intensity curve is fitted to correct for contrast leak

1.6 Cerebral blood volume in grading glioma tumours

Several methods have been applied to measure the cerebral blood volume in the tumour area to grade glioma. Measurements of hot spot within the tumour is a common method used. Basically, the aim of using a hot spot area

is to identify the part of the tumour with the largest CBV. As the absolute value of the CBV obtained from the tumour area is affected by physiological factors, the relative value of CBV is typically used to nullify these effects. The relative CBV values were significantly correlated ($r = 0.82$) with glioma grades (Law et al., 2004b; Bulakbasi et al., 2005). This method is highly accurate in differentiating low grade glioma from high grade glioma, with a sensitivity of 100% and a specificity of 91% for a two fold increase in CBV (Hakyemez et al., 2005) and a sensitivity of 91% in a different study (Shin et al., 2002), a specificity of 83% for a 2.93 fold increase in CBV. Most previous studies did not attempt to differentiate between glioblastoma multiforme (grade 4) and anaplastic glioma (grade 3); however, Calli et al. (2006) only reported a significant difference between the two grade types but did not report the accuracy. A few limitations were encountered in those studies: First, most of those studies assessed the accuracy value on a small sample of patients; Second, the MR settings and post-processing methods were not optimized to reduce confounding effects; Third, most of those studies did not use an independent test data set to assess the reliability of their model predictions.

The assessment of tumor grades may be complicated by the presence of different tumour cell lines (astrocytic or oligodendroglioma), which may differ in terms of rCBV values and clinical outcome. For example, oligodendroglioma had higher CBV values compared to astrocytic glioma of the same grade (Lev et al., 2004). Furthermore, differences due to genotype were also detected within the oligodendroglioma cell line: the CBV in oligodendroglioma 1p/19q deleted alleles was higher than in the oligodendroglioma

with intact alleles (Jenkinson et al., 2007; Whitmore et al., 2007). The clinical response of glioma to treatment is also different. Oligodendroglioma cell line tumours respond better to chemotherapy (Pinto et al., 2008) or surgical resection (Nagy et al., 2009) which translates into improved survival (Kitange et al., 2005). The sensitivity of oligodendroglioma tumour to chemotherapy and radiotherapy was ascribed to the existence of cytogenetic markers with the loss of heterozygosity of the alleles 1p and 19q (Sugahara et al., 1998).

1.7 MR perfusion in predicting survival time

Glioblastoma patients have poor outcomes, with a median survival time of about 7 months (Park et al., 2010a), which is slightly improved, to 14 months, after treatment with Temozolomide and radiotherapy (Stupp et al., 2005). Several factors may influence the survival time of glioma patients. Factors such as age ($P = 0.001$) (Law et al., 2008), sex ($P = 0.029$) (Hirai et al., 2008), treatment with Temozolomide ($P < 0.006$) (Valeriani et al., 2006; Mineo et al., 2007), delay in radiotherapy treatment ($P = 0.01$) (Irwin et al., 2007), and performance status ($P = 0.024$) (Durmaz et al., 2008), have been reported as being able to predict survival for glioma patients. Treatment was identified as one of the survival predictors in glioma patients (Lamborn et al., 2008). Treatment with Temozolomide improved 6 months progression free survival (66%) and survival rate, compared to untreated patients ($P < 0.001$) (Lamborn et al., 2008). Recently, genetic markers with loss of chromosomes ($P < 0.009$) as it promotes favourable response to Temozolomide (Wemmert et al., 2005) and tumour location (insular) ($P < 0.001$) (Talachchi et al., 2010)

were identified as survival predictors for glioma patients.

Conventional MR techniques had earlier been used to predict glioma patients' survival. This included features such as contrast enhancement (Guillermo et al., 2001) and tumour growth (Brasil Caseiras et al., 2009) in survival predicting. However, these parameters are not consistent, and are difficult to assess using conventional MR techniques (Yang et al., 2002). Furthermore, oedema in glioblastoma multiforme (hazard ratio (HR)= 1.6) and necrosis in anaplastic glioma (HR = 4.4) have been reported to be survival predictors (Pope et al., 2005). The extent of oedema and necrosis were found negatively correlated with the survival rate (Pope et al., 2005). For instance, anaplastic glioma patients with extensive tumour necrosis have a shorter survival time than those without (Pope et al., 2005).

Perfusion MRI has been used in predicting survival in glioma patients. Hyperaemic status in the brain tumours (Sugahara et al., 1999; Shin et al., 2002; Law et al., 2003; Lev et al., 2004) may aid indirectly in glioma grading (Lupo et al., 2007). The relative CBV helped predict one year survival (Bisdas et al., 2009) and time to progression (Law et al., 2008). Permeability perfusion parameters such as K^{trans} had significant prognostic value in predicting patient survival, independently of tumour grade ($P = 0.008$) (Mills et al., 2006). However, few high grade glioma patients were presented with both high permeability but longer survival time.

Low grade glioma patients with $\text{rCBV} < 1.75$ were found to have a longer time to progression (median = 144 months) compared to same grade patients with $\text{rCBV} > 1.75$ (median = 8 months) (Law et al., 2006a). Interestingly, low grade glioma patients with high rCBV had a survival time comparable to

those with high grade glioma (Law et al., 2006a). The prediction of survival may be poorer when including tumours of mixed tissue cell types (Pope et al., 2005). Oligodendroglioma with high rCBV have survived longer than astrocytic cell type (Pope et al., 2005). The influence of cell phenotype variation on rCBV will be assessed and discussed in Chapter 6.

1.8 Advanced glioma imaging with non-MRI techniques

Endothelial proliferation, mitotic activity, cellular pleomorphism, and necrosis are characteristics of malignant glioma tumours (Kleihues et al., 1993). The increase in vascular density causes an increase in blood volume and flow (Packard et al., 2003). Diagnostic modalities other than MRI techniques can be used to detect tumour characteristics such as vascular proliferation and cell mitosis (Ellika et al., 2007; Jain et al., 2008).

CT perfusion was shown to be better than conventional MRI in detecting cerebral tumours (Ellika et al., 2007) and in detecting glioblastoma multiforme (Jain et al., 2008). CT perfusion, similar to magnetic resonance perfusion (MRP), allows generating maps of the cerebral blood volume (CBV), cerebral blood flow (CBF), permeability surface area product (PS), and mean transit time (MTT), the same parameters used in the MR technique for grading cerebral glioma. Computed tomography (CT) perfusion had a higher sensitivity (93%) and specificity (100%) in differentiating high from low grade gliomas, whereas conventional MR images had a sensitivity of 86% and a

specificity of 60% (Ellika et al., 2007). The difference among high grade glioma was also significant ($P = 0.039$) using CBV derived perfusion CT (Jain et al., 2008). The main drawbacks of this technique are its long acquisition time and less anatomical coverage of brain areas, which may conceal important tumour features.

Functional imaging using single photon emission computed tomography (SPECT) is also used for brain tumours characterisation. Tracers such as ^{99m}Tc -methoxy isobuty-isonitrile (MIBI) (Le Jeune et al., 2006; Palumbo et al., 2006) and Thallium-201 (Tie et al., 2008; Ortega-Lozano et al., 2009; Iida et al., 2011) are used to differentiate between tumour recurrence and radiation necrosis and in grading glioma (Walker et al., 2004). The use of ^{99m}Tc -MIBI has showed an accuracy of 91% (Le Jeune et al., 2006) and 93% (Palumbo et al., 2006) in differentiating tumour recurrence from radiation necrosis. Thallium-201 was a predictor of overall survival (HR = 2.3) in patients with newly diagnosed glioblastoma multiforme (Vos et al., 2011).

Positron emission tomography (PET) functional imaging has been used in grading cerebral glioma, demonstrating significant differences between high and low grade oligodendroglioma (Derlon et al., 2000). The tracer uptake was based on the idea that the increase in cellular proliferation and increase in energy demand was reflected in high glucose consumption (hyper-metabolic) in high grade glioma (Padma et al., 2003). 2-[F18] fluoro-2-deoxy-d-glucose (^{18}F -FDG), a commonly used PET tracer, provides a good-to-background contrast and differentiates between tumour recurrence and radiation necrosis. The drawback of this glucose label radiotracer (^{18}F -FDG) is that it had an elevated uptake in non-malignant inflammatory tissue, the same as in

tumoural areas (Weber et al., 1997). Another drawback is that ^{18}F -FDG is less sensitive: half of the oligodendroglioma subtype of anaplastic glioma were classified as hypo-metabolic (Walker et al., 2004). ^{11}C -Choline as a PET tracer was developed for the investigation of gliomas (Hara et al., 2003) with the advantage that they are not taken up by inflammatory tissue (Hara et al., 1997). However, others found no difference in the tracer uptake between low and high grade glioma and the uptake is variable among tumours with the same histological diagnosis (Utriainen et al., 2003). In addition, The tendency of this tracer to pass the blood–brain barrier limited its accuracy in post-operative and post-treated brain tumours. ^{11}C -methionine (MET), a different PET tracer, was tested against the cerebral blood volume obtained from MR perfusion (Sadeghi et al., 2007). A positive and significant correlation ($r = 0.65$) between the two parameters was found in the tumoural, peri-tumoural, and infiltrated tissue. Albeit both modalities show the same sensitivity of 69%, the specificity of MET uptake was deemed higher (80%) than that of rCBV (70%). This was explained by the strong correlation of MET uptake with mitotic activity and endothelial vascular proliferation (Sadeghi et al., 2007). The low spatial resolution of PET images makes it difficult to define tumoural and peri-tumoural areas precisely.

1.9 Distinction of glioma tumours from other brain tumours using MR techniques

Differentiation of brain tumours using only conventional MR is challenging, as the technique does not assess specifically the different cellular characteristics of different types of brain tumours. Tumour characteristics such as location and the pattern of contrast enhancement may be similar for many brain tumours. Meningiomas, for example, are relatively benign extra-axial tumours with display a homogeneous and strong enhancement with gadolinium contrast, and can be easily distinguished from gliomas. Nonetheless, malignant meningioma may infiltrate into the brain parenchyma and become difficult to be distinguished from intra-axial tumours (Cha et al., 2002). Meningiomas exhibit strong contrast enhancement, similar to that of high grade gliomas, due to the absence of the blood–brain barrier in both lesions (Bruening et al., 1998).

Single brain metastatic lesions sometimes have a similar appearance to glioblastoma, which makes it challenging to distinguish between them (Bulakbasi et al., 2005; Calli et al., 2006). A sensitivity of 89% and a specificity of 73% were achieved in differentiating between glioblastomas and single metastatic lesions using a histogram distribution of normalized CBV (Ma et al., 2010). Other studies, however, were unsuccessful in demonstrating any significant difference between metastasis and high grade glioma (Calli et al., 2006) or low grade oligodendroglioma (Bulakbasi et al., 2005). On the other hand, a significant difference was detected for the peri-tumoural area: peri-tumoural CBV was higher in HGG than that in metastatic lesions

(Law et al., 2002; Chiang et al., 2004). The higher levels of CBV in the peri-tumoural area was explained by the presence of infiltrating tumoural cells in high grade gliomas (HGG) but not in metastatic lesions. However, this effect might be reversed by the effect of the tumour mass or oedema around the tumour (Hossman and Bloink, 1981). Finally, the peak of signal intensity and contrast enhanced tumour volume measurements did not reveal any statistical difference between the two lesions (Cha et al., 2007).

Primary cerebral lymphoma (PCNSL), one of the main differentials of glioma tumours, constitutes about 6% of central nervous system tumours (Jellinger and Paulus, 1992). The point in differentiating between the two tumour types is that surgery is not recommended for PCNSL and the standard therapy results in poor outcomes (van Besien et al., 2008). A different treatment regime, with systemic and intraventricular chemotherapy, showed a median survival of about 50 months (Pels et al., 2003). A recent study showed less median survival (34 months) on using only high-dose systematic chemotherapy (Chamberlain and Johnston, 2010). Bihemispheric butterfly appearance involvement at the corpus callosum commonly occurs in glioblastoma multiforme and may occasionally be present in cerebral lymphoma (Toh et al., 2006). Conventional MR is not considered a powerful discriminatory tool in differentiating between these two tumours, as both have marked enhancement on contrast enhanced T_1 -weighted images (Hartmann et al., 2003). Lymphoma with ring enhancement, mostly presented in immunodeficient patients, resembles the appearance of glioblastoma. In contrast, glioblastoma showed a higher transient drop of signal intensity and a higher relative CBV than that of PCNSL ($P < 0.0001$) in perfusion dynamic susceptibility MR

imaging (Hartmann et al., 2003).

1.10 MR perfusion techniques for evaluating tumour response to treatment

To date, response to treatment is assessed by clinical and radiological criteria (Macdonald et al., 1990). Tumour size changes and contrast enhancement are the main characteristics in defining treatment response in conventional MR images (Macdonald et al., 1990). However, conventional MR criteria are usually not indicative of tumour progression as the degree of contrast enhancement or oedema may also appear in pseudo progression cases after treatment (Taal et al., 2008). In addition, these criteria have failed in evaluating the clinical response to anti-angiogenic drugs (Taal et al., 2008). That is because changes in tumour volume are not strongly correlated with clinical outcomes (Vredenburgh et al., 2007; Kreisl et al., 2009). Anti-angiogenic drugs are targeted at the vascular supply of the tumour, to cut off its growth (Anderson et al., 2008). Hence MR perfusion is thought to be more suitable for detecting treatment efficacy than conventional MR, based on the changes in blood volume (Tomoi et al., 1999) and flow (Akella et al., 2004). Interestingly, a reduction in absolute CBV values was also noted within the tumoural area after fractionated radiotherapy in low grade astrocytoma (Wenz et al., 1996). However, a transient increase in CBV may be noticed in the peritumoural area (Jain, 2005), due to relief of the compression to the blood vessels, followed by a CBV drop due to radiation damage to the vascular

endothelium (Wenz et al., 1996).

Distinguishing tumour recurrence from post-radiation necrosis is of clinical importance for treatment management and during follow-up. Regrettably, they can not be differentiated based on conventional MR imaging as they are manifested with variable degrees of contrast enhancement and oedema (Dooms et al., 1986; Sugahara et al., 2000; Hu et al., 2009). In contrast, cerebral blood volume derived perfusion MR imaging achieved a sensitivity range of 89%–92% in differentiating recurrent tumour from post-radiation necrotic tissue (Barajas, Jr. et al., 2009; Hu et al., 2009). In general, rCBV is higher in patients with tumour progression than in those with post-treatment necrosis (Matsusue et al., 2010; Henry et al., 2000). An earlier study (Sugahara et al., 2000) reached statistical significance ($P < 0.03$) in differentiating recurrence from post-radiation necrosis, but the results were not verified by histological diagnosis for the majority of the included patients.

Steroid usage in glioma tumours is the mainstay and first line treatment to alleviate pressure symptoms caused by the tumours (Sinha et al., 2004). Steroids reduce the vascular wall permeability within the tumour and hence reduce the oedema around the tumour, and may lead to an increase in cerebral blood flow (Bastin et al., 2006). That study assesses the effect of steroids on glioblastoma patients by quantitatively measuring perfusion parameters using the MR technique. Borderline levels of significance of increased cerebral blood flow was detected in the peri-tumoural area after three days of treatment with steroids (Bastin et al., 2006). The effect of steroids on rCBV changes will be discussed later in Chapter 6.

1.11 Conclusion

Gliomas are the most common primary brain tumours encountered in adults with high mortality and poor outcome, especially for high grade gliomas. Treatment planning is different for different glioma grades and types, so appropriate tumour grading is crucial. The heterogeneity of gliomas, however, predisposes to sampling error in stereotactic biopsy, which may result in tumour misclassification. Vascular proliferation, besides other histopathological criteria, have been mainly used to grade brain gliomas. Conventional MR imaging is less sensitive (72%) in differentiating high from low grade glioma. In addition, conventional MR is less accurate (50%) in distinguishing between tumour recurrence and post-radiation necrosis. Several functional imaging techniques are available to index angiogenesis that may be used for non-invasive glioma grading. Among the MR-perfusion based, CBV mapping seems to be the best predictor of tumour grades and survival. However, current knowledge is limited due to the variable accuracy being reported from mostly studies with small sample sizes and variation of techniques. To address this knowledge gap for better patient management, we propose to undertake (i) A systematic review of the studies using CBV derived from MR perfusion in differentiating high from low grade glioma; (ii) Assessing the accuracy of tumour blood volume (TBV) using 3T gradient echo in differentiating high versus low grade and whether TBV allows of differentiating grade IV from grade III, and (iii) To assess whether TBV independently predicts survival and tumour progression in potential patients. A systematic review will be carried out in Chapter 2. The general methods of my thesis

will be discussed in Chapter 3, and assessing the diagnostic and prognostic value of TBV in glioma grading and survival prediction will be discussed in Chapters 4, 5 and 6.

Chapter 2

Systematic review of DSC-MR perfusion in grading cerebral glioma

2.1 Introduction and purpose

The national cancer database for the distribution of brain cancer in the years 1985–1994 has revealed about 30,000 glioblastoma and 15,000 astrocytoma tumours with intracranial primary site of 75% and 67%, respectively (Davis et al., 1999). Glioblastoma extension within the supra-tentorial area presents in about 17% (Davis et al., 1999). Gliomas are classified according to the WHO classification (Kleihues and Ohgaki, 2000), based on severity, into diffuse low grade glioma (grade II), anaplastic gliomas (grade III), and glioblastoma multiforme (GBM) (grade IV). Recurrence after treatment is high in malignant glioma due to its tendency to infiltrate into the adjacent brain tissue (Kaba and Kyritsis, 1997). An accurate determination of glioma grades is important, as the treatment differs for different grades (Louis et al., 2001).

Conventional MR has been used as an indicator of the degree of tumour aggressiveness based on contrast enhancement; however, some low grade glioma tumours do enhance while some high grade gliomas do not (Aronen et al., 1994; Knopp et al., 1999). This is because the contrast enhancement is not only an indicator of blood flow but also may indicate a vascular leak from a disrupted blood–brain barrier (Abbott et al., 1999). Stereotactic biopsy is then directed towards contrast enhanced lesions in the tumour area, however, contrast enhanced areas did not necessarily match with high malignant tissue, which may lead to sampling error (Aronen et al., 1994). A high success rate of stereotactic biopsy was achieved when 4–5 target sites were taken (Shastri-Hurst et al., 2006); however, postoperative complications such as stroke and haematoma may occur. The occurrence of post operative intrac-

erebral haematoma in brain tumours accounts for about 4.4% (Licata and Turazzi, 2003).

Advanced MR imaging techniques have been used in brain tumour differentiation as an effective tool in providing physiological information of tumour haemodynamic (Law et al., 2004b). Endothelial proliferation and neovascularisation, signs of tumour growth and aggressiveness, were recognized by dynamic MR perfusion techniques (Knopp et al., 1999). Most of the previous literature has focused on the role of MR perfusion as a non-invasive technique for the accurate differentiation of cerebral glioma grades (Law et al., 2003; Cho et al., 2002; Hakyemez et al., 2005; Schmainda et al., 2004; Arvinda et al., 2009). Consequently, cerebral gliomas were grouped based on their genetic phenotype as clinical outcome and treatments were reported differently for different glioma grades (Spampinato et al., 2007; Whitmore et al., 2007; Di Costanzo et al., 2008). The relative cerebral blood volume (rCBV), MR perfusion parameter, was found to be strongly correlated with the histological grading (Law et al., 2006c). However, a literature review (chapter 2) of these studies found differences in the threshold values and accuracy measures obtained. Few studies have reported a high rCBV accuracy (Spampinato et al., 2007; Bulakbasi et al., 2005; Arvinda et al., 2009; Lee et al., 2001; Shin et al., 2002), and the majority (Cho et al., 2002; Hakyemez et al., 2005; Shin et al., 2002; Lee et al., 2001; Sadeghi et al., 2006) recruited only a small number of patients. Others included non-glioma tumours and used different MR sequences and parameters (Schmainda et al., 2004). A critical appraisal was required of those studies as to whether the differences in accuracy values is population based or based on technical characteristics.

The aim of this study is to identify and appraise the quality of those other studies and to provide a summary of the accuracies of using relative cerebral blood volume in grading glioma. A systematic review was used to combine and address the relevant studies in determining the role of MR perfusion as a diagnostic tool.

2.2 Methodology

2.2.1 Eligibility Criteria

All the diagnostic studies performing MR perfusion in diagnosing cerebral glioma were included, regardless of authors names, country, or year of publication. For a study to be included in the systematic review, it had to include histological diagnosis as the standard reference for all subjects. Studies with recurrent or post-surgery or post-therapy subjects were excluded due to the effect of these treatments on the perfusion values, which may affect the accuracy measures of those studies. Table 2.1 gives the inclusion and exclusion criteria in detail.

2.2.2 Search Strategy

The search strategy was planned before beginning the study, with prior literature review knowledge (Figure 2.1). The search was conducted in September 2010 without restriction to publication date. The PubMed electronic search engine <http://www.ncbi.nlm.nih.gov/pubmed/> was searched for the keywords 'MR perfusion', 'brain or cerebral' and 'glioma or tumour or tumor'

Criteria type	Criteria
Inclusion	<p>Articles in the English language</p> <p>Studies including high and low grade cerebral glioma</p> <p>Contrast enhanced MR perfusion studies using relative cerebral blood volume as perfusion metric with clear accuracy or quantitative measures</p> <p>Newly diagnosed glioma patients who have pre-operative pre-treatment MRP scans</p>
Exclusion	<p>Studies with no histological diagnosis</p> <p>Studies aimed at differentiating glioma from other intracranial tumours</p> <p>Studies merging pilocytic astrocytoma (grade 1) with diffuse glioma into one group and whose accuracy measures could not be separated</p> <p>Case control and case report studies</p>

Table 2.1: Inclusion and exclusion criteria used in the systematic review

(Figure 2.2). The articles that were included on the basis of their titles or abstracts were then retrieved for the sake of systematic analysis but the corresponding authors were not contacted to clarify any ambiguous results.

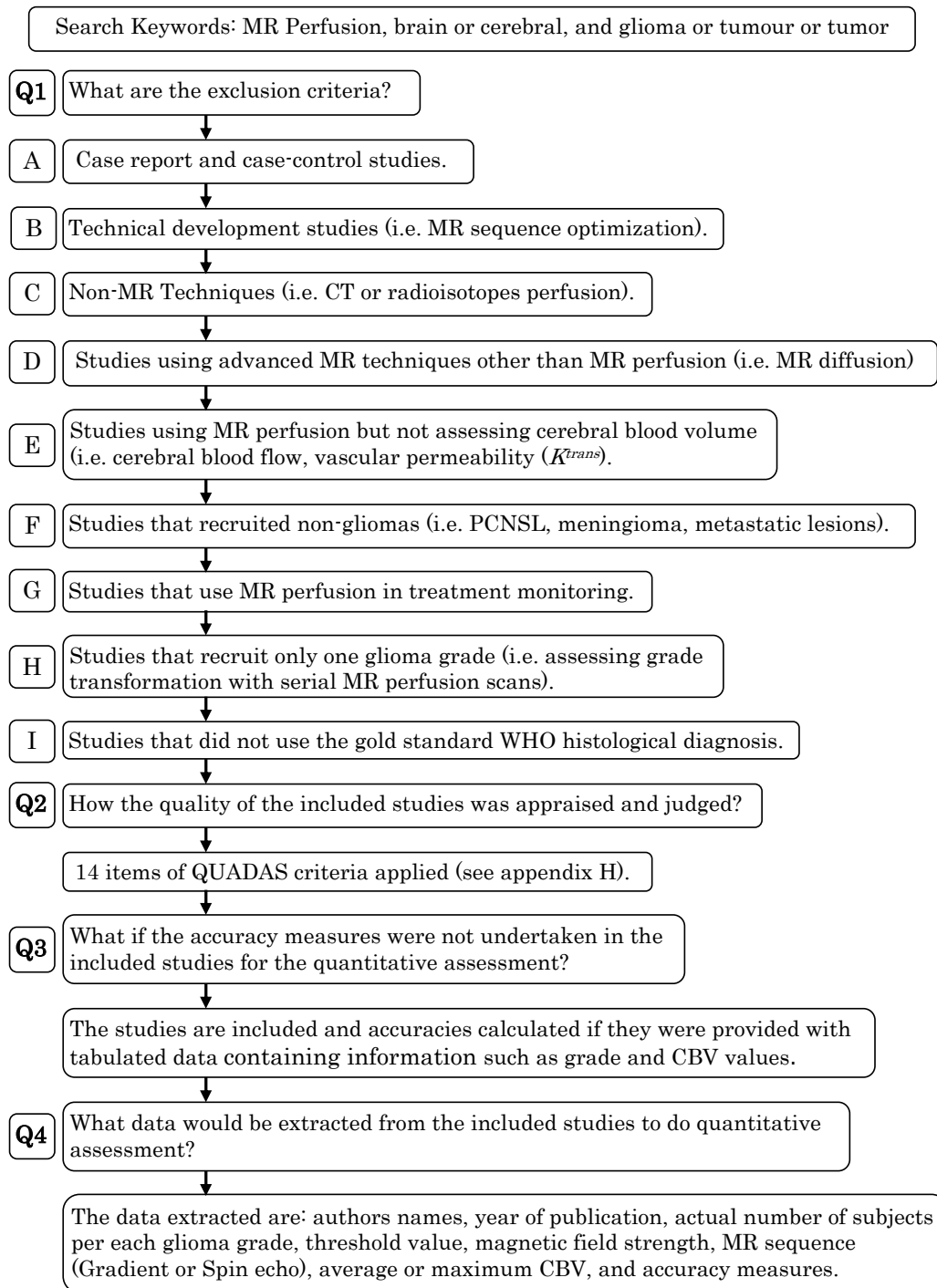


Figure 2.1: Flow chart of search strategy

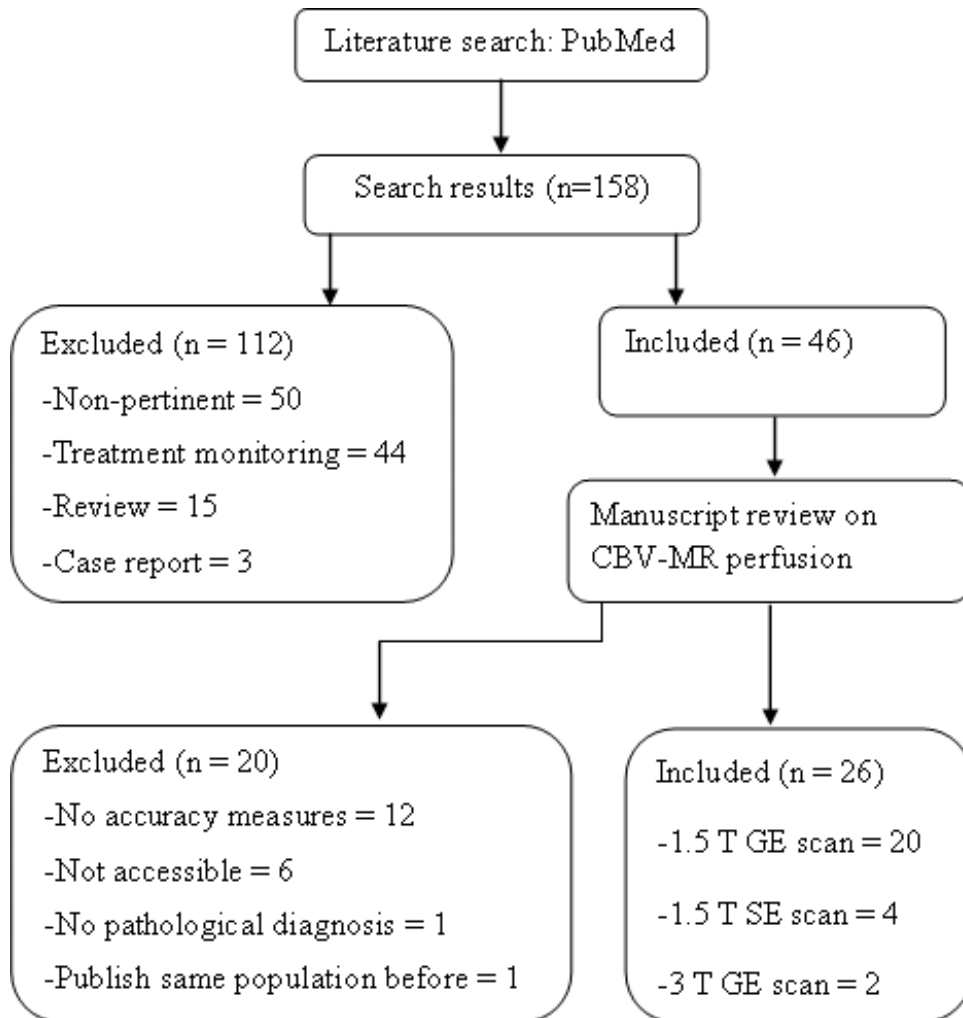


Figure 2.2: Literature search flow diagram; where GE and SE denote the gradient echo and spin echo sequence, respectively

2.2.3 Study selection

The potential studies were reviewed by one researcher with prior experience in systematic review. That reviewer applied the inclusion criteria to the potential studies (Table 2.1). All studies concerned with using MR perfusion with or without other multimodal MR imaging to differentiate high from low grade glioma were included, with no lower limit on the number of glioma

patients. Studies that include, in addition to cerebral glioma, other brain tumours were also included in the systematic review but the accuracy data of only glioma patients was considered wherever possible. Included studies should have a clear report of the accuracy measures or at least tabulated $rCBV_{max}$ and grades of each subject for accuracy measurement calculations. Accuracy measures were calculated for studies provide only CBV values and the highest accuracy values selected for the final analysis. Selection bias was not expected at this step as all articles that matched the inclusion criteria were included.

2.2.4 Data extraction

The quality assessment of the studies of diagnostic accuracy (QUADAS) was applied to the selected MR perfusion studies as a tool for quality assessment of the included studies (Appendix H) (Whiting et al., 2003). Data extraction and review of QUADAS items was performed by one researcher. A general statistical consensus report was presented, based on 14 standard items of QUADAS criteria for the included studies, but does not conform to the accuracy measure assessment. The second part of the extracted data was for the purpose of quantitative analysis and the data extracted were the authors' names, year of publication, type (dynamic contrast-enhanced or dynamic susceptibility contrast), sequence of MR perfusion (gradient or spin echo), magnetic field strength, threshold value, method of calculating cerebral blood volume, number subjects, and accuracy measures.

2.2.5 Data analysis

Meta-disc software (version 1.4) was introduced in 2006 (Zamora et al., 2006) for the meta-analysis of diagnostic tests. The software is publicly available at http://www.hrc.es/investigacion/metadisc_en.htm.

The data sheets used were introduced in form of accuracy parameters (true positive, false positive, false negative, and true negative). The accuracy results were presented by meta-disc software in the form of tables and forest plots or receiver operating characteristic curves (ROC) for ease of data interpretation. The main pitfall in pooling data from different studies is the heterogeneity which is either attributed to inconsistency of thresholds, variation in study populations, chance occurrences, or differences in technique settings and operators (Lijmer et al., 2002; Zamora et al., 2006). To assess the effect of threshold variation, both receiver operating characteristic curves and Spearman's correlation coefficient were used.

Forest plots of sensitivity, specificity, and diagnostic odds ratio were used to illustrate any variation between the included studies. The diagnostic odds ratio was used to describe the chance of occurrence of positive results in patients with disease (i.e., high grade glioma) to the chance of occurrence of positive results in patients without disease (i.e., low grade glioma). Summary receiver operator characteristic (sROC) was used to provide a smooth presentation, where each study on the curve contributed one pair of sensitivity and specificity at a certain point on the curve (Deville et al., 2002). The random effects model (DerSimonian and Laird, 1986) was used to combine the diagnostic odds ratios of the included studies and determine the best-fitting

ROC curve regardless of different thresholds (Zamora et al., 2006) .

2.3 Results

The electronic search via PubMed had 158 hits. A flow chart of this systematic review illustrates the number of included and excluded studies (Figure 2.2). There were 26 studies finally eligible for methodological appraisal. Authors, year of publication, location of study, technical settings, and threshold values of the studies included in the systematic review are presented in Table 2.2. The articles were selected based on the availability of accuracy measures, which were to be subjected to quantitative assessment. The initial review of the included studies revealed that a good number of studies used a gradient echo sequence on a 1.5-T magnetic field while only a few studies used spin echo sequence or performed an MR scan on a 3-T magnetic field.

2.3.1 Quality assessment using QUADAS criteria

Table 2.3 gives the refined 14 items of QUADAS criteria (Whiting et al., 2003) used for assessing the quality of the included papers. A systematic review revealed that three items in the QUADAS criteria were not fulfilled by most of reviewed articles. A quick review disclosed criteria such as time between standard reference test and radiological test, description of histological procedures, and whether or not clinical data were available at the time of diagnosis, were not recorded in most articles. Criteria such as appropriate choice of patient spectrum, clear description of selection criteria, and verifications with a standard reference, were described in most studied articles.

Authors	year	country	pt No.	cut-off	MR sequence	field strength
Aronen et al.	1994	USA	19	1.5	SE	1.5
Sugahara et al.	1998	Japan	30	2.5	GE	1.5
Knopp et al.	1999	USA	29	2.32	GE	1.5
Lee et al.	2000	S. Korea	22	2.6	GE	1.5
Ludemann et al.	2001	Germany	24	1.88	SE (T1)	1.5
Cho et al.	2002	S. Korea	29	NA	GE	1.5
Shin et al.	2002	S. Korea	17	2.93	GE	1.5
Yang et al.	2002	Japan	17	1.55	GE	1.5
Law et al.	2003	USA	160	1.75	GE	1.5
Schmainda et al.	2004	USA	72	1.5	GE & SE	1.5
Lev et al.	2004	USA	30	1.5	SE	1.5
Hakyemez et al.	2005	Turkey	33	2	GE	1.5
Bulakbasi et al.	2005	Turkey	58	3.9	GE	1.5
Law et al.	2006	USA	73	NA	GE	1.5
Sadeghi et al.	2006	Belgium	18	2.4	GE	1.5
Hou et al.	2006	USA	22	1.1	GE	1.5
Boxerman et al.	2006	USA	41	1.63	GE	1.5
Spampinato et al.	2007	USA	14	2.14	GE	1.5
Zonari et al.	2007	Italy	105	1.16	GE	1.5
Whitmore et al.	2007	USA	30	2	SE	1.5
Law et al.	2007	USA	92	2.15	GE	1.5
Lu et al.	2008	USA	39	NA	GE	1.5
Arvinda et al.	2009	India	51	2.91	GE	1.5
Park et al.	2009	S. Korea	41	1.92	GE	3
Bisdas et al.	2009	USA	34	1.7	GE	1.5
Park et al.	2010	S. Korea	48	2.12	GE	3

Table 2.2: List of included studies using relative cerebral blood volume for glioma grading

The most important criteria concerned for quality control in diagnostic tests were those related to use and verification of the standard test (histology) and the blind interpretation of the radiological test to the standard test.

2.3.2 Quantitative analysis

As mentioned earlier, 26 articles fit into the main aim, which is the use of CBV in differentiating high from low grade glioma. Twenty-two studies

Item	Criteria	Yes (No.)	No (No.)	Unclear (No.)
1	Patient spectrum representative of the brain glioma	25	1	0
2	Clear selection criteria	24	0	2
3	Use of standard reference	26	0	0
4	Clearly defined time between standard and radiological test	5	3	18
5	Verification of standard test on entire sample	26	0	0
6	Using the same reference standard	26	0	0
7	Independence of reference standard	26	0	0
8	Full description of the radiological test	26	0	0
9	Full description of the histological test	2	6	18
10	Radiological diagnosis blindly interpreted to histological diagnosis	7	0	19
11	Histological diagnosis blindly interpreted to radiological diagnosis	5	0	21
12	Availability of clinical data at time of radiological diagnosis	2	2	22
13	Reporting uninterpretable results	26	0	0
14	Explaining patient withdrawal if any	26	0	0

Table 2.3: QUADAS criteria were applied on the candidate 26 studies.

performed T_2^* gradient echo sequence, three studies performed T_2 spin echo sequence, and one study used T_1 spin echo sequence. Among the 22 studies performing T_2^* gradient echo sequence, 20 studies applied a field strength of 1.5 T, and 2 studies applied a field strength of 3 T. All other studies of spin echo used field strengths of 1.5 T. As the difference in MRI sequence and field strength may contribute to variations in the MRI parameters, only studies that performed gradient echo on a 1.5 T magnetic field were selected for quantitative analysis. The total cohort of those studies was 834 patients. A descriptive analysis showed the normality of the distribution of the threshold

values, as the skewness falls within the range of the twice standard error of skewness. The descriptive statistic showed that the mean of the threshold values is 2.13, close to the threshold values in most of the included studies (Table 2.4).

The cause of variation between the studies was assessed as to whether it was the threshold effect or chance. Spearman's correlation coefficient test of the threshold on heterogeneity gave a positive correlation between sensitivity and specificity, indicating no effect of threshold values between the studies (Table 2.5). The β is equal to zero (0.018), indicating that the odds ratio is constant regardless of the variation in the threshold. The variation in accuracies between studies may be due to chance alone.

variable	Min.	Max.	mean	SD	skewness	std error of skewness
Threshold value	1.1	3.9	2.13	± 0.71	0.88	0.55

Table 2.4: Descriptive statistics illustrated the normal distribution of threshold values for all included studies.

Subjective analysis of the forest plot (Figures 2.3 and 2.4) showed that both the sensitivity and the specificity were within the confidence interval of each study. The diagnostic odds ratio (Figure 2.5) gives the variation of

variable	coefficient	standard error	T	P value	
a	3.698	0.455	8.136	< 0.001	Tau-squared
b	0.018	0.229	0.077	0.939	

estimate = 0.6258 (Convergence is achieved after 5 iterations)
 Restricted Maximum Likelihood estimation (REML)
 Logit (TPR) vs Logit (FPR). Mosess model ($D = \alpha + \beta S$)
 Weighted regression (Inverse Variance)

Table 2.5: Analysis of Diagnostic Threshold. The effect of threshold variation was tested for the diagnostic performance of the odds ratio, where TPR denotes the true positive rate, FPR, the false positive rate, T, the predicted probabilities test.

both the sensitivity and specificity within the 95% confidence interval. The degree of heterogeneity between the included studies was medium (57%) for sensitivity values and medium to high (62%) for specificity values. As the Spearman's correlation coefficient test found a positive correlation between the sensitivity and specificity values, we expect the difference is because of chance only.

A summary receiver operator characteristic curve (sROC) was made out of the included studies ($n = 20$): the sensitivity and specificity of each study is represented and a smooth curve is fitted to these points. It was tested previously that the diagnostic odds ratio is constant between the studies and the threshold variation did not effect between-study variation. So, the symmetric was used to conclude the summary of accuracy measures between the included studies. The area under curve was 93% indicating that a large percentage of patients with cerebral glioma within the included studies were diagnosed correctly (Figure 2.6). The equations for producing the sROC were described in detail elsewhere (Zamora et al., 2006).

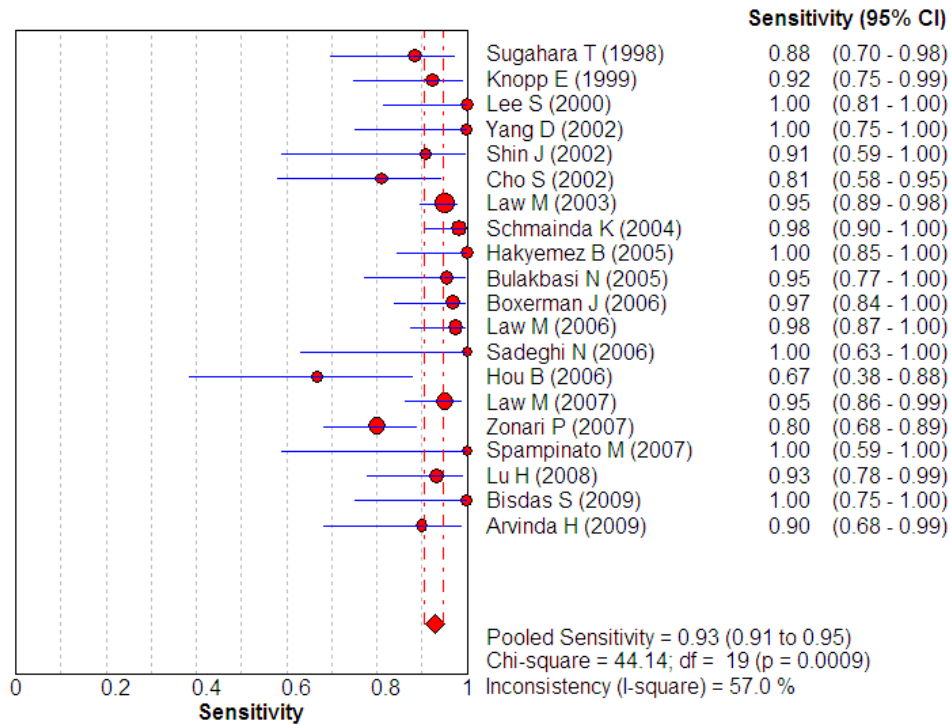


Figure 2.3: Forest plot of pooled sensitivity among the candidate 20 studies that used 1.5 T gradient echo sequence

A variation in threshold values usually affects the shape of a conventional ROC curve as it based on values, not percentages. On the contrary, the diagnostic odds ratio and summary ROC are not been affected by this variation, as they represent the relations between sensitivity and specificity of each study. Table 2.6 summarises the diagnostic odds ratio with weighting factors. (It is interesting to note that the three outlier studies had high percentage weights and at the same time low diagnostic ratios though they recruited only a small number of subjects.)

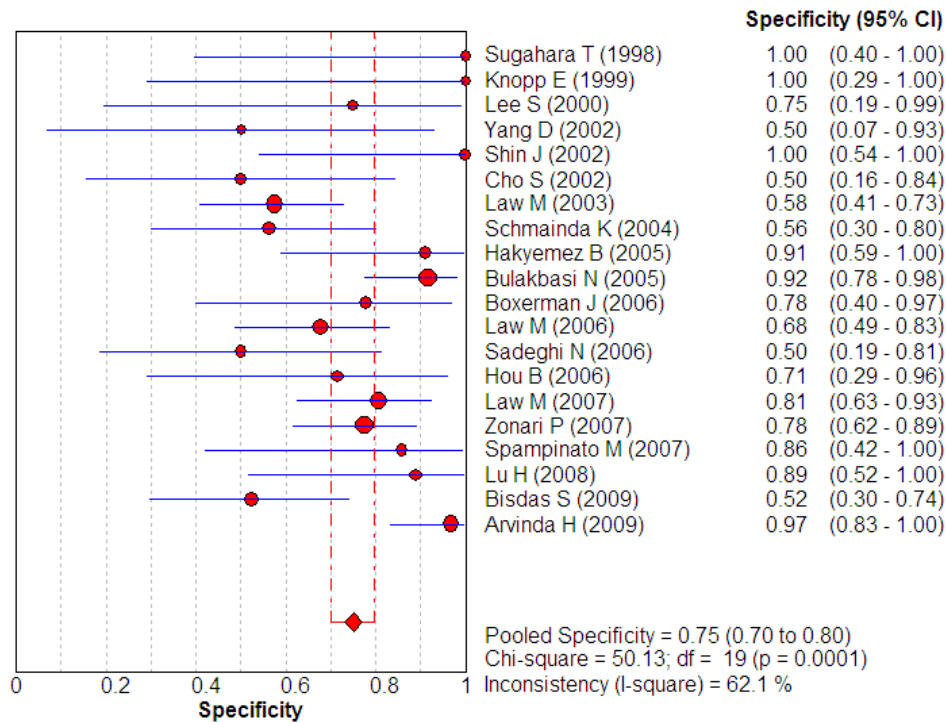


Figure 2.4: Forest plot of pooled specificity of the candidate 20 studies that used 1.5 T gradient echo sequence

2.4 Discussion

The WHO histological diagnosis is the standard reference to date for grading cerebral glioma. Typically, surgical debulking is the appropriate approach for grading; however, not all high grade glioma underwent surgical resection. Glioblastoma patients were mostly (88%) subjected to debulking but a small percentage (12%) were subjected to stereotactic biopsy (Filippini et al., 2008). In clinical practice, misdiagnosis due to sampling error was about 10% in addition to the occurrence of major complication (6%)(Teixeira et al., 2009). Therefore, the diagnostic work-up requires a non-invasive techniques to diagnose and differentiate cerebral glioma.

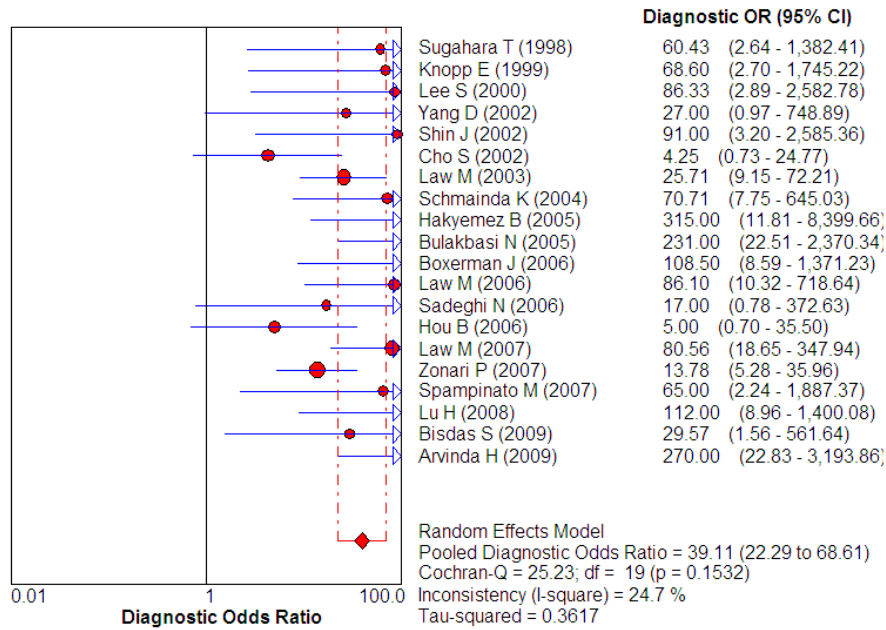


Figure 2.5: Diagnostic odds ratio of 20 studies performing perfusion analysis on 1.5 T gradient echo sequence

To my knowledge this is the first study performing a systematic review of MR perfusion studies in evaluating the diagnostic performance of relative cerebral blood volume ($rCBV_{max}$) in distinguishing high from low grade glioma. The reason for choosing $rCBV_{max}$ in our systematic review is that it was reported frequently as a powerful diagnostic tool for glioma grading (Law et al., 2006c).

The analysis was made on two independent elements; qualitative evaluation using QUADAS criteria (Whiting et al., 2003) for quality appraisal of the all studies performing $rCBV_{max}$ in glioma grading. Most of the included studies lacked a clear methodological description, which makes the techniques used irreproducible. The diagnostic reliability of MR perfusion could not be judged appropriately based on those deficient criteria, though

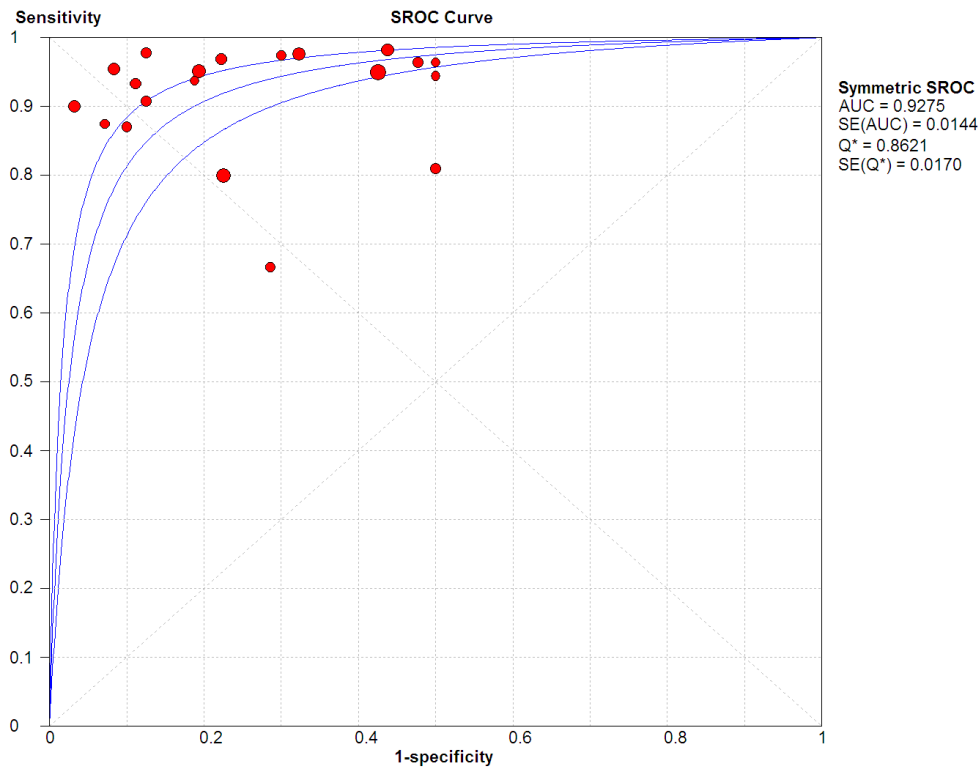


Figure 2.6: Pooled summary ROC for all studies; where AUC denotes the area under curve; SE, the standard error; Q^* , the point of equal sensitivity and specificity; SE (Q^*), the standard error of Q^*

all 26 studies standardized the result to histological diagnosis. The quantitative analysis was conducted for the same studies assessed qualitatively, but the studies basically sub-divided themselves into 20 studies using a 1.5 T gradient echo sequence (GE), 2 studies with 3 T GE, and 4 studies with 1.5 T Spin echo sequence (SE). This classification has created a homogeneity among the studies, as technical factors may contribute to differences in $rCBV_{max}$ values.

Almost all studies included patients with only glioma brain tumours while two studies included also non-glioma tumours or pilocytic astrocytoma (grade

Study	DOR	95% confidence interval	% weight
Sugahara (1998)	60.4	2.6–1382.4	2.82
Knopp (1999)	68.6	2.7–1745.2	2.66
Lee (2001)	86.3	2.9–2582.8	2.44
Yang (2002)	27.0	0.9–748.9	2.54
Shin (2002)	91.0	3.2–2585.4	2.51
Cho (2002)	4.3	0.7–24.8	7.03
Law (2003)	25.7	9.2–72.2	12.86
Schmainda (2004)	70.7	7.8–645.0	5.03
Hakyemez (2005)	315.0	11.8–8399.7	2.60
Bulakbasi (2005)	231.0	22.5–2370.3	4.64
Boxerman (2006)	108.5	8.9–1371.2	4.04
Law (2006)	86.1	10.3–718.6	5.36
Sadeghi (2006)	17.0	0.8–372.6	2.89
Hou (2006)	5.0	0.7–35.5	6.04
Law (2007)	80.6	18.7–347.9	8.95
Zonari (2007)	13.8	5.3–35.9	13.68
Spampinato (2007)	65.0	2.2–1887.4	2.48
Lu (2008)	112.0	8.9–1400.1	4.07
Bisdas (2009)	29.6	1.6–561.6	3.14
Arvinda (2009)	270.0	22.8–3193.9	4.22

Table 2.6: Summary of diagnostic odds ratio (random effects model), illustrating the power of each study based on the inverse variance of the log of the DOR

1). For instance, one study (Bulakbasi et al., 2005) included, in addition to gliomas, 10 patients with pilocytic tumour. Another study (Schmainda et al., 2004) included one ependymoma patient and one neurocytoma patient which could not be excluded from the analysis.

The variation in threshold was the mainstay to assess when performing the meta-analysis. Luckily, the threshold values were close to the arithmetic mean and they were normally distributed as evident by descriptive analysis. In addition, a positive Spearman’s correlation with coefficient close to zero

confirmed a flat effect of threshold variation. A close observation of the sensitivity and specificity of each study shows there are three studies [Law et al. (2004), Cho et al. (2002), and Lu et al. (2008)] which did not state the threshold values, while two studies [Hou et al. (2006) and Zonari (2006)] employed a relatively low threshold value.

The pooled sensitivities and specificities of the twenty studies with gradient echo had a sensitivity and specificity of 93% and 75%, respectively. Forest plot disclosed certain degrees of heterogeneity between the studies more marked in between specificities values. The outliers in the pooled sensitivity graph were mainly from three studies possessing sensitivity measures $\leq 81\%$.

Two models were proposed for analysis and statistical pooling: a fixed effects model considering the weighting average of each study and assuming the difference is only due to chance; and a random effects model based on DerSimonian–Laird method, which considers also the differences due to technical procedures and study populations (Deville et al., 2002). The details of the mathematical procedures and equations of these two models were published elsewhere (Rutter and Gatsonis, 2001).

In this study, the 27 preferred reporting items for systematic review and meta-analysis (PRISMA) (Moher et al., 2009) were followed except that the studies' authors were not contacted for any citing references and the other technical variables were not regressed for their effect on the calculated accuracy measures. The Cochrane tool for assessing the risk of bias in the systematic review was checked, and it revealed that no such selection, performance, detection, or reporting bias was present, partly because the papers

included were not clinical trial studies and partly because of following the QUADAS criteria for quality assessment.

Though such a study has not been conducted before showing the preliminary data of the possible clinical application of cerebral blood volume-derived MR perfusion in grading cerebral glioma, several limitations were encountered at every step of systematic review. First, only a few key search words were used and it would be interesting to use combinations of search words, such as cerebral, blood volume, neoplasm, tumor, tumour, magnetic resonance, and CBV. Second, only the PubMed search engine was used and not other web sources such as EMBASE or the Cochrane library database. Both of these have advantages over PubMed, as the EMBASE indexes many European and non-English journals, while the Cochrane library includes evidence-based practice, unpublished clinical trials, and systematic review articles. Third, the reference lists of the retrieved articles were not searched. The above limitations were due to the short time available within the period of post-graduate study, and the fact that one researcher was responsible for data selection and extraction. It would be appropriate to verify the data search and extraction with a second researcher. Fourth, selection bias is expected in favour of English publication as only English key words and papers published in the English language were included in this systematic review, although some non-English articles had abstracts in English. However, qualitative analysis and data extraction could not be carried out based on an abstract alone. Fifth, only one software for the meta-analysis was used and the output was not compared or verified using different meta-analysis software. Sixth, two studies included in the analysis recruited, in addition to

glioma tumours, non-glioma tumours or pilocytic astrocytoma, and the accuracy data of the glioma tumours could not be assessed separately, which may affect the final results. Finally, 6 articles were excluded from the systematic review as they were inaccessible for review though their title and abstract indicated the conducting of accuracy measures.

In conclusion, this study aimed at assessing the diagnostic performance of the relative cerebral blood volume parameter derived from MR perfusion in differentiating between high and low grade glioma. The initial assessment in this study shows that CBV-derived MR perfusion is not able to promptly differentiate high from low grade glioma. Two main issues need to be addressed in grading glioma: first, assessing the low specificity of this technique with a large number of low grade gliomas and without the inclusion pilocytic astrocytoma (grade I); second, assessing the diagnostic performance of CBV in differentiating among high grade gliomas. These two issues will be assessed and discussed in the next chapters.

Chapter 3

General methods:

Dynamic susceptibility contrast

MR perfusion and Dynamic
contrast enhanced MR

perfusion applied to cerebral
gliomas

3.1 Introduction

This chapter describes the recruitment process, patient clinical data, conventional and perfusion MR technical settings, and the histological procedures. The theoretical assumption, the existence of a correlation between contrast concentration and change in signal intensity, and the post-processing techniques, including the methods for drawing and measuring ROI, will also be given in detail in this chapter. The aim of this chapter is to provide the methodology used in the studies (Chapters 4 and 5) that assessed the diagnostic and prognostic values of the maximum relative tumour blood volume ($rTBV_{max}$) derived from dynamic susceptibility contrast (DSC) MR perfusion applied to cerebral gliomas.

3.2 Subject Recruitment and Patient Criteria

The MRI examinations were performed as part of clinical workups between August 2006 and January 2010. In total, two hundred and five patients with cerebral glioma were recruited, based on the approaches mentioned below. Potential patient approach and recruitment were performed in parallel in the two groups.

The first group was recruited based on research ethical approval (Appendix D). The recruiting approach to the potential participants, the design and duration of the study, and the transferral and storage of the MR images are explained in detail in the research protocol (Appendix A). Po-

tential patients were identified via the documentation of neuro-oncology in Multi-disciplinary team (MDT) meetings, the low grade glioma clinic and neurosurgery department (Queen's Medical Centre), and the neuro-oncology clinic (Nottingham City Hospital). Based on the research protocol, the potential patients were approached at any time after they were informed from their clinical team that they had brain glioma. The potential patients were contacted by me once they had been informed by the clinical care team and agreed to take part in the study. During the interview, a brief introduction to the study's aim and the study information sheet (Appendix C) was given to the patients, explaining the study. The patients were given the opportunity to read the information sheet and to ask questions and sign the consent form (Appendix B) if they were happy to take part in the study. One hundred and six patients with primary cerebral glioma were recruited based on local research protocol.

The second group was recruited based on clinical audit approval (Appendix E) under project number 1272. The recruitment under this part was part of assessing the performance of multimodality MR in brain tumour differentiation. The potential patients recruited under the audit approval were those who had either primary cerebral lymphoma (PCNSL), cerebral glioma, or brain metastasis. However, only patients diagnosed with primary cerebral glioma are being included in the present thesis. Patients in this category were approached via the neuro-oncology documentation of the Multi-disciplinary team (MDT) or histopathological data source. A research information sheet and consent form are not required to qualify for accessing patient data. The process of transferring and storing MR images followed the same procedures

as for the first group. Ninety-nine patients diagnosed with primary cerebral glioma were recruited based on audit approval.

The inclusion criteria were as follows:

- Patients with histologically confirmed newly diagnosed cerebral glioma
- Patients having undergone a pre-operative and pre-treatment MR Perfusion (MRP) scan
- Signing the consent form if they had been recruited via the research approval (group one).

Exclusion criteria were as follows:

- Patients aged less than 18 years
- Patients who received an MR Perfusion scan at 1.5-T magnetic field
- Failure to sign the consent form if they had been recruited via the research approval study (group one)
- Patients with too long a time interval between the histological diagnosis and the MR perfusion.

One hundred and twenty-three patients matched the inclusion criteria (53 women and 70 men, median age 53 years, age range 18–83 years) were confirmed histologically with cerebral glioma. The diagnosis of glioma was

confirmed by surgical resection ($n = 67$) or stereotactic biopsy ($n = 56$). Of these, 105 patients were astrocytic cell phenotype and 18 patients were of oligodendrogliotic cell type. All the tumours were graded according to the WHO grading system (Kleihues et al., 1995; Kleihues and Sobin, 2000) as revised in 2007 (Louis et al., 2007).

Eighty-two patients were excluded from the two recruited groups because they matched the inclusion and exclusion criteria: 12 patients had not had a histological diagnosis, 38 patients had not had any perfusion MR imaging scans, 3 patients had received their perfusion scans at 1.5 T, 19 patients had received a post-operative MR perfusion scan, 9 patients had too long a time interval between their histological diagnosis and their MR perfusion scan, and one patient was diagnosed later with a brain infection. The interval between the WHO histological diagnosis and the MR perfusion scan was defined as too long if it was more than 540 days in the case of low grade glioma, or 390 days in the case of anaplastic glioma, or 90 days in the case of glioblastoma multiforme. Figure 3.1) is a detailed patient recruitment flowchart.

The tumour grades broke down as follows: 39 patients had diffuse glioma (grade II), 24 patients had anaplastic glioma (grade III), and 60 patients had glioblastoma multiforme (grade IV). Prior to the MR scan, no patient had received any cancer treatment except corticosteroids ($n = 91$). The duration of taking the steroids before MR perfusion scans was variable (8 ± 4).

The time interval between taking the histological sample and performing the MR perfusion was carefully reviewed, for fear of a grade transformation or change in the characteristics of the tumour if too wide a gap were to be allowed. However, a relatively long interval was permitted for low grade

gliomas and anaplastic gliomas if there was no clinical or radiological evidence of disease progression that might have raised the suspicion of a histologic grade transformation.

The most common presenting clinical symptom at the time of diagnosis was a neurological manifestation ($n = 50$) such as mono- or hemi-paresis followed by seizures ($n = 44$). 30 out of 50 patients with neurological manifestation were diagnosed as having GBM while half of the patients with low grade glioma presented initially with seizures. Thirty-six (60%) out of 60 GBM patients had had surgical debulking, while the remaining GBM patients had had stereotactic biopsy. Fifty-four per cent of low grade glioma and 42% of anaplastic glioma patients underwent surgical debulking.

3.3 MR Imaging Protocol

All MR imaging was performed as part of a clinical work up protocol using a 3 Tesla Philips Achieva (Philips Healthcare, Best, Netherlands). The MR perfusion imaging protocol followed a standardised procedure for all patients as part of a tumour multimodal MRI protocol at 3 T. A localizing sagittal T_1 -weighted image was obtained followed by axial non-enhanced T_2 -weighted test spin echo (TR, 3000 ms; TE, 80 ms; echo train length 15), coronal non-enhanced T_1 -weighted image spin echo (TR, 500 ms; TE, 10 ms; echo train length 1), axial contrast-enhanced T_1 -weighted image spin echo (TR, 425 ms; TE, 10 ms; echo train length 1) or axial high resolution contrast-enhanced (MPRAGE) T_1 -weighted image fast field echo (TR, 8.1 ms; TE, 3.73 ms; echo train length 205) and coronal contrast-enhanced T_1 -weighted image spin

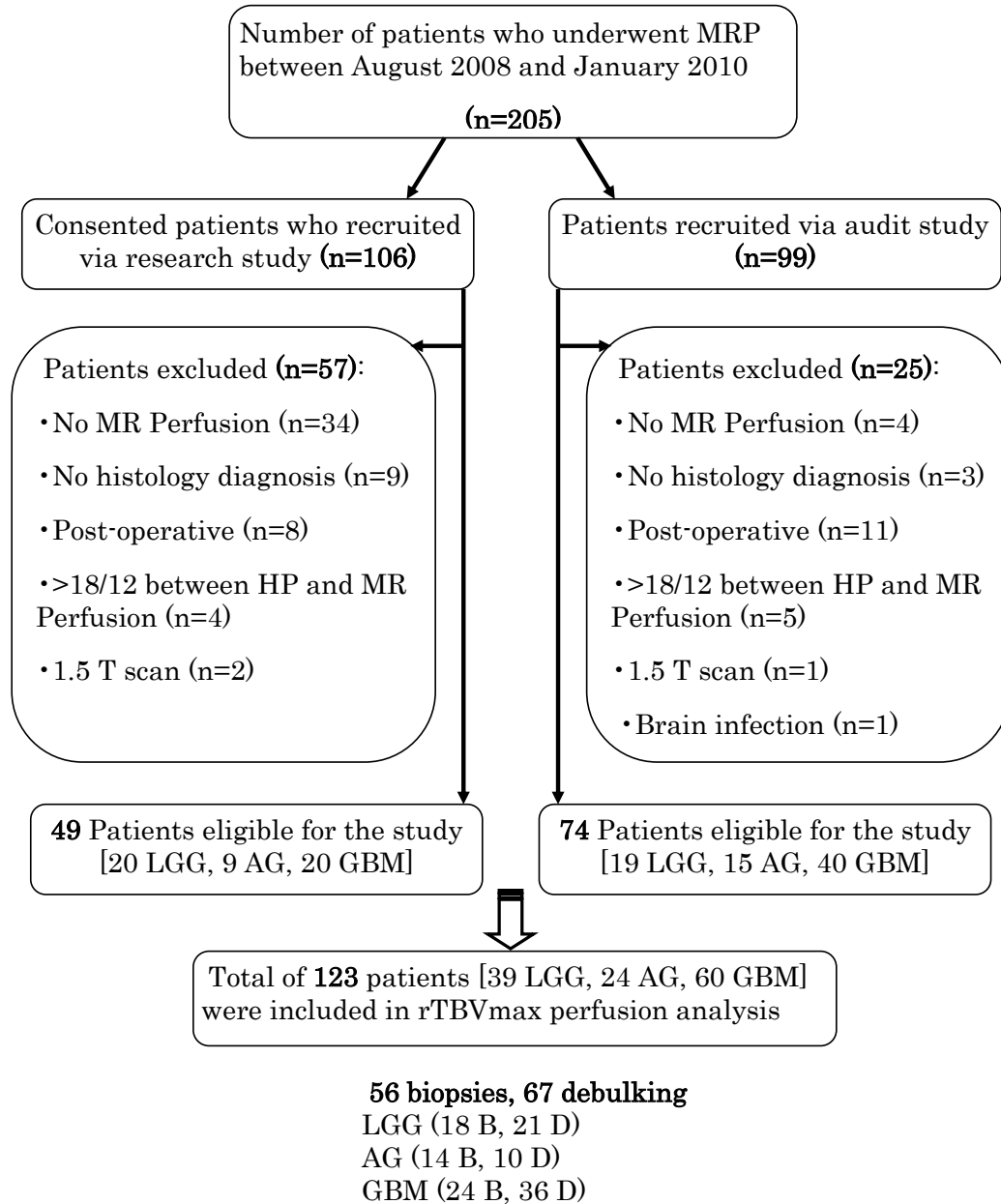


Figure 3.1: Flow chart of patient recruitment: HP (histopathology); OP (operative); LGG (low grade glioma); AG (anaplastic glioma); GBM (glioblastoma multiforme); B (biopsy); and D (debulking)

echo (TR, 423 ms; TE, 10 ms; echo train length 1). The post-contrast T_1 -weighted or high resolution contrast-enhanced T_1 -weighted images were obtained after acquisition of dynamic susceptibility contrast-enhanced MR perfusion images.

Dynamic susceptibility contrast-enhanced (DSC) T_2^* -MR perfusion images were obtained using 3D gradient echo PRESTO scans during the first pass of the bolus of the contrast agent. The MR perfusion 3D slab was positioned to cover a large area of the brain in 30 slices. A series of 60 images were acquired at intervals of 1.2 seconds. The first five volumes before contrast arrivals were used as the baseline for the signal intensity of the brain. The perfusion imaging parameters were as follows: acquisition matrix 128×128 ; pixel size 1.8×1.8 ; TR 15.78 ms; TE 23.8 ms, flip angle 7° ; field of view $230 \text{ mm} \times 105 \text{ mm} \times 187 \text{ mm}$; slice thickness 3.5 mm. A bolus of contrast material was injected intravenously at a dose of 0.1 mmol/Kg of Gadobutrol (Gadovist/ Bayer Schering Pharma). An MRI-compatible power injector (Medrad/ Spectris Solaris) was used for contrast injection at a rate of 3 ml/s followed by a bolus injection of 10 ml saline at the same rate.

Forty-three patients [9 LGG, 7 AG, and 27 GBM] underwent a dynamic contrast enhanced (DCE)- T_1 prior to the T_2^* -weighted perfusion images. In this subset of patients, the total bolus dose was the same (0.1 mmol/kg) but a quarter of the calculated dose was injected during the T_1 perfusion and the remaining three quarters were injected during the T_2^* perfusion. This improved protocol was introduced as a pre-load dose to minimize potential leakage effects in the T_2^* DSC perfusion.

The T_1 perfusion images were acquired using T_1 perfusion turbo field

echo (TFE) to obtain 45 sequential volumes in 10 sections with imaging parameters as follows: acquisition matrix 128×128 , pixel size 2×2 mm; TR, 3.62 ms; TE, 2.36 ms; flip angle 5° ; field of view $224 \times 176 \times 100$ mm; slice thickness 10 mm; temporal resolution 2.4 sec. The contrast agent Gadovist (BAYER/Schering Pharma, UK) was injected using an automatic MR compatible injector system (MedRad Spectris, PA, USA). The total required dose was calculated based on patient weight at a dose of 0.1 mmol/Kg and rate of 3 ml/sec; however 25% of the total dose was injected to perform the T_1 -DCE perfusion scan. The T_1 and T_2^* MR perfusion scans were separated by a time gap of about three minutes.

The T_1 sequence used in this study is the turbo field echo (TFE), which is a gradient echo sequence applied after a 180 degree pulse. The short TR resulted in incomplete relaxation and hence low T_1 contrast. Moreover, a short TR creates a low flip angle known as the Ernst angle effect. Radio frequency spoiling was performed for T_1 contrast optimization. The idea of the T_1 MR perfusion in this study is not different from that of the T_2^* MR perfusion but tissue signals in T_1 had an increased signal intensity while in T_2^* there was a decrease in signal intensity.

3.4 Post-Processing and CBV Map Generation

The radiographic analysis was performed blind to the histological diagnosis, to test the accuracy of MR perfusion in glioma grading. All MR images

including the dynamic MR perfusion images were anonymised before being transferred as digital imaging (DICOM) through a compact disc and stored in the server at the radiological and imaging science division (Queen's Medical Centre) according to research protocol (Appendix A). The process of anonymisation was performed at two levels: first, at the hospital data base in which the option of anonymised data was selected and hence the patient's name was stored in the compact disc as a coded number; second, at the radiological division server in which the DICOM images transferred to analyze images and every patient is coded and given a unique identity code. The identity code is composed of the first two letters of the patient's surname and the first letter of the patient's first name, followed by the scan date, so the patient's name and information can not be traced back or identified by any third party users. However, the identity code and the patients' hospital numbers were matched and kept in a secure place in case any clinical data were requested. The details of data retention and period of keeping these data were mentioned in Appendix A. The DICOM images were transferred to analyze images using a Linux workstation code. The MR perfusion analysis was performed using Java Image software (www.xinapse.com). An exponential relation was assumed between the concentration of contrast agent in the blood vessels and the reduction in the signal intensity of the brain tissue (Rosen et al., 1990). A Gamma variate was used to correct for the recirculation of contrast agents based on the following equation (Tofts, 2003).

$$C(t) = K(t - t_0)^\alpha e^{(t-t_0)/\beta} \quad (t > t_0)$$

in which $C(t)$ indicates the concentration of the contrast agent in the sup-

plying artery; K is a constant scale factor; α and β are constants describing the shape of the contrast bolus; t is the time of the first pass contrast, and t_0 is the contrast arrival delay.

The software package uses a standard algorithm for deconvolution of the tissue signal intensity (Ostergaard et al., 1999), which was used to generate cerebral blood volume maps from the MR perfusion raw images (Figure 3.2).

During the first pass of contrast bolus, T_2^* is reduced, which is demonstrated by signal reduction in the T_2^* -weighted images. The change in relaxation time (ΔR_2^*), the reciprocal of T_2^* , is calculated based on the equation

$$\Delta R_2^* = -\ln(S(t)/S_0)/TE,$$

where $S(t)$ is the signal intensity at time t , S_0 is the baseline intensity, and TE is the echo time (Aronen et al., 1994). Arterial input function was measured by localizing the region of interest to the internal carotid artery or middle cerebral artery (Figure 3.3). Arterial sampling aimed at determining the correlation between the contrast concentration and the change in signal intensity. Only the first pass was included in the analysis through truncating the signal curve from the point of signal drop to the half maximum signal recovery.

In this study, the term tumour blood volume (TBV) is used as it is exclusive to the tumour area rather than the term cerebral blood volume (CBV), which may indicate any brain area. ROIs placed over the tumour area to measure the TBV corresponds to the area under the curve (figure 3.4).

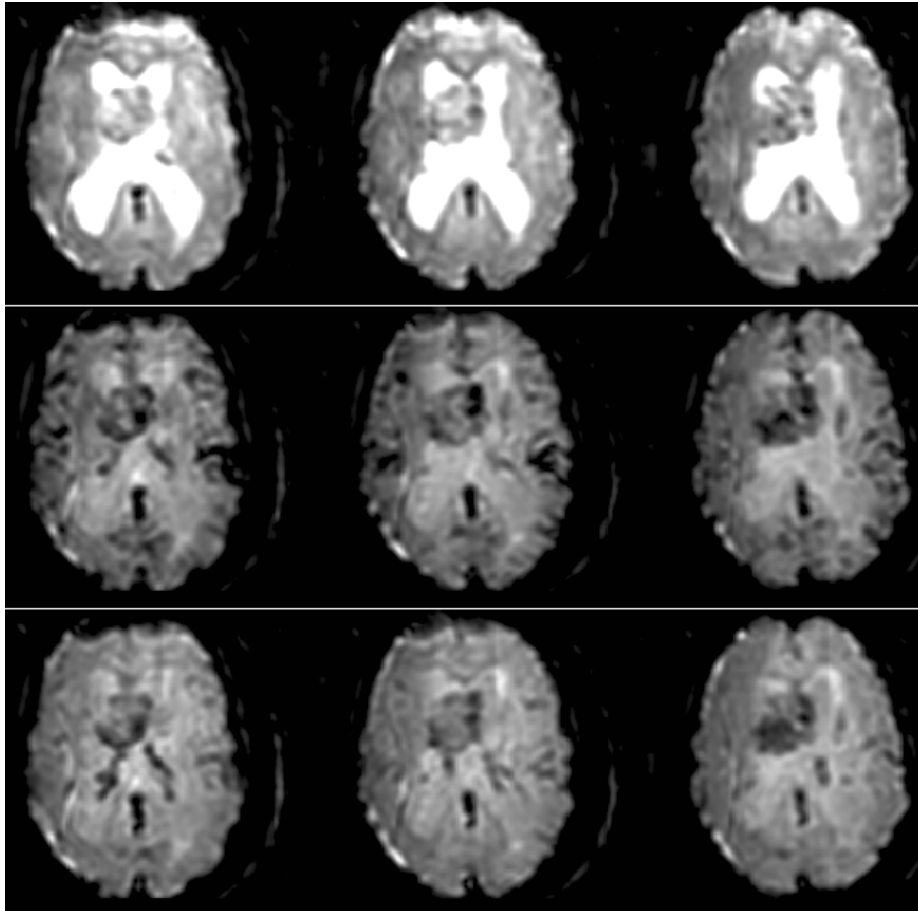


Figure 3.2: A few cuts of perfusion raw images of histologically diagnosed glioblastoma multiforme were obtained using 3T T_2^* -DSC at 3D gradient echo PRESTO scans. The upper row is the baseline before contrast injection, the middle row is at the maximum signal change (20 seconds), and the lower row is after signal recovery and recirculation (40 seconds). Note the reduction in signal intensity (middle row) compared to baseline signal intensity (upper row). Tissue change in signal intensity over time was assessed over the whole volume to detect changes in signal intensity.

3.5 Calculation of Maximum rTBV

The relative TBV_{max} analysis was performed blind to the histological diagnosis. Both post-contrast T_1 -weighted images (spin echo or MPRAGE) and T_2 weighted images were used to define the solid portion of the tumour and

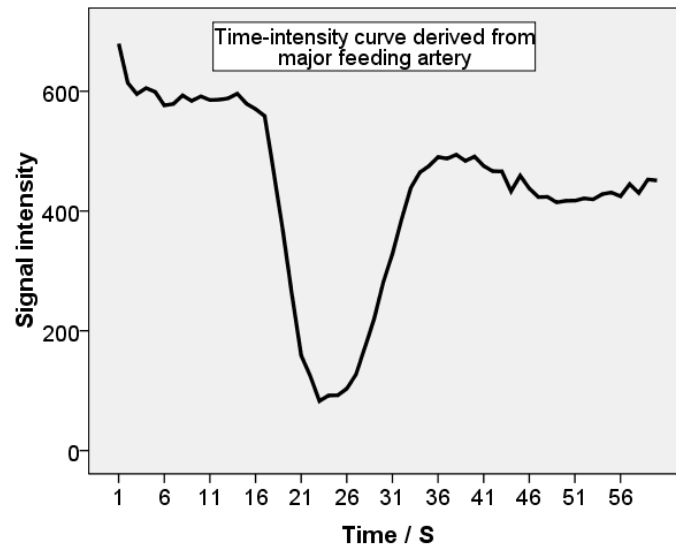


Figure 3.3: Time-intensity curve sampled from internal carotid artery. The curve showed arterial signal drop as a result of contrast injection

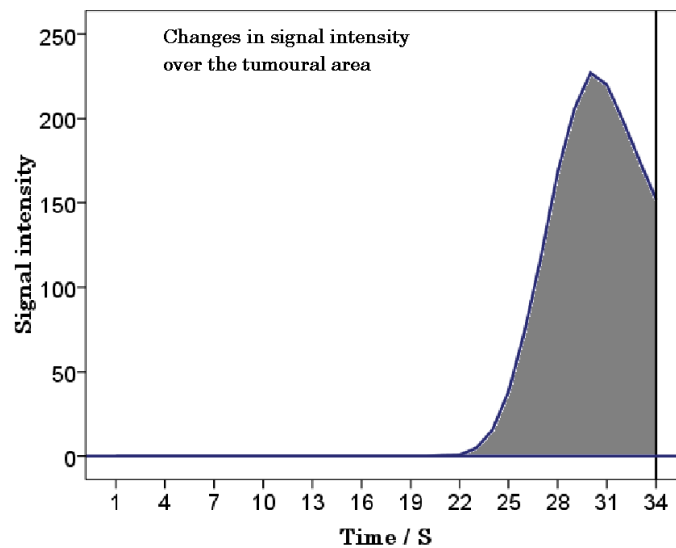


Figure 3.4: Changes in tumour relaxivity: the shaded area under the curve indirectly reflects the cerebral blood volume.

to delineate the blood vessels. The radiological criteria for defining a glioma tumour (Kornienko, 2008) were based on the appearance in the T_1 -weighted image (T_1WI), post-contrast T_1WI , and T_2WI . Defining the tumour area

of the tumour was based on the following criteria: The solid portion of the tumour appears as isointense to hypointense on T_1WI , with heterogeneous signal and poorly defined margins. The tumour in T_2 weighted images appears as a heterogeneous signal intensity. Contrast enhancement may be affected by a blood–brain barrier breach and may vary from ill-defined poor enhancement, focal enhancement, to strong peripheral ring enhancement. Peri-tumoural oedema is not typical in low grade glioma whereas in high grade gliomas, a marked oedema with mass effect is expected. Areas of central necrosis, cysts, and haemorrhagic foci are criteria of GBM. Unfortunately, tumour margins were difficult to define due to micro-infiltration into normal brain tissue. The criteria used to define the blood vessels were an enhanced linear structure that runs through a few slices in post-contrast T_1 -weighted images, and/or linear signal void structures in T_2 -weighted images.

The term hot spot is defined to include the most hyperemic areas in the tumour, indicating a high value in the look up colour scale. In the CBV map, the hot spot areas appear in the range of red to yellow colours within the solid portion of the tumour. Multiple regions of interest (ROIs) of not more than 28 mm² were drawn on the CBV map over the solid portion of the tumour. The small size of the ROIs used in this study was to avoid erroneous sampling from adjacent normal brain tissue or blood vessels. Although large blood vessels were excluded from the analysis, small blood vessels were retained as long as they were contained within the tumour. This is because a complex vascular network across the tumour precludes complete exclusion. The time spent on drawing ROIs on the CBV map within the tumour area and guided by conventional MR images (T_2 and T_1 post-contrast) was in the

range of 10–20 minutes. The mean value of TBV of each region of interest was considered and then the maximum value (TBVmax) among the ROIs was taken as representative of the most aggressive part of the tumour. The absolute TBVmax was normalized to the CBV value obtained from normal white matter. Within the normal white matter (i.e., Centrum semiovale) two large regions of interest (ROIs) of about 140 mm² were drawn for normalization. The reason for drawing a large ROI within the normal white matter is to extract a representative value. The average of both ROIs was reported and used to normalize the representative tumour value. Figures (3.5, 3.6, and 3.7) present patients with diffuse glioma, anaplastic glioma, and glioblastoma multiforme respectively. Radiological conventional images illustrate the tumour and peri-tumoural signal intensity, and the CBV maps illustrate the hot spot area and ROI in the tumoural area.

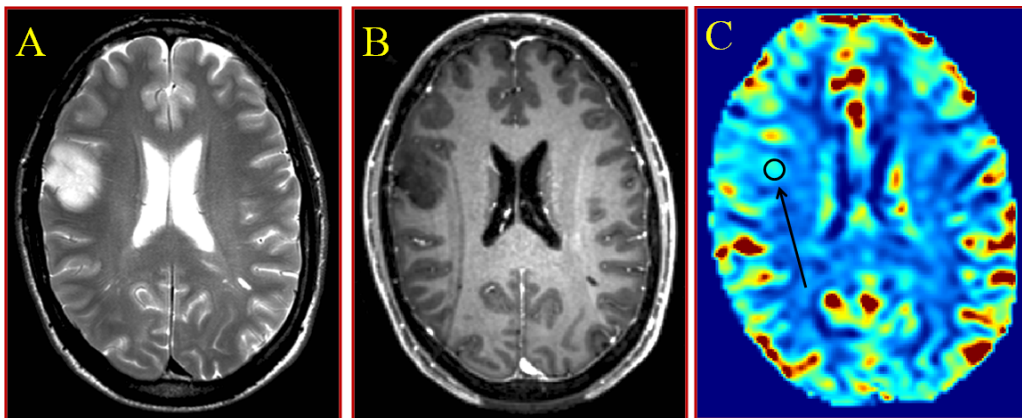


Figure 3.5: Images of a 41 year old male with histological diagnosis of low grade glioma (grade II). A, axial T_2WI hyperintense lesion in Rt posterior frontal gyrus. B, contrast-enhanced T_1WI shows hypointense lesion. C, CBV map shows mild hyperaemic signal (ROI) in the same area, with a $rTBV_{max}$ value of 1.59.

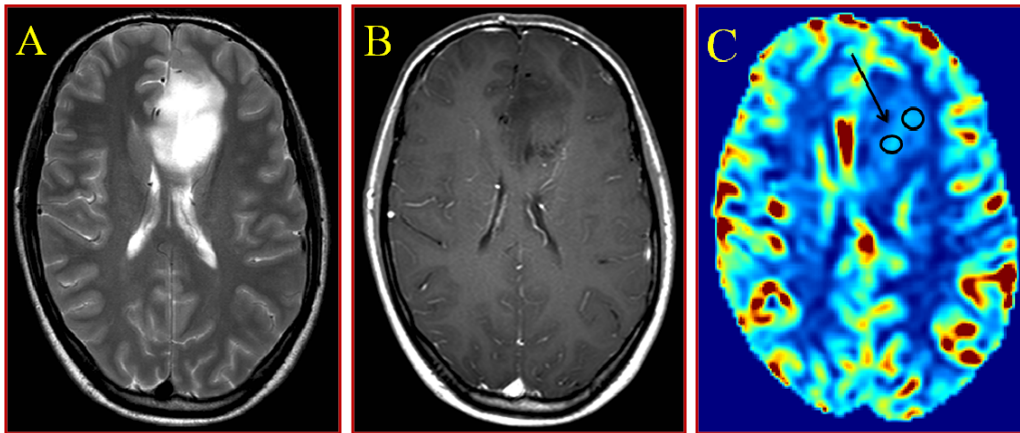


Figure 3.6: Images of 25-year-old male with histological diagnosis of anaplastic glioma (grade III). A, axial T_2WI shows hyperintensity in Lt frontal lobe with involvement of corpus callosum. B, T_1WI shows the tumour is partly heterogeneous with cystic appearance in tumour area. C, CBV map shows moderate hyperaemia (ROIs) with $rTBV_{max}$ value of 7.2

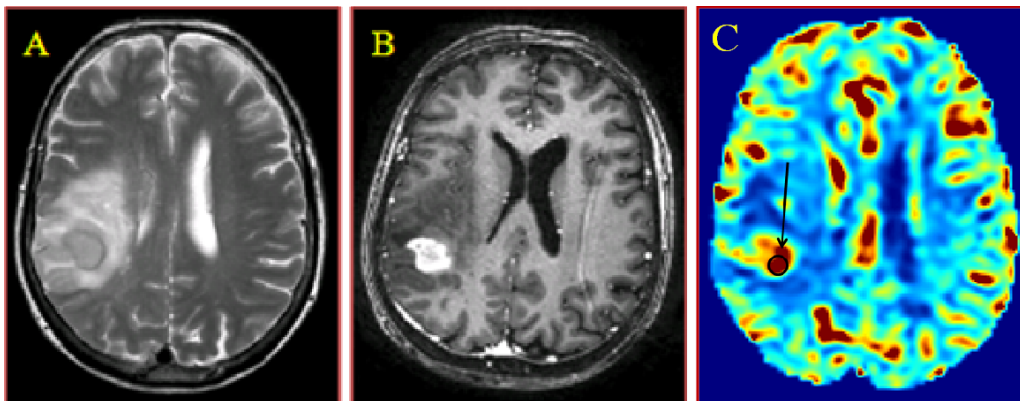


Figure 3.7: Images of a 72 year old female with a histological diagnosis of glioblastoma multiforme (grade IV). A, T_2 axial weighted image shows hypointense lesion within a large surrounding oedema at right inferior parietal lobule. B, axial MPRAGE contrast enhanced shows lesion at the same area with mass effect and effacement of the overlying sulci. C, CBV map shows severe hyperaemic lesion in corresponding area (ROI) with a $rTBV_{max}$ value of 10.62.

3.6 Histological Procedures

All specimens were analysed as part of clinical care by two neuropathologists who have more than 20 years experience. They were blind to the perfusion MR imaging findings. The grading was based on the WHO grading system into diffuse low grade glioma (grade II), anaplastic glioma (grade III), and glioblastoma multiforme (grade IV) (Kleihues et al., 1995; Kleihues and Ohgaki, 2000; Louis et al., 2007). The main features in this grading system are mitosis, vascular proliferation, and nuclear pleomorphism.

3.7 Statistical Analysis

SPSS software (version 17.0) was used for the statistical analysis. In brief, the receiver operating characteristic was used as a binary classifier to assess the diagnostic performance of $rTBV_{max}$ in grading glioma. The Cox regression model was used to assess the prognostic value of $rTBV_{max}$ as survival predictor. ANOVA was performed to assess the influence of confounders on $rTBV_{max}$ variation. The statistical analysis was mentioned in full detail in the context chapters.

Cross validation was performed through double entry of clinical, demographic, and radiological data. 10% of the total included potential subjects were randomly selected by the SPSS software. The cross validation process included 13 potential subjects and 16 variables. The same criteria in the initial data extraction were followed for cross validation.

Chapter 4

The Diagnostic Value of Dynamic Susceptibility Contrast-Enhanced MR Perfusion in Predicting the Grade of Cerebral Gliomas

4.1 Introduction

Brain cancer incidence, adjusted for age, is about 7 per 100,000, and accounts for 2% of all adult cancer deaths (Legler et al., 1999). The incidence rate increases rapidly after the age of 45 and declines after age 79 (Legler et al., 1999). Cerebral gliomas are the most common brain tumours (Principi et al., 2003) and mostly are of high grade (Daumas-Duport et al., 1988).

The WHO histological classification of cerebral glioma has been revised four times since its first publication four decades ago (Scheithauer, 2008). This is because the classification primarily is based only on cellular differentiation rather than cellular phenotype. Clinical outcomes differ with different cellular phenotypes; for instance, the variant of glioblastoma, small cell glioblastoma, has a poor prognosis compared to non-small glioblastoma (Perry et al., 2004), although a different study showed no difference in overall survival (Homma et al., 2006). Another main component in tumour classification is tumour necrosis, which has been found to be associated with poor survival in high grade gliomas (Miller et al., 2006).

High mitotic activity of tumour cells requires more oxygen consumption and hence more blood flow to the tumour (Murat et al., 2009). This is accomplished by selecting pre-existing blood vessels (Winkler et al., 2009) and by the formation of new ones (Anderson et al., 2008). The process of blood vessel formation (angiogenesis) is controlled by molecular regulation through over expression of certain growth factors as a result of cell hypoxia (Behin et al., 2003). Consequently, vascular density increases in the tumoural area with the increased number of large newly formed vessels (Cao et al.,

2006; Anderson et al., 2008). Hence it is expected that the process of blood vessel formation would be more prominent in high grade glioma and especially in glioblastoma.

The WHO histological grading is the gold standard in grading cerebral glioma. In patients deemed ineligible for debulking surgery, histological grading is based on tissue sampled from stereotactic biopsy. The brain biopsy of tumours carries a small but significant risk of mortality and morbidity (Hall, 1998). Two main issues arise as a result of biopsy procedures: first, there is a chance of 10% sampling error, as reported in clinical practice (Shastri-Hurst et al., 2006); second, major complications (6%) may occur after stereotactic biopsy, such as intra-cerebral haemorrhage, which may pass to hemiparesis and death (Teixeira et al., 2009; Dammers et al., 2010; Shastri-Hurst et al., 2006; Jackson et al., 2001). Other centres have reported complication rates ranging between 3% and 20%, including intracerebral haemorrhage, sub-arachnoid haemorrhage, deep venous thrombosis, wound infection, hydrocephalus, and infarct (Coffey et al., 1988; Vecht et al., 1990; Kreth et al., 1993; Bernstein and Parrent, 1994; Kelly and Hunt, 1994; Bernstein, 2001).

Standard MRI images fail to accurately grade cerebral glioma as radiological criteria such as contrast enhancement are weakly correlated with the histological findings of tumours (Lev and Rosen, 1999; Law et al., 2006a). The radiological findings of different cerebral glioma grades may appear similar in standard MRI images (Sugahara et al., 1999; Scott et al., 2002). It has been shown that standard MRI has poor sensitivity (73%) and specificity (65%) for diagnosing tumour type and grade, compared with histological analysis (Law et al., 2003).

Recently there has been a move towards using advanced MRI techniques which provide information on the tissue micro-environment to characterise brain tumours. The tumour growth has been correlated with an increase in blood flow and volume derived from perfusion MR (Cha et al., 2002). Previous studies showed $rCBV_{max}$ to be correlated with the histological grading and with an increased vascularity of the tumour (Aronen et al., 1994; Sugahara et al., 1998; Knopp et al., 1999; Cha et al., 2002). The use of MR perfusion promises to provide more detail in evaluating tumour properties such as vasculogenesis, cellularity, and tissue composition. Advanced perfusion MRI using relative cerebral blood volume was reported as the metric best correlated with histological diagnosis (Law et al., 2006c). A literature review performed by me has revealed a good number of studies using the relative cerebral blood volume for differentiating high from low grade glioma. Two studies evaluated the accuracy of relative cerebral blood volume using 3 T in glioma grading; however, again they had only a small sample size. The main issue in those studies is the difference in the threshold value, which makes pooling the data cumbersome. A systematic review (Chapter 2) found a low specificity in differentiating between high and low grade glioma. The advantage of using a strong magnetic field of 3 T for perfusion scanning, compared to 1.5 T, is its higher signal to noise ratio, which can be used for higher spatial resolution (Tofts, 2003). Accordingly, the temporal resolution will be improved without a large decrease in the spatial resolution. This may result in early picking up of the signal during the first pass of contrast, and an easy detection of hot spot areas within the tumour area (Tofts, 2003). The aim of this study is to assess the diagnostic accuracy of MRP at 3 T in grading

cerebral gliomas against the standard WHO histopathological diagnosis.

4.2 Methods

The subject recruitment, MR imaging protocol, post-processing, and histological diagnosis were described in Chapter 3. The demographic and clinical data are tabulated in Appendix F.

4.2.1 MR imaging protocol

The imaging protocol was described in detail in Chapter 3.

4.2.2 Post-processing and CBV map generation

Post-processing and CBV map generation was described in detail in chapter 3.

4.2.3 Histological procedures

Histological procedures was described in detail in chapter 3.

4.2.4 Statistical analysis

SPSS software (version 17.0) was used for the statistical analysis. The inter-class correlation (reliability test) was evaluated as part of quality control, in the form of assessing the intra and inter-observer agreement. A diagnostic accuracy test was performed for the first 50 recruited patients of different

glioma grades. In order to test the reproducibility of the diagnostic accuracy in this study, the threshold values obtained as a result were applied to the next 73 recruited patients. Receiver operator characteristic curves were generated from $rTBV_{max}$ values for different values of sensitivities and specificities in differentiating high from low grade gliomas and in differentiating between all three histological grades. The threshold values were obtained to differentiate high from low grade gliomas, anaplastic glioma versus low grade glioma, and among high grade gliomas. Statistical significance was defined to be $p < 0.05$.

4.3 Results

The intra-class correlation was obtained for a subset of 41 patients with different gliomas to test the reliability of $rTBV_{max}$ derived MR perfusion in grading glioma. Almost perfect consistency value (0.95) and substantial agreement (0.79) (Landis and Koch, 1977) were found within the same observer measures (Table 4.1).

Intra-class correlation	95% CI		F test			
	lower limit	upper limit	value	Df1	Df2	Sig.
0.792	0.644	0.883	8.56	40	40	<0.001

Table 4.1: Intra-class correlation coefficient (Kappa) showed high consistency for two readings of $rTBV_{max}$ performed blindly to each other. CI denotes the confidence interval; df, the number of degrees of freedom; Sig., that the level of significance < 0.05

Twenty patients with different glioma grades were selected randomly by

a computer using SPSS software. The data were analysed independently by a different observer to grade glioma lesions using the same method in calculating $rTBV_{max}$ and defining hot spot areas (Chapter 3). The inter-class correlation coefficient is indicative of substantial agreement (Landis and Koch, 1977) (Table 4.2).

Inter-class correlation	95% CI		F test			
	lower limit	upper limit	value	Df1	Df2	Sig.
0.80	-0.488	0.920	4.94	19	19	<0.001

Table 4.2: Inter-class correlation indicates substantial agreement between the two observers; df denotes the number of degrees of freedom; Sig., that the level of significance < 0.05 .

The diagnostic accuracy in predicting the grade was assessed with various cut-offs of the relative cerebral blood volume ($rTBV_{max}$) on the first recruited 50 patients with different glioma grades (18 LGG, 9 AG, and 23 GBM), using the standard reference WHO histological grading system. The best threshold values were selected based on the optimum sensitivity and accuracy in differentiating the grades of glioma. The accuracy measures with the $rTBV_{max}$ for the best threshold values at distinguishing tumour grades are presented in Table 4.3. The optimal cut-off values were estimated to provide the maximal accuracy in differentiating between glioma grades.

The threshold values were assessed for their reproducibility on the next 73 recruited glioma patients (21 LGG, 15 AG, and 37 GBM) using the same standard reference. The results are summarized in Table 4.4.

Tumour Grade	Threshold value	SEN. %	SPEC. %	PPV %	NPV %	Accuracy %	P value
LGG vs HGG	7.0	97	94	97	89	96	< 0.001
II vs III	7.0	89	94	89	94	93	< 0.001
III vs IV	9.6	100	56	85	100	88	< 0.001

Table 4.3: Sensitivity and specificity for the first set of glioma patients are represented with their significance values. The chi square test was used to produce the p value. PPV denotes the positive predictive value; NPV, the negative predictive value. The AUC for the difference between high and low grade glioma, between low grade glioma and anaplastic glioma, and between anaplastic glioma and glioblastoma multiforme, were 94%, 87%, and 94%, respectively.

Tumour Grade	Threshold value	SEN. %	SPEC. %	PPV %	NPV %	Accuracy %	P value
LGG vs HGG	7.0	96	95	98	91	96	< 0.001
II vs III	7.0	87	95	93	91	92	< 0.001
III vs IV	9.6	97	73	90	92	90	0.002

Table 4.4: Re-testing accuracy measures on the defined threshold value on the next recruited new 73 glioma patients. The AUC for the difference between high grade glioma (HGG) and low grade glioma (LGG), between low grade glioma (LGG) and anaplastic glioma (AG), and between glioblastoma multiforme (GBM) and anaplastic glioma (AG), were 97%, 91%, and 89%, respectively.

The threshold values obtained from the first set had produced about the same accuracy in differentiating between high and low grade glioma and between low grade glioma and anaplastic glioma. However, testing the threshold in differentiating among high grade gliomas yielded an even higher accuracy value than the first set. Figure 4.1 presents the ROC graphs comparing the accuracy obtained from the first and the second set of recruited patients.

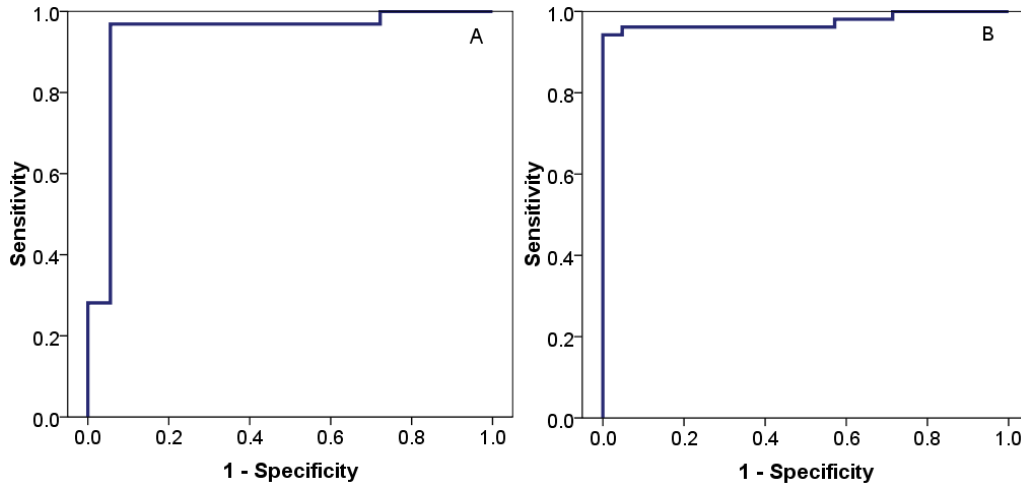


Figure 4.1: A comparison of ROC curves between high and low grade gliomas for A, the first set of glioma patients ($n = 50$) and B, the second set of glioma patients ($n = 73$)

We also pooled all 123 patients to test the accuracy of $rTBV_{max}$ -derived MR perfusion against the histological grades as a standard reference. The receiver operator characteristic (ROC) curve is applied to assess the accuracy measures of $rTBV_{max}$ in differentiating between high grade ($n = 84$) and low grade glioma ($n = 39$) (Table 4.5). Four high grade gliomas were misclassified as low grade. All the misclassified cases were anaplastic gliomas. Two patients with diffuse astrocytoma were misclassified as high grade. The ROC graph illustrates the predictive value for detecting high grade glioma, with 95% sensitivity, 95% specificity, and 95% accuracy ($P \leq 0.001$) (Figure 4.2).

An ROC curve analysis was performed for both low grade glioma ($n = 39$) and anaplastic glioma ($n = 24$). The sensitivity is 88% and specificity 97% (Table 4.6) with a significant difference between the two grades ($P < 0.001$) and AUC of 0.89 (Figure 4.3.)

Threshold value	Sensitivity (%)	Specificity (%)	PPV (%)	NPV (%)	Accuracy (%)
7	95	95	98	90	95

Table 4.5: Threshold value with corresponding accuracy measures in distinguishing between high and low grade glioma; PPV denotes the positive predictive value; NPV, the negative predictive value.

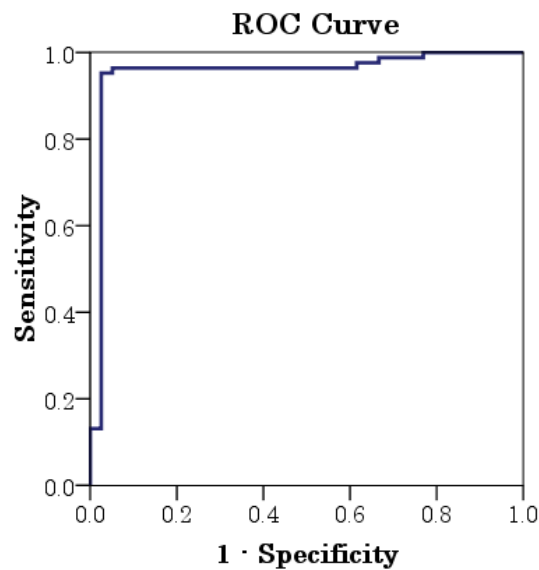


Figure 4.2: ROC curve demonstrating the diagnostic accuracy of $rTBV_{max}$ for analysis high grade glioma (HGG) and low grade glioma (LGG). The AUC for each threshold is 0.96.

The ROC curve was applied to test the diagnostic value of $rTBV_{max}$ in differentiating glioblastoma multiforme ($n = 60$) from anaplastic glioma ($n = 24$). The test had a high sensitivity (98%) but low specificity (67%). Fifty-nine out of 60 GBM patients were correctly diagnosed (Table 4.7). One patient with GBM was falsely classified due to a low $rTBV_{max}$ value, however, this patient had a long period of survival and tumour progression after one year. Sixteen patients with anaplastic glioma (grade III) had a low

Threshold value	Sensitivity (%)	Specificity (%)	PPV (%)	NPV (%)	Accuracy (%)
7	88	97	95	93	94

Table 4.6: Threshold values with corresponding accuracy measures of $rTBV_{max}$ in differentiating anaplastic glioma (grade III) from low grade glioma (grade II)

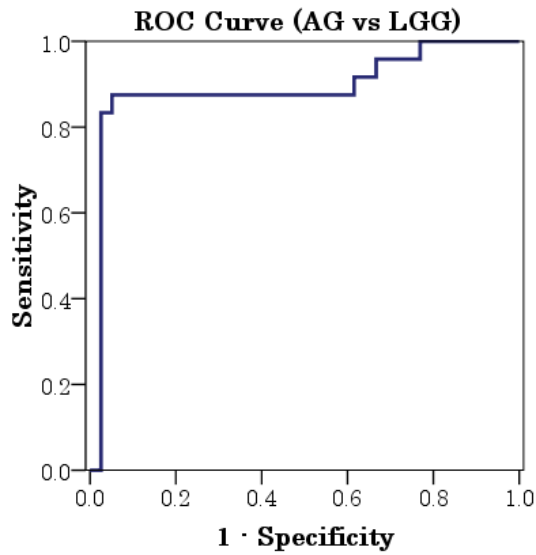


Figure 4.3: ROC curve analysis showing difference between low grade and anaplastic glioma with AUC of 0.89

$rTBV_{max}$ value compared with those having GBM. Eight anaplastic glioma patients were falsely classified by the MR perfusion as GBM, with higher $rTBV_{max}$ of more than 9.6. Three out of eight patients had high $rTBV_{max}$ and the remaining ($n = 5$) had $rTBV_{max}$ values close to the threshold value. One out of three patients with a high $rTBV_{max}$ were diagnosed based on stereotactic biopsy that showed oligodendrogliotic subtype. Interestingly, all misclassified anaplastic glioma presented with clinical symptoms such as neurological manifestations and seizures. A discriminant analysis showed a

significant difference between high grade glioma ($P < 0.001$) with an AUC of 90% (Figure 4.4).

Threshold value	Sensitivity (%)	Specificity (%)	PPV (%)	NPV (%)	Accuracy (%)
9.6	98	67	88	94	89

Table 4.7: Accuracy measures in differentiating glioblastoma multiforme (grade IV) from anaplastic glioma (grade III)

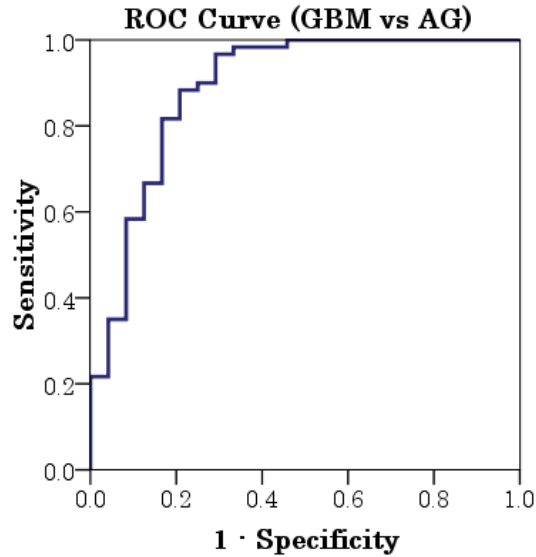


Figure 4.4: ROC curve analysis illustrating the differences among high grade glioma. AUC was 90% with significant difference ($P < 0.001$).

4.4 Discussion

A new hyperaemia-based radiological grading system was suggested in this study for human adult cerebral gliomas. The maximum value of tumour

blood volume demonstrated consistently high accuracy (96%) in differentiating between high and low grade glioma and even better accuracy (90%) in distinguishing glioblastoma from anaplastic glioma, compared to the training set accuracy (88%).

In this study we used 2D gradient PRESTO technique at 3 T MR scan to assess the diagnostic accuracy of the perfusion parameter ($rTBV_{max}$) in grading glioma. All patients recruited underwent a pre-treatment MR perfusion scan. Both short echo time (23.8 s) and low flip angle (7°) improved the T_2^* signal changes and reduced the T_1 effect. In addition, the total acquisition time for obtaining the perfusion scans was 72 seconds as of 1.2 second per image volume, so the contrast bolus can be tracked within the tumour and without much loss of SNR. PRESTO is less sensitive than EPI to field inhomogeneity (Liu et al., 1993) and gives fast three-dimensional volumes without significant geometric distortion (Tofts, 2003). In contrast, Echo planar imaging (EPI) causes image distortion at arterial input function curve. In addition, the temporal resolution in 3-Dimension acquisition of EPI is about two seconds per image volume (Yang et al., 1998), which is insufficient for bolus tracking (Tofts, 2003). The less geometric distortion in PRESTO compared to EPI is attributed to a relatively shorter time interval between the first and last echo (van Gelderen et al., 1995).

Two main problems are usually encountered when calculating tumour blood volume. First, the T_1 effect due to contrast leak within the extracellular space as a result of porous tumour blood vessels, which is minimized to a large extent by the use of a low flip angle and short echo time. Second, contrast agent re-circulation to the tumour area, which may falsely increase

the reading of the tumour blood volume. This contrast re-circulation was mitigated by considering first pass bolus via fitting to a gamma variate curve and by truncating the time intensity curve to the point of mid half-maximum of signal recovery. The techniques among the studies were different in terms of reducing the T_1 effect for optimization of the T_2^* signal. Many studies used a relatively long echo time or a large flip angle (Yang et al., 2002; Bulakbasi et al., 2005; Hakyemez et al., 2006; Whitmore et al., 2007; Hirai et al., 2008), which may result in under-estimating the actual tumour volume and hence in affecting the MR perfusion sensitivity in grading gliomas. Another technique attempting to reduce the T_1 effect was to inject a pre-load contrast dose; however the accuracy in grading glioma was not improved (Schmainda et al., 2004; Boxerman et al., 2006; Whitmore et al., 2007).

The technical settings of MR perfusion and the methods of selecting and drawing ROI used in this study were slightly different from what had been published previously; hence the threshold values were expected to differ as well. A systematic review (Chapter 2) identified the range of $rCBV_{max}$ threshold values as being between 1.1 and 3.9 (mean 2.13) to distinguish high from low grade (Hou et al., 2006; Bulakbasi et al., 2005). This study analysis generated threshold values for radiological grading of gliomas from the first 50 patients. These threshold values were tested on the second recruited patient group ($n = 73$) and showed a high reproducibility and substantial reliability.

The diagnostic performance in detecting high grade glioma was 97% in the training set ($n = 50$) and 96% on the test data ($n = 73$), which is in line with the performance achieved by other studies using 1.5 T (Hakyemez et al.,

2005; Lu et al., 2008; Park et al., 2010b; Spampinato et al., 2007; Bulakbasi et al., 2005; Arvinda et al., 2009; Lee et al., 2001) and 3 T (Park et al., 2010b, 2009; Morita et al., 2010). Two studies (Law et al., 2003; Zonari et al., 2007) recruited a large number of glioma patients. The specificity in these studies ranges from 57%–78%. The improvement in diagnostic accuracy compared to other studies (Law et al., 2003; Schmainda et al., 2004; Zonari et al., 2007; Bisdas et al., 2009; Law et al., 2007b) was due to the optimization in the MR technical parameters such as the flip angle and echo time, in addition to the post-processing technique to reduce contrast leakage and recirculation. The lower accuracy of those studies may be attributed to the inclusion of other tumour types such as brain metastasis, ependymoma, and neurocytoma (Cho et al., 2002; Schmainda et al., 2004), or to including the paediatric age group with pilocytic astrocytoma (Bisdas et al., 2009). Four patients histologically confirmed as high grade glioma had a low $rTBV_{max}$ value. All four patients were, however, anaplastic astrocytoma. Three out of four patients were diagnosed based on surgical debulking and one patient was diagnosed based on stereotactic biopsy. Two low grade glioma patients had high $rTBV_{max}$. Both had undergone surgical debulking and one patient died six months after diagnosis.

This study also showed a high ability in differentiating between glioblastoma multiforme (grade IV) and anaplastic glioma (grade III). The diagnostic accuracy was 88% in the training set and 90% in the test set. The clinical importance of this separation is that the survival and treatment plans differ for the two tumour grades (Louis et al., 2007). Only two studies (Lu et al., 2008; Park et al., 2009), to the best of my knowledge, have attempted to

distinguish between the two tumour grades: one had low accuracy (57%) and the other produced comparable accuracy (86%) although the result was not validated. In this study only one glioblastoma patient presented with low $rTBV_{max}$. The histological diagnosis confirmed a GBM arising in a low grade tumour with focal vascular proliferation and incipient necrosis. Eight anaplastic glioma patients were falsely diagnosed as GBM, based on radiological classification. Three out of eight patients had high $rTBV_{max}$ values; two patients died a few months after diagnosis and had a histological report of high cellularity and mitotic activity, the other patient died after two years and was diagnosed based on stereotactic biopsy. The remaining five anaplastic glioma patients had a $rTBV_{max}$ value close to the threshold value. Three out of five patients were diagnosed based on stereotactic biopsy and two of them had the histological phenotype of oligodendroglioma.

However, the diagnostic accuracy of stereotactic biopsy may reach up to 93% when two target sites are undertaken (Shastri-Hurst et al., 2006). A larger percentage of glioblastoma multiforme patients were subjected to surgical debulking while the rest (40%) were biopsied, either because the tumour was inaccessible or the patients clinical status did not permit of doing so. We see that no such under-grading of tumour grade occurred within the glioblastoma multiforme (GBM) group; however, false negative results of GBM may ensue at lower grades.

Although we demonstrated a high accuracy and reproducibility in grading cerebral gliomas, a few limitations were encountered in this study. First, the interval between the histological and radiological diagnosis was too wide for four glioma patients (two low grade glioma patients and two anaplas-

tic glioma patients). The two anaplastic glioma patients had more than a one year difference, and there was an even longer period for the two low grade glioma patients. However, the tumour characteristics, based on clinical and radiological criteria, were stable for those patients during the follow-up period. Second, 32 patients (51%) with low grade and anaplastic glioma underwent surgical biopsy rather than surgical debulking. In patients deemed ineligible for debulking surgery, histological grading is based on stereotactic biopsy. In fact, 10 out of 14 misclassified patients had a higher radiological grade than histological grade. Third, the reproducibility of this technique needs to be applied in a multi-centre study as the threshold values depend mainly on local MR perfusion setting and post-processing technique. Finally, although the patients recruited in this study were consecutive, they were less than half of the cerebral glioma patients diagnosed during the time of the study. Selection bias is unlikely, as the MR perfusion was mainly driven by scanner availability.

4.5 Conclusion

In this study we have shown that the $rTBV_{max}$ derived from dynamic susceptibility MR perfusion at 3 T affords high accuracy for the grading of cerebral gliomas. This suggests that a single physiological tumour parameter, namely the increase in blood volume, is almost as powerful as the panel of cellular changes to predict tumour aggressiveness. The substantial agreement of post-processing of the perfusion MR images was indicative of the reproducibility of this method, although our cut-offs are higher than those

previously reported. Importantly, non-invasive assessment of this parameter through MR perfusion highlights its clinical diagnostic utility. The clinical application of MR perfusion would be valuable during the follow-up period of low grade glioma patients to assess tumour progression (Law et al., 2006a). In my opinion, by knowing the value of $rTBV_{max}$ during the follow-up period, the surgical decision and the risk-to-benefit of an operation can be judged appropriately. In chapter 6, the diagnostic performance of $rTBV_{max}$ -derived MR perfusion in tumour grading will be assessed against the histological diagnosis in predicting survival in conjunction with other previously reported survival predictors.

Chapter 5

The diagnostic value of DCE- T_1
MR perfusion in predicting
cerebral glioma grades

5.1 Introduction

Tumour growth is associated with the development of several immature and hyper-permeable blood vessels which differ from those in normal brain tissue. The increase in the vascularity of the tumour is associated with high malignancy (Macchiarini et al., 1992; Weidner et al., 1991). The increase in vascular permeability is greatly affected by the vascular endothelial growth factor (VEGF) (Puduvalli and Sawaya, 2000), which increases the vascular density, which, in return may result in an increase in relative CBV. Hence, CBV maps are used to assess patients with brain tumours (Rosen et al., 1991; Knopp et al., 1999; Aronen and Perki, 2002; Wetzel et al., 2002; Law et al., 2003). A strong relationship between the histological grade of cerebral glioma and the CBV readings has been found by several studies (Aronen et al., 1994; Ludemann et al., 2001; Sugahara et al., 2001; Law et al., 2003, 2004b; Mills et al., 2006; Sadeghi et al., 2007).

T_2^* -DSC MR perfusion is the most common method (Aronen et al., 1995; Aronen and Perki, 2002), applied and explained in detail in Chapters 3 and 4. The main disadvantage of this method is the susceptibility effect wherein the residual relaxivity is affected by contrast leakage into the extravascular space (Siegal et al., 1997). The major blood vessels in T_2^* CBV maps are broader and appear distorted compared to those displayed in T_1 CBV maps. The susceptibility effect has resulted in concealing vascular structure details (Haroon et al., 2007).

T_1 -DSC perfusion analysis of glioma has demonstrated a significant ability to distinguish between grade II and grade IV (Mills et al., 2006), and a good

correlation between the CBV obtained from T_1 -DCE and from T_2^* DSC MR perfusion (Li et al., 2003; Haroon et al., 2007) and the arterial spin label method (Zhang et al., 2012).

The aim of this study is to assess the diagnostic accuracy of T_1 -DCE MR perfusion in grading glioma and compare it to that obtained from T_2^* -DSC MR perfusion.

5.2 Methods

The subject recruitment, MR imaging protocol, post-processing and histological diagnosis were described in Chapter 3. The demographic and clinical data are tabulated in Appendix F.

5.2.1 MR imaging protocol

The imaging protocol was described in detail in Chapter 3

5.2.2 Perfusion images post-processing

The DCE- T_1 perfusion images were post-processed using JIM software (www.xinapse.com) where DICOM images (Figure 5.1) are downloaded and transformed into Analyze image format to perform the perfusion analysis. Rapid and consecutive turbo field echo images were used over the brain area with 10 slices and 45 repeats. The concept of generating a T_1 MR signal is the same as in T_2^* MR perfusion, but the contrast arrival into the area of interest produces an increase in signal intensity, which is in contrast to the signal

changes occurring in T_2^* . The arterial input function (AIF) was determined by manual registration of the signal changes over the internal carotid artery or the middle cerebral artery and then saved as an AIF file. The time-intensity curve obtained from the AIF (Figure 5.2), an indicator of changes in signal intensity, was registered on raw data T_1 perfusion images to create the CBV map of T_1 perfusion. In the signal-intensity-time curve, the time from escalating signal intensity to the end of T_1 perfusion scanning time was used for the analysis.

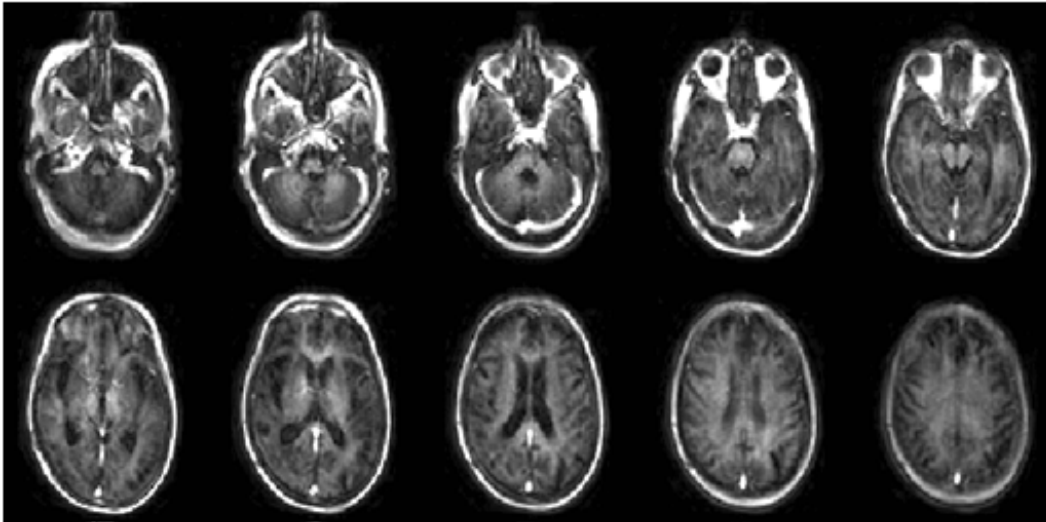


Figure 5.1: Raw data of T_1 MR perfusion used to generate dynamic CBV map

5.2.3 Calculation of $rTBV_{max}$

Calculation relative tumour blood volume was the same described in chapter 3. The appearance of different glioma grades with an example of ROIs over the tumour is shown in Figure 5.3.

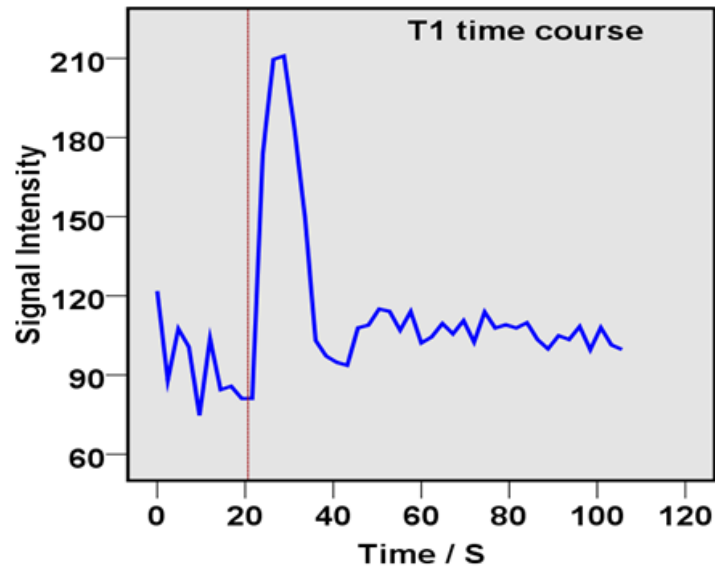


Figure 5.2: Signal intensity time curve obtained from major feeding artery to produce T_1 dynamic perfusion images

5.2.4 Histological procedures

The histological procedures for grading glioma based on the WHO grading system were given in detail in Chapter 3.

5.2.5 Statistical analysis

SPSS (17.0) was used to perform the statistical analysis. ROC was used as a binary classifier to assess the diagnostic accuracy of this T_1 MR perfusion technique in grading glioma. ROC was also used for groups of patients where T_2^* DSC perfusion was performed without pre-load dose. The accuracy values obtained from the three different techniques were compared, to assess their accuracy in grading gliomas.

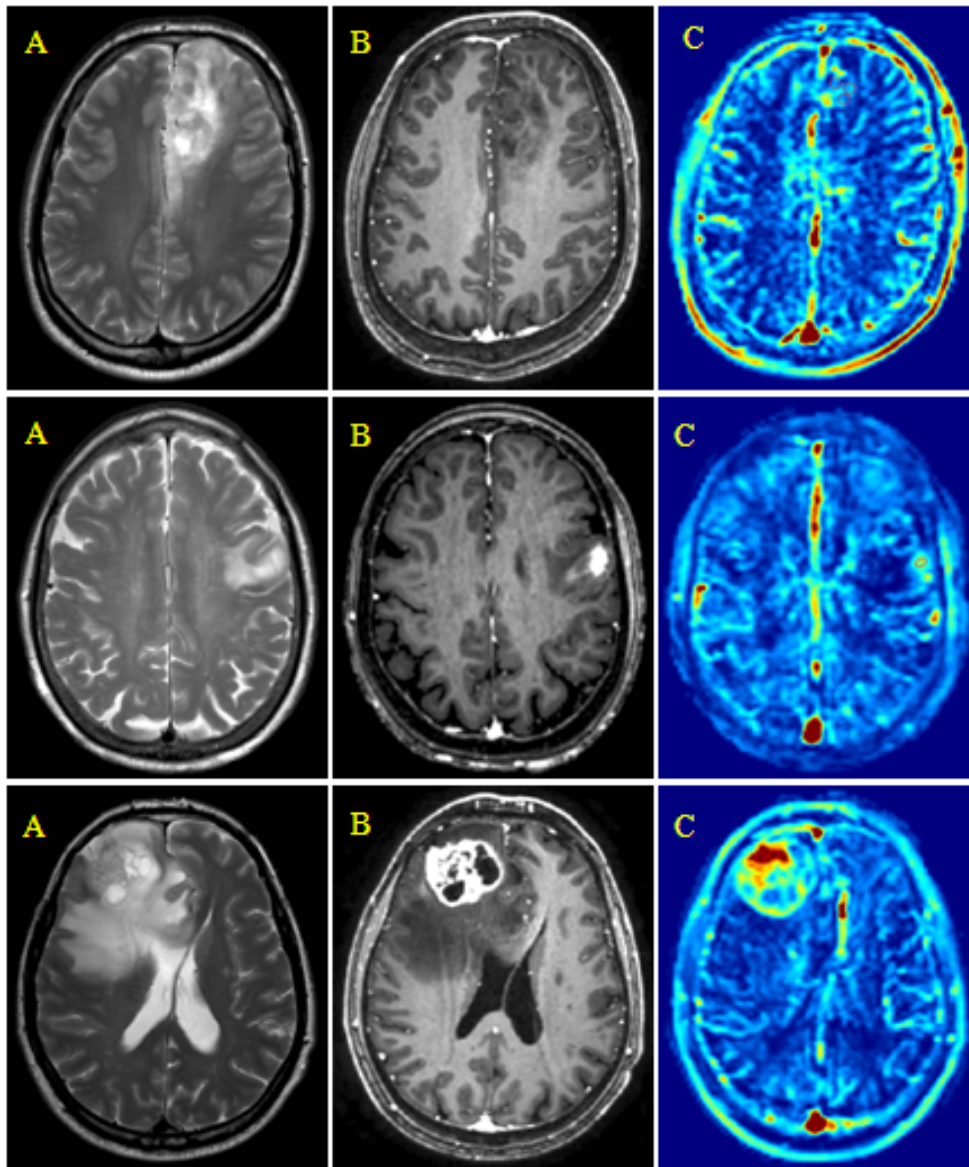


Figure 5.3: Conventional images and CBV map of DCE-MR perfusion. A is T2-weighted; B, MPRAGE images; C, T_1 perfusion images of low grade glioma (upper row), anaplastic glioma (middle row), and glioblastoma multiforme (lower row). Multiple ROIs were placed over the hyperaemic area on CBV map C.

5.3 Results

ROC curves (Figure 5.4) were also applied to assess the diagnostic accuracy of T_1 perfusion, T_2^* MR perfusion techniques with and without pre-load dose of contrast (Tables 5.1, 5.2, and 5.3).

Tumour grade	Threshold value	Sensitivity %	Specificity %	PPV %	NPV %	Accuracy %	P value
HGG vs LGG	3.7	97	78	94	88	93	<0.001
AG vs LGG	3.7	86	78	75	88	81	0.02
GBM vs AG	6.4	93	100	100	78	86	<0.001

Table 5.1: Optimised thresholds for T_1 perfusion technique and accuracy in distinguishing glioma grades

Tumour grade	Threshold value	Sensitivity %	Specificity %	PPV %	NPV %	Accuracy %	P value
HGG vs LGG	7	98	93	96	97	96	<0.001
AG vs LGG	7	94	93	89	97	94	0.001
GBM vs AG	9.6	100	59	83	100	86	<0.001

Table 5.2: Optimised thresholds and accuracy for T_2^* perfusion without pre-load dose contrast in differentiating glioma grades

Tumour grade	Threshold value	Sensitivity %	Specificity %	PPV %	NPV %	Accuracy %	P value
HGG vs LGG	7	94	100	100	82	95	< 0.001
AG vs LGG	7	71	100	100	82	88	0.05
GBM vs AG	9.6	96	100	100	88	97	<0.001

Table 5.3: Optimised thresholds and accuracy for T_2^* perfusion with pre-load dose contrast in grading gliomas

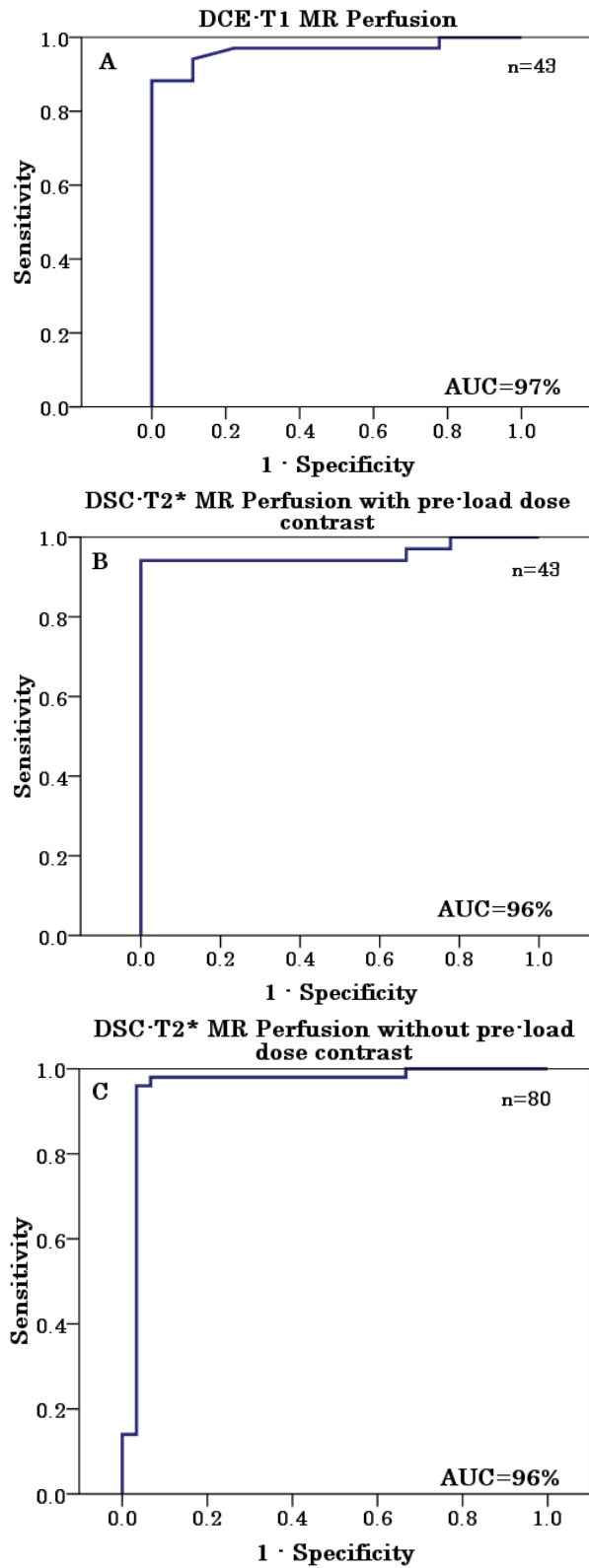


Figure 5.4: Diagnostic accuracy of $rTBV_{max}$ in differentiating high from low grade glioma was assessed. ROC curves A, B and C represent AUC of T_1 MR perfusion, T_2^* MR perfusion with pre-load dose, and T_2^* MR perfusion without pre-load dose of contrast, respectively.

5.4 Discussion

In this chapter the objective was to test the diagnostic accuracy of T_1 perfusion in differentiating between high and low grade gliomas and between different glioma grades for possible use in the future as a clinical tool.

ROC was obtained to test the accuracy of T_1 MR perfusion in diagnosing glioma. The highest sensitivity and accuracy was in separating high from low grade glioma and in separating glioblastoma multiforme from anaplastic glioma. This technique was introduced recently in our institution aiming at being a radiological tool supplementing T_2^* MR perfusion. The separation within high grade glioma is important clinically as both the treatment regimens and survival times are different.

The optimum threshold values in separating glioma grades for T_1 perfusion were lower than for T_2^* perfusion, which may be attributed to the small sample size, the low contrast dose, and the lesser susceptibility to signal changes. The accuracy of T_1 perfusion in differentiating high from low grade gliomas is comparable to that of T_2^* perfusion. In addition, T_1 perfusion showed a high sensitivity and specificity in differentiating between glioblastoma and anaplastic glioma. In distinguishing high from low grade glioma, one high grade patient possessed a low $rTBV_{max}$, and two low grade patients had high $rTBV_{max}$. One of these two cases showed clinical deterioration and later received radiotherapy and chemotherapy. Our results were in line with the previously reported significant difference between high and low grade glioma (Pauliah et al., 2007) using T_1 -dynamic contrast enhanced MR perfusion. On the other hand, others (Hu et al., 2010) have reported

improved accuracy only when using a combination of a higher pre-load dose and a baseline subtraction method.

In terms of the comparison between the two different techniques of T_2^* perfusion, the accuracy in differentiating high from low grade glioma was about the same when a threshold value of 7 was selected. The slight difference between the two techniques in other accuracy measures may be attributed to the difference in distribution of glioma cases within each tumour grade. T_2^* MR perfusion without a pre-load dose had a lower specificity in differentiating among high grade gliomas. In total, seven anaplastic glioma patients had high $rTBV_{max}$, two patients were diagnosed histologically based on surgical biopsy. Those two cases died less than one year after diagnosis. Our result found no statistical difference between DSC- T_2^* MR perfusion with, and without, pre-load dose. This contradicts data previously reported (Boxerman et al., 2006).

5.5 Conclusion

T_1 perfusion demonstrated a comparable accuracy to that of T_2^* perfusion. However, its robustness in glioma grading still needs to be assessed on a larger scale.

Chapter 6

Is relative cerebral blood volume-derived MR perfusion a significant predictor of survival in patients with brain glioma?

6.1 Introduction

The prognosis for cerebral gliomas remains poor despite the introduction of combined therapy (Stupp et al., 2005). The glioma prognosis is variable within the same histological grade, which may be indicative of other factors implicated in survival (Gilles et al., 2000). Although histological diagnosis is the gold standard reference in grading gliomas, tumour heterogeneity and sampling error from stereotactic biopsy make grade verification inadequate (Jackson et al., 2001; Behin et al., 2003).

Several factors have been assessed for their influence on predicting survival in glioma patients. Gender has been reported as a significant predictor in high grade glioma wherein females have a better prognosis than males (Hirai et al., 2008). In other studies, age and performance status were the most prognostic variables encountered in survival prediction (Behin et al., 2003; Chang et al., 2009). This is, however, in contradiction with others who found that age and performance status did not elicit any prognostic significance for progression free survival in low grade glioma patients (Dhermain et al., 2009). The same factors were found not significant survival predictors within a group glioblastoma multiforme (Hirai et al., 2008; Stark et al., 2007)

Tumour resection, radiotherapy and re-operation of recurrence not chemotherapy were prognostic factors in elderly patients survival for glioblastoma multiforme (Stark et al., 2007). The extent of surgical resection was a predictor of survival within high grade glioma patients (Hirai et al., 2008). Glioblastoma patients with gross total resection have a longer survival time than those who have a subtotal resection or biopsy; however, the difference did not reach

statistical significance (Saraswathy et al., 2009). Assessment of the effect of post-operative radio- and chemotherapy in low grade glioma showed that post-operative treatment did not improve overall survival (Schomas et al., 2009b). In addition, radiotherapy and chemotherapy did not improve survival in patients with anaplastic oligodendroglioma (van den Bent et al., 2010).

Regardless of tumour grading, histological cell lines showed different blood volume values (Maia, Jr. et al., 2005; Whitmore et al., 2007) and variable survival time (Engelhard et al., 2003; Derlon et al., 2000). Low grade glioma with oligodendroglial elements showed a longer median survival and patients do better than their counterparts with astrocytic elements (Schomas et al., 2009b). Oligodendrogliomas with loss of heterozygosity demonstrated radio- and chemosensitivity, with a longer survival rate (Cairncross et al., 1998; Bauman et al., 2000). The genetic loss of 1p/19q showed a strong correlation with overall survival and progression free survival (van den Bent et al., 2010).

Radiological features were revealed as prognostic parameters in glioma patients survival. Tumour size (> 4 cm) and location were reported to be independent predictors of overall survival when adjusted for performance status and age (Chang et al., 2009). Contrast enhanced derived from conventional imaging, relative CBV, and microvascular leak have been presented as survival predictors (Dhermain et al., 2009). Cerebral blood volume was found to be an independent predictor of 2-year survival within high grade glioma patients (Hirai et al., 2008). Low grade oligodendrogliomas with heterozygous chromosomal loss showed high tumoural blood volume compared

to the astrocytic cell type of the same grade (Whitmore et al., 2007). The non-invasive evaluation of tumour behaviour with MRI perfusion (rCBV) was reported to be an independent predictor among high grade glioma and within the glioblastoma multiforme grade (Hirai et al., 2008; Saraswathy et al., 2009). An increase of cerebral blood volume of more than three times the CBV of normal white matter was significantly associated with poor survival (Saraswathy et al., 2009).

Changes in cerebral blood volume may also predict tumour transformation in which rCBV was elevated over a period of time compared to the baseline measures in non-transformers (Danchaivijitr et al., 2008). A high relative CBV was associated with a short time to progression, irrespective of tumour grade, and has shown a significant association even when adjusted for histological grading (Law et al., 2008). The shortfalls in those studies were either their small sample size and few death events or in their assessing survival within one tumour grade. Confounders such as age, treatment, steroid intake, surgical resection, and performance status, were not analysed beside the perfusion parameters in order to assess whether the $rTBV_{max}$ is an independent survival predictor. Furthermore, $rTBV_{max}$ as a perfusion parameter was adjusted to the histological diagnosis (Law et al., 2008) while the study aimed at evaluating $rTBV_{max}$ for possible future use as a substitute for histological diagnosis in survival prediction.

The aim of the present study is to assess the prognostic value of relative tumour blood volume ($rTBV_{max}$) derived from MR perfusion in survival prediction of glioma tumour patients. The predictive value of $rTBV_{max}$ was also assessed within glioblastoma multiforme patients. The prognostic value

of $rTBV_{max}$ in survival prediction will be assessed with demographic and clinical factors.

6.2 Methods

6.2.1 Patient population

The patient population and criteria were described in detail in Chapter 3.

6.2.2 MR Imaging protocol

The imaging protocol was described earlier in Chapter 3.

6.2.3 Post-processing of dynamic images

The post-processing method was described in Chapter 3.

6.2.4 Histological technique

The histological technique was described in Chapter 3.

6.2.5 Survival analysis

The clinical follow-up period ranged from 1 to 255 days (median 33 days). Overall survival and time to progression were used as the primary end points. Overall survival was defined from the time of the first MR images confirming the diagnosis of brain tumour to the date of the last visit or date of death. Time to progression was defined from the date of the first diagnosis with MR

images to the date of disease progression. Disease progression was defined by the MacDonald criteria (Macdonald et al., 1990) which is based on either or both radiological and clinical criteria. Tumour progression was identified by an increase in tumour size by 25%, the appearance of a contrast-enhanced new lesion, clinical deterioration with neurological symptoms, and an increase or dependence on steroid dose. On MR scan, the tumour was measured with two lines perpendicular to each other at the largest cross sectional diameter. The assessment of the increase in size of the tumour was established by measuring the tumour size in the latest MR images and comparing it to that in the first MR images at diagnosis. The appearance of neurological symptoms such as paresis, seizures, and a drop of performance score below 50 (Karnofsky scale) are signs of disease progression (Kocher et al., 2008).

There were 53 events distributed as follows: glioblastoma multiforme ($n = 44$), anaplastic glioma ($n = 4$) and low grade glioma ($n = 5$). The remaining patients ($n = 70$) were registered as censored. The censored patients were those who were still alive or lost to follow-up. The age variable was used for survival analysis as a continuous variable.

To assess the predictive value of treatment in our cohort study, the patients were sub-grouped into three treatment-groups. Treatment grouping was based on a study which showed Temozolomide as an independent survival predictor associated with improved survival (Stupp et al., 2009). The three treatment groups were as follows: patients not having received any treatment; patients receiving either of or a combination of radiotherapy and Procarbazine, Chloro-ethyl-nitrosourea and Vincristine (PCV), and a third group comprising patients who receiving any of the above treatments plus

Temozolomide.

The relative tumour blood volume-derived MR perfusion ($rTBV_{max}$) was reconstructed into three categorical groups. The classifier was based on threshold values obtained with high accuracy (Chapter 4): the mild hyperaemic group ($rTBV_{max} \leq 7$), the moderate hyperaemic group ($rTBV_{max}$ 7.1-9.6), and the severe hyperaemic group ($rTBV_{max} > 9.6$).

Cytogenetic profiles grouped the patients into two groups: the first group being those with a histological diagnosis of astrocytoma, and the second group those having either or both oligodendroglioma and oligoastrocytoma cell line.

The Karnofsky performance status scale has been published elsewhere: (Crooks et al., 1991) describes numerically, in incremental order, the patient's ability to perform daily tasks. The score is on a point scale between 0 and 100 points with 10 point increments. However, in our analysis, the scale was re-arranged into five groups by combining two consecutive scale points and the 0 point scale (dead) was omitted as it used as the end point of the survival outcome (Table 6.1). For some analyses, the Karnofsky scale was sub-classified into two groups, wherein the value 50 was taken as the cut-off. This is because too few events makes it impossible to run a multivariate analysis on the extended Karnofsky scale.

6.2.6 Statistical analysis

SPSS (version 17.0) was used for the statistical analysis. Both The Kaplan–Meier survival curve and the Cox regression model of survival were used to

Score	Description
90–100	Patient is fully active, few symptoms of disease
70–90	Patient caring for himself, but not capable of normal activity or work
50–70	Patient can look after himself but not enough to work
30–50	Patient in bed or sitting in chair for more than half day, needing some help to look after himself
10–30	Patient in bed or chair all the time and needs a lot of looking after.

Table 6.1: Karnofsky scale for describing performance status.

assess the relative tumour blood volume, histological grading, age, gender, performance status, treatment, steroid intake, cytogenetic profile, and surgical resection as survival predictors. Both Mann–Whitney and Chi square tests were used to assess the significance level for continuous and categorical data, respectively. For illustration, the Kaplan–Meier curve presents the graphs of the WHO histological classification and the three-tier radiological classification for comparison. The Cox regression model was used to test each variable in a univariate analysis for the hazard ratio and level of significance. Significant variables were combined to check for independency in survival prediction. The number of variables in the Cox regression model was determined by the number of events (EPV) in the study (Concato et al., 1995). In a multiple regression, a small number of events may affect test accuracy and produce a misleading association between the tested variable and survival prediction. The log rank test was used, in which a p value less than 0.05 is indicative of statistical significance.

6.3 Results

6.3.1 Descriptive analysis

Descriptive statistics were obtained for variables such as age, gender, performance status, treatment, steroid intake, surgical procedure, and glioma phenotype, in addition to the maximum relative tumour blood volume ($rTBV_{max}$), to reveal the statistical significance of each variable in terms of confounding factors for survival time (Table 6.2).

Patients with cerebral glioma were treated differently according to the tumour grades and this was manifested clearly for the variables treatment, steroid intake, and surgical procedures, in addition to the tumour genetic profile. Therefore, when performing this statistical analysis to test for statistical significance, the patients were grouped based on these variables (Tables 6.3 and 6.4). The analysis was performed in two steps: step one includes univariate analysis for each variable to assess its significance; step two combines all statistically significant variables in a multivariate analysis.

6.3.2 Kaplan–Meier plot for overall survival and time to progression: A graphical comparison of the WHO histological classification and the three-tier radiological classification

The Kaplan–Meier survival analysis and log rank test were used to assess the effects of the WHO histological diagnosis and the three-tier radiological classification ($rTBV_{max}$) on overall survival and time to progression (Figures 6.1–6.4). MR perfusion imaging values were transformed into categorical

Variable	Total ($n = 123$)	Event (death)		p value
		Yes (%)	No (%)	
WHO histological grading	LGG (39)	9.4	48.6	< 0.001
	AG (24)	7.5	28.6	
	GBM (60)	83.0	22.9	
rTBV _{max} (3-Tier classification)	Mild hyperaemia (41)	7.5	52.9	<0.001
	Moderate (16)	9.4	15.7	
	Severe (66)	83.0	31.4	
Age (continuous)	Mean(dead) 59.6 ± 11.7 Mean (alive) 45.1 ± 15.4	53	70	<0.001
Age (categorical)	≤ 52 yrs (61)	24.5	68.6	<0.001
	> 52 yrs (62)	75.5	31.4	
Gender	Male (70)	64.2	52.9	0.142
	Female (53)	35.8	47.1	
Performance status	90–100 (28)	15.1	28.6	0.026
	70–90 (68)	50.9	60.0	
	50–70 (20)	24.5	8.6	
	30–50 (5)	5.7	2.9	
	10–30 (2)	3.8	0.0	
Treatment	No treatment (39)	18.9	40.0	0.032
	Partial treatment (42)	39.6	34.3	
	Full treatment (42)	41.5	25.7	
Steroid intake	No steroid (34)	13.2	40.0	0.001
	Steroid intake (89)	86.8	60.0	
Surgical procedure	Biopsy (56)	52.8	40.0	0.109
	Debulking (67)	47.2	60.0	
Phenotype	Astrocytoma (105)	98.1	75.7	<0.001
	Oligoastro cell type (18)	1.9	24.3	

Table 6.2: Mann–Whitney and Chi square tests were used for all glioma grades to test the statistical significance of continuous and categorical variables, respectively. The distribution in percentages is illustrated within each variable. The tests evaluate the relative frequencies of occurrence of the observed events and a p value < 0.05 indicates significant difference between groups of each variable.

Variable	Total ($n = 84$)	Event (death)		p value
		Yes (%)	No (%)	
WHO histological grading	AG (24)	8.3	55.6	< 0.001
	GBM (60)	91.7	44.4	
rTBV _{max} (3-tier classification)	Moderate hyperaemia (17)	4.2	41.7	<0.001
	Severe hyperaemia (67)	95.8	58.3	
Age (continuous)	Mean (dead) 59.6 ± 12 Mean (alive) 48 ± 15.9	48	36	0.001
Age (categorical)	≤ 52 yrs (31)	22.9	55.6	0.002
	> 52 yrs (53)	77.1	44.4	
Gender	Male (51)	64.6	55.6	0.270
	Female (33)	35.4	44.4	
Performance status	90–100 (14)	14.6	19.4	0.386
	70–90 (44)	47.9	61.1	
	50–70 (19)	27.1	13.9	
	30–50 (5)	6.3	5.6	
	10–30 (2)	4.2	0.0	
Treatment	No treatment (16)	14.6	22.2	0.664
	Partial treatment (29)	39.6	36.1	
	Full treatment (39)	45.8	41.7	
Steroid intake	No steroid (11)	10.4	19.4	0.196
	Steroid intake (73)	89.6	80.6	
Surgical procedure	Biopsy (38)	50.0	38.9	0.215
	Debulking (46)	50.0	61.1	
Phenotype	Astrocytoma (77)	100.0	80.6	0.002
	Oligoastro cell type (18)	0.0	19.4	

Table 6.3: Mann–Whitney and Chi square tests illustrating the significance of the variables for high grade glioma. A p value was considered significant if it is < 0.05 .

Variable	Total ($n = 60$)	Event (death)		p value
		Yes (%)	No (%)	
rTBV _{max} (50 th percentile)	1 st (30)	43.2	68.8	0.072
	2 nd (30)	56.8	31.3	
Age (continuous)	Mean (dead) 59.7 ± 12 Mean (alive) 51.8 ± 15.8	44	16	0.082
Age (categorical)	≤ 52 yrs (18)	22.7	50.0	0.045
	> 52 yrs (42)	77.3	50.0	
Gender	Male (34)	63.6	37.5	0.066
	Female (26)	36.4	62.5	
Performance status	90–100 (10)	15.9	18.8	0.854
	70–90 (24)	43.2	37.5	
	50–70 (19)	29.58	31.3	
	30–50 (5)	6.8	12.5	
	10–30 (2)	4.5	0.0	
Treatment	No treatment (8)	15.9	0.0	0.036
	Partial treatment (18)	38.6	18.8	
	Full treatment (34)	45.5	81.3	
Steroid intake	No steroid (5)	11.4	6.20	0.488
	Steroid intake (55)	88.6	93.8	
Surgical procedure	Biopsy (24)	47.7	18.8	0.039
	Debulking (36)	52.3	81.3	

Table 6.4: Mann–Whitney and Chi square tests were performed for continuous and categorical data, respectively, on patients with glioblastoma multiforme (grade IV). The patient distribution and percentage of patients with and without events is given for each variable.

data (three-tier radiological classification) as mentioned earlier based on the threshold values of the highest accuracy. The starting point for determining the overall survival was taking from the date of the first MR scan at time of diagnosis to the date of the last visit or the date of death. The time to progression was defined from the time point of the MR scan at diagnosis to the appearance of radiological and/or clinical criteria based on the Macdonald criteria (Macdonald et al., 1990). The graphical presentation of the Kaplan–Meier survival curve aims at determining whether the WHO histological grading and $rTBV_{max}$ were able to correctly classify patients with cerebral glioma based on their overall survival and time to progression.

Both overall survival and time to progression are survival parameters which are very close for low grade glioma and anaplastic glioma when applying the WHO histological grading. On the other hand, our $rTBV_{max}$ using the three-tier radiological classification showed that patients with mild hyperaemia have a long period of survival and time to progression compared to patients with moderate hyperaemia, while patients with severe hyperaemia have the shortest cumulative survival time among all groups.

The second stage was to assess $rTBV_{max}$ in predicting both overall survival and time to progression in patients with glioblastoma multiforme. A median $rTBV_{max}$ value (14.0) within GBM patients was chosen and used as the cut-off value to create two groups. The Kaplan–Meier survival curve did not show any significant difference between the two groups (Figures 6.5 and 6.6). Despite the fact that $rTBV_{max}$ had statistical significance in predicting survival for all glioma grades, it failed to show any difference within glioblastoma multiforme. This may be attributed to the difference in age,

performance status, treatment, and surgical resection among the GBM patients. Therefore, a Cox regression model was run to assess the influence of these factors on both survival and time to progression in all glioma grades and within each glioma grade.

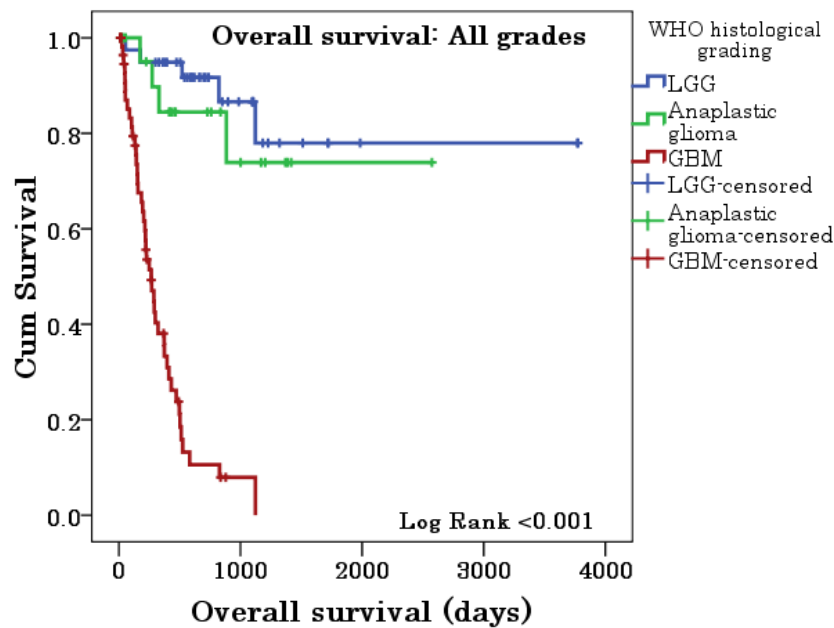


Figure 6.1: Kaplan–Meier survival curve according to WHO grade in cerebral gliomas. The curves of both low grade glioma and anaplastic glioma were close to each other, indicating failure of the WHO histological diagnosis in separating the two glioma grades.

6.3.3 Assessment of the effect of co-variables on survival and time to progression performed for all glioma grades: Univariate and multivariate analyses

For assessing the prognostic power of different variables, the Cox proportional hazard model was used to assess the influence of certain factors assumed to affect glioma patients survival and time to progression. One hundred and

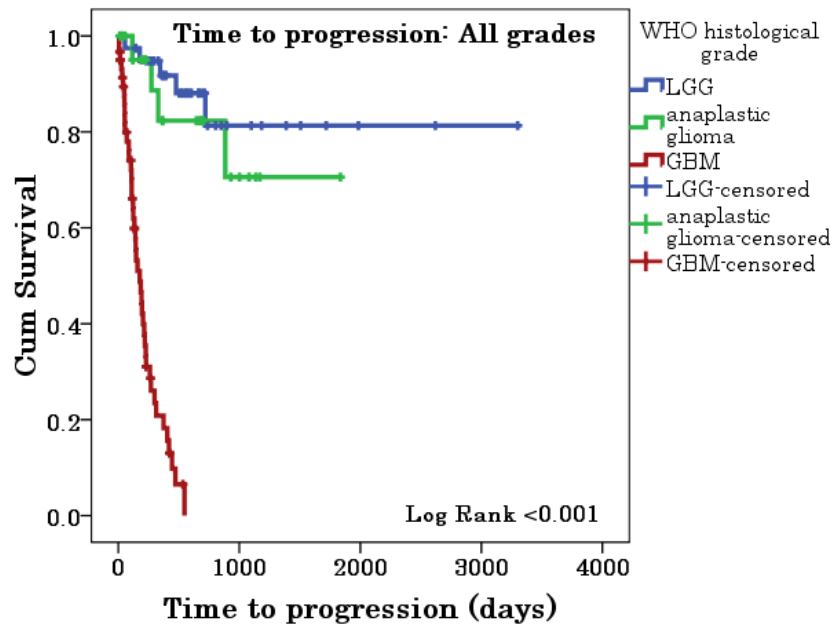


Figure 6.2: Kaplan–Meier curve of time to progression of all glioma grades based on WHO histological diagnosis.

twenty-three patients with different glioma grades [39 LGG, 24 AG and 60 GBM] were subjected to survival analysis.

The first step was to assess these factors separately in univariate analyses to determine their influence on glioma patient survival and time to progression. Age, $rTBV_{max}$, WHO histological grade, treatment, performance status, and steroid intake were recognised co-variables showing statistical significance in predicting overall survival (Table 6.5). $rTBV_{max}$ was much better in predicting the survival in the intermediate groups of glioma patients (moderate hyperaemia) than was the WHO histological grading. This was shown earlier in Figure 6.1, where both the graphs of low grade glioma and of anaplastic glioma were inseparable. Patients with performance status <70 had shorter survival times compared to those with good performance

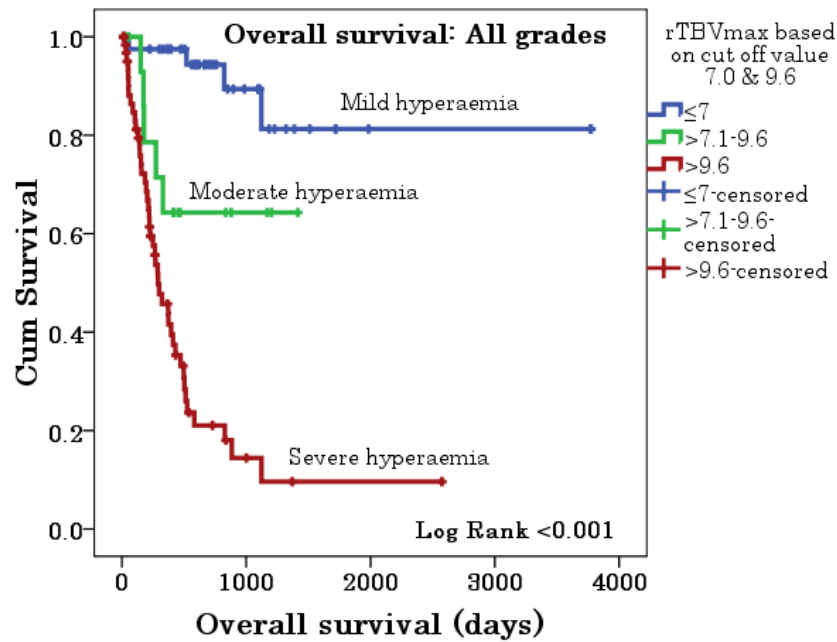


Figure 6.3: Kaplan–Meier survival curve illustrating the overall survival based on the three-tier radiological classification obtained at the point of high accuracy in differentiating glioma grades.

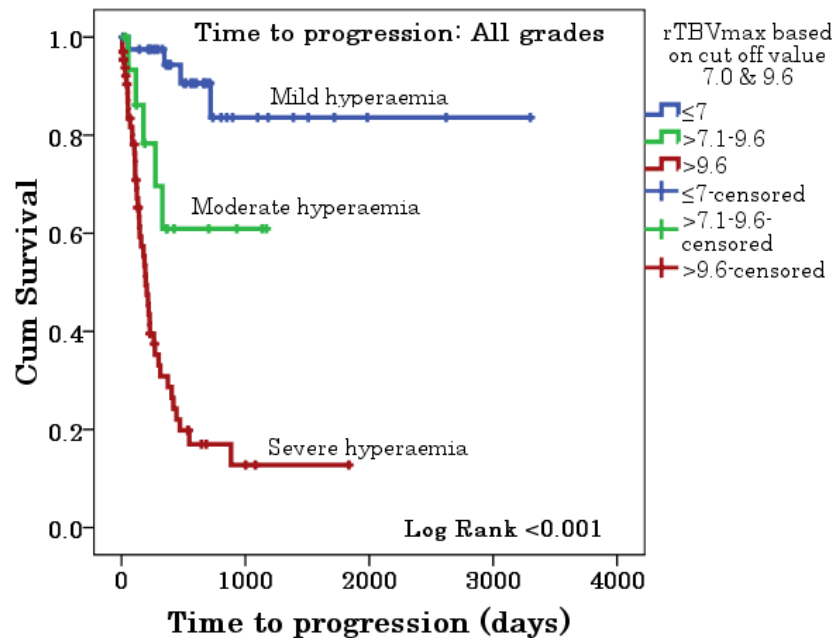


Figure 6.4: Kaplan–Meier curve illustrating time to progression based on $rTBV_{max}$, which shows better separation between glioma grades.

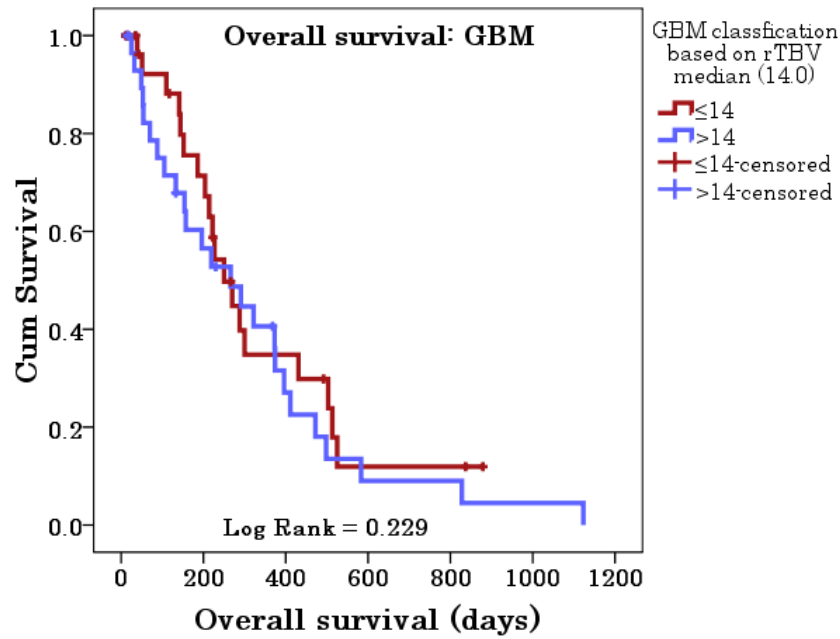


Figure 6.5: Kaplan–Meier survival curve illustrating survival within the two groups of GBM patients. Log rank was also not significant.

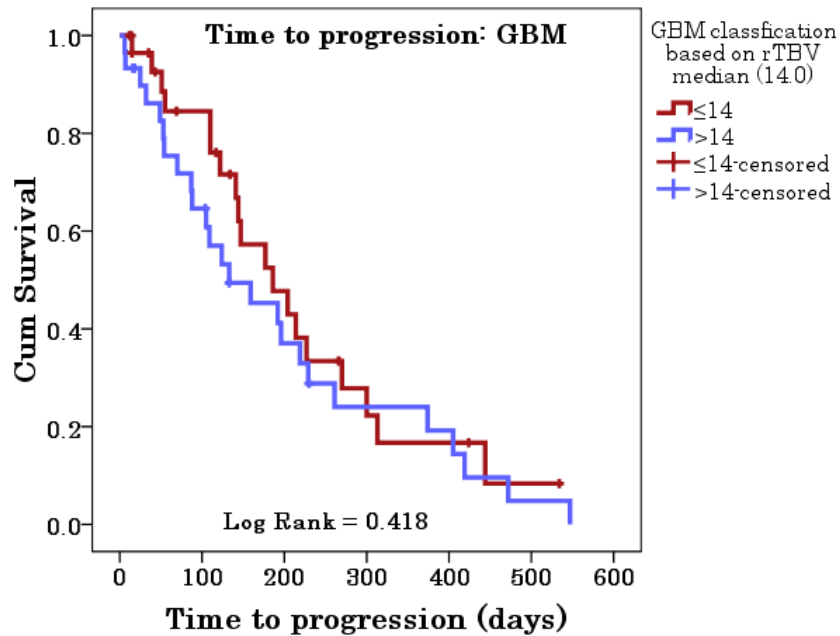


Figure 6.6: Kaplan–Meier curve of GBM patients illustrating time to progression based on $rTBV_{max}$ -derived MR perfusion. The difference among two groups GBM was non-significant (0.418).

status. In the same table, variables such as gender, surgical resection, and genetic phenotype showed no statistical significance. The multivariate analysis of the significant variables, Tables 6.6 and 6.7, demonstrated that $rTBV_{max}$, the WHO histological grading, and age were independent predictors of survival. However, the histological grading failed to predict survival in grade 3 patients. Referring to the three-tier radiological classification, patients with moderate and severe hyperaemia were at higher risk (short survival) than those with mild hyperaemia. Treatment, performance status and steroid intake were not significant for predicting survival.

The same variables were also assessed for their effect on predicting tumour progression. Age, $rTBV_{max}$, WHO histological grading, performance status, and steroid intake were predictors of tumour progression, see Table 6.8. Factors such as gender, treatment, genetic phenotype, and surgical resection were not predictors of progression. The combined effect of the significant variables showed that age, $rTBV_{max}$, WHO histological grading, and performance status were the only independent predictors of tumour progression (Tables 6.9 and 6.10). $rTBV_{max}$ was able to predict progression in glioma patients with moderate hyperaemia but the WHO histological grading failed to do the same for the equivalent group of anaplastic glioma (grade 3) patients. Steroids failed to demonstrate any significance in predicting tumour progression.

Co-variate	HR	95% CI	<i>p</i> value
Age	1.07	1.04–1.09	<0.001
Gender (Male)	1.44	0.82–2.53	0.203
<i>r</i> TBV _{max}			
Moderate hyperaemia	4.74	1.27–17.68	0.021
Severe hyperaemia	15.76	5.61–44.29	< 0.001
WHO histological grading			
Grade 3	1.66	0.44–6.18	0.453
Grade 4	17.94	6.90–46.59	<0.001
No treatment	2.50	1.08–5.78	0.032
Partial treatment	1.96	1.04–3.68	0.036
Performance status			
70–90	1.48	0.67–3.26	0.330
50–70	4.50	1.86–10.89	0.001
30–50	11.47	2.90–45.33	0.001
10–30	21.88	4.34–110.30	<0.001
Surgery (Biopsy)	1.25	0.73–2.14	0.419
No steroid intake	0.281	0.13–0.63	0.002
Phenotype			
Astrocytic tumour	4.57	0.58–36.18	0.151

Table 6.5: Cox regression model (univariate analysis) assessing the influence of each co-variable on predicting survival for patients with cerebral glioma grades

Co-variate	HR	95% CI	<i>p</i> value
Age	1.07	1.04–1.10	<0.001
rTBV _{max}			
Moderate hyperaemia	4.49	1.14–17.77	0.023
Severe hyperaemia	12.88	4.05–40.97	<0.001
No treatment	1.14	0.46–2.85	0.776
Partial treatment	1.03	0.54–1.98	0.923
Performance status			
70–90	1.21	0.50–2.93	0.674
50–70	1.34	0.52–3.45	0.540
30–50	3.28	0.80–13.44	0.099
10–30	6.77	0.96–47.88	0.055
No steroid intake	0.83	0.30–2.32	0.728

Table 6.6: Cox regression model (multivariate analysis) for the effect of co-variables including radiological classification on predicting survival for patients with all glioma grades

Co-variate	HR	95% CI	<i>p</i> value
Age	1.06	1.03–1.09	<0.001
WHO histological grading			
Grade 3	1.47	0.37–5.88	0.588
Grade 4	25.55	7.50–87.07	<0.001
No treatment	3.03	1.08–8.50	0.03
Partial treatment	1.51	0.78–2.93	0.223
Performance status			
70–90	1.22	0.52–2.86	0.643
50–70	0.92	0.35–2.41	0.866
30–50	2.70	0.66–11.04	0.168
10–30	2.96	0.41–21.44	0.283
No steroid intake	0.73	0.25–2.15	0.570

Table 6.7: Cox regression model (multivariate analysis) for the effect of co-variables including the WHO histological diagnosis on predicting survival for patients with all glioma grades

Co-variate	HR	95% CI	<i>p</i> value
Age	1.07	1.04–1.09	<0.001
Gender (Male)	1.47	0.84–2.58	0.181
rTBV _{max}			
Moderate hyperaemia	4.70	1.26–17.54	0.021
Severe hyperaemia	15.33	5.47–42.99	< 0.001
WHO histological grading			
Grade 3	1.58	0.42–5.92	0.495
Grade 4	23.38	8.50–64.33	<0.001
No treatment	1.73	0.72–4.15	0.223
Partial treatment	1.53	0.83–2.85	0.175
Performance status			
70–90	1.37	0.62–3.03	0.430
50–70	4.02	1.65–9.75	0.002
30–50	9.55	2.40–37.96	0.001
10–30	99.64	115.83– 627.02	<0.001
Surgery (Biopsy)	1.22	0.71–2.10	0.466
No steroid intake	0.27	0.12–0.61	0.001
Phenotype			
Astrocytic tumour	4.93	0.63–38.64	0.129

Table 6.8: Cox regression model (univariate analysis) for the influence of co-variables on predicting tumour progression of all glioma grades

Co-variate	HR	95% CI	<i>p</i> value
Age	1.06	1.04–1.09	<0.001
rTBV _{max}			
Moderate hyperaemia	4.69	1.22–17.96	0.024
Severe hyperaemia	13.86	4.46–43.11	<0.001
Low performance status	3.41	1.25–9.27	0.016
No steroid intake	1.23	0.50–3.00	0.650

Table 6.9: Cox regression model (multivariate analysis) for the combined effect of co-variables including radiological diagnosis on predicting time to progression of all cerebral glioma grades. Low performance status includes patients with Karnofsky scores <50.

Co-variate	HR	95% CI	<i>p</i> value
Age	1.05	1.03–1.08	<0.001
WHO histological grading			
Grade 3	1.88	0.48–7.41	0.367
Grade 4	21.16	6.48–69.09	<0.001
Low performance status	3.11	1.15–8.44	0.026
No steroid intake	1.23	0.50–3.00	0.650

Table 6.10: Cox regression model (multivariate analysis) for the combined effect of co-variables including histological diagnosis on predicting time to progression of all cerebral glioma grades. Low performance status includes patients with Karnofsky scores <50.

6.3.4 Assessment of the influence of certain co-variables on survival and time to progression performed within high grade glioma: Univariate and multivariate analysis

The Cox regression model was applied to patients with high grade glioma (grades 3 and 4) to assess the influence of certain factors on survival and time to progression. Age, $rTBV_{max}$, histological grading system, treatment and performance status were recognized factors in predicting survival for high grade glioma (Table 6.11). MR perfusion found patients with a $rTBV_{max}$ value above 9.6 have a higher risk and shorter survival compared to those with a value below 9.6. This threshold value was based on the highest accuracy value in differentiating between glioblastoma multiforme (grade 4) and anaplastic glioma (grade 3) mentioned earlier in Chapter 4. Multivariate analysis (Tables 6.12 and 6.13) showed that $rTBV_{max}$, histological grading system, and age are independent predictors of survival of GBM. Treatment and performance status were inconsistent as they had a varying significance

level for survival prediction. The influence of the same variables on predicting tumour progression was also assessed wherein factors of $rTBV_{max}$, histological grading, age and performance status were significant predictors (Table 6.14). $rTBV_{max}$ as MR perfusion parameter was able to significantly showed short period to tumour progression in patients with $rTBV_{max} >9.6$ compared to those below 9.6. Only high grade glioma patients with performance status <50 showed short period to tumour progression compared to those with high performance status. Although the combined effect of those three variables were independent predictors of tumour progression within high grade glioma, only patients with low performance status below (<50 ; Karnofsky scoring) showed short period of tumour progression (Tables 6.15 and 6.16).

Co-variate	HR	95% CI	<i>p</i> value
Age	1.07	1.04–1.10	<0.001
Gender (Male)	1.11	0.62–2.01	0.723
$rTBV_{max} (>9.6)$	10.00	2.42–41.45	0.001
WHO histological grading Grade 4	10.65	3.69–30.80	<0.001
Surgical resection Biopsy	1.10	0.62–1.93	0.757
No treatment	2.48	1.02–6.05	0.045
partial treatment	1.90	1.00–3.63	0.050
Performance status			
70–90	1.20	0.51–2.79	0.681
50–70	2.42	0.96–6.06	0.060
30–50	6.08	1.50–24.68	0.011
10–30	11.47	2.22–59.18	0.004
No steroid intake	0.854	0.34–2.16	0.739

Table 6.11: Cox regression model (univariate analysis) for high grade glioma was performed to assess the effect of variables on survival prediction.

Co-variate	HR	95% CI	<i>p</i> value
Age	1.06	1.03–1.10	<0.001
rTBV _{max} (>9.6)	8.67	2.02–37.26	0.004
No treatment	1.15	0.46–2.89	0.766
partial treatment	1.13	0.60–2.15	0.701
Low performance status	3.42	1.24–9.43	0.018

Table 6.12: Cox regression model (multivariate analysis) was performed to assess the influence of combined variables including radiological classification in predicting survival among high grade glioma.

Co-variate	HR	95% CI	<i>p</i> value
Age	1.06	1.03–1.09	<0.001
WHO histological grading Grade 4	14.60	4.21–50.62	<0.001
No treatment	2.89	1.04–7.98	0.041
partial treatment	1.48	0.76–2.87	0.246
Low performance status	2.49	0.86–7.21	0.092

Table 6.13: Cox regression model (multivariate analysis) was performed to assess the influence of combined variables including histological diagnosis in predicting survival among high grade glioma.

Co-variate	HR	95% CI	<i>p</i> value
Age	1.06	1.04–1.09	<0.001
Gender (Male)	1.23	0.68–2.23	0.491
rTBV _{max} (>9.6)			
Severe hyperaemia	9.17	2.22–37.85	0.002
WHO histological grading			
Grade 4	14.88	4.43–49.94	<0.001
Surgical resection			
Biopsy	1.04	0.59–1.84	0.888
No treatment	1.77	0.69–4.52	0.235
partial treatment	1.47	0.78–2.77	0.230
Performance status			
70–90	1.02	0.44–2.37	0.970
50–70	1.99	0.79–5.02	0.147
30–50	4.56	1.12–18.51	0.034
10–30	47.22	7.41–301.00	<0.001
No steroid intake	0.95	0.37–2.41	0.914

Table 6.14: Cox regression model (univariate analysis) for the influence of co-variables on time to progression for patients with high grade glioma

Co-variate	HR	95% CI	<i>p</i> value
Age	1.06	1.03–1.08	<0.001
rTBV _{max} (>9.6)			
Severe hyperaemia	6.76	1.61–28.30	0.009
Low performance status	3.40	1.25–9.25	0.017

Table 6.15: Cox regression model (multivariate analysis) was performed to assess the influence of combined co-variables including radiological classification in predicting tumour progression in patients with high grade glioma.

Co-variate	HR	95% CI	<i>p</i> value
Age	1.05	1.02–1.07	0.001
WHO histological grading Grade 4	11.02	3.09–39.22	<0.001
Low performance status	3.14	1.16–8.55	0.025

Table 6.16: Cox regression model (multivariate analysis) was performed to assess the influence of combined co-variables including histological diagnosis in predicting tumour progression in patients with high grade glioma.

6.3.5 Assessment of the influence of variables on predicting survival and time to progression in glioblastoma multiforme: Univariate and multivariate analysis

Further univariate and multivariate analyses were performed only for glioblastoma multiforme patients, to investigate the prognostic value of $rTBV_{max}$ in addition to other co-variables in survival and tumour progression. Age, treatment and performance status were significant variables in predicting patients' survival (Table 6.17). Patients who had not received treatment had a survival shortened by 70% compared to patients receiving full treatment including Temozolomide. Patients with performance status < 30 demonstrated shortened survival times by 85% compared to patients with high performance status. Both steroid intake and $rTBV_{max}$ did not show any significance in predicting survival for glioblastoma multiforme. Only the variables that showed statistical significance were incorporated in the multivariate analysis (Table 6.18). Age and treatment were independent predictors of overall survival in glioblastoma multiforme patients.

Time to progression was assessed for patients with glioblastoma multiforme to define the co-variables that may influence their survival. Table 6.19

displays the univariate analysis of performance status, steroid and age, as influencing tumour progression. Patients with performance status < 30 were at a higher risk with a shorter period for tumour progression compared to those with higher performance status. Patients who did not receive steroids had their time to progression decreased by 70%. $rTBV_{max}$, using their median value, in addition to gender, treatment and surgical resection, did not predict tumour progression in glioblastoma patients. Further assessment of the combined effect of co-variables using multivariate analysis (Table 6.20) revealed that performance status, steroid and age were independent factors in tumour progression.

Sixteen patients with GBM survived longer than one year; 6/16 patients were younger than 52 years, 10/16 patients presented initially with high ($=80$) Karnofsky score; 11/16 patients received complete treatment, and 8/16 patients were subjected to surgical debulking. One patient with an overall survival of about 3 years was diagnosed with brain stem glioma at the age of 34 years.

Co-variate	HR	95% CI	<i>p</i> value
Age	1.06	1.03–1.09	<0.001
Gender (Male)	1.38	0.73–2.58	0.320
rTBV _{max} (>14)	1.26	0.69–2.31	0.454
No treatment	3.48	1.45–8.38	0.005
Partial treatment	2.09	1.07–4.08	0.031
Performance status			
70–90	1.27	0.53–3.04	0.585
50–70	1.15	0.45–2.93	0.775
30–50	3.51	0.87–14.18	0.078
10–30	6.55	1.28–33.60	0.024
No steroid intake	1.43	0.56–3.68	0.457

Table 6.17: Cox regression model (univariate analysis) for the influence of co-variables on survival in glioblastoma patients

Co-variate	HR	95% CI	<i>p</i> value
Age	1.06	1.03–1.10	<0.001
No treatment	5.37	1.92–15.02	0.001
Partial treatment	1.62	0.80–3.29	0.180
Low performance status	1.95	0.65–5.91	0.236

Table 6.18: Cox regression model (multivariate analysis) for the influence of co-variables on survival in glioblastoma multiforme patients

Co-variate	HR	95% CI	<i>p</i> value
Age	1.04	1.02–1.07	0.002
Gender (Male)	1.62	0.87–3.03	0.130
rTBV _{max} >14	1.28	0.70–2.33	0.431
No treatment	2.39	0.93–6.10	0.070
Partial treatment	1.62	0.84–3.12	0.148
Performance status			
70–90	0.68	0.28–1.68	0.409
50–70	0.67	0.26–1.75	0.415
30–50	1.89	0.48–7.48	0.366
10–30	19.71	3.16–122.83	0.001
Surgery (Biopsy)	0.84	0.46–1.53	0.565
No steroid intake	3.10	1.18–8.14	0.022

Table 6.19: Cox regression model (univariate analysis) of GBM patients for the influence of co-variables on tumour progression

Co-variate	HR	95% CI	<i>p</i> value
Age	1.04	1.01–1.07	0.006
Low performance status	3.54	1.28–9.80	0.015
No steroid intake	3.10	1.17–8.21	0.023

Table 6.20: Cox regression model (multivariate analysis) for the influence of combined effect of co-variables on tumour progression

6.4 Discussion

Perfusion MR imaging is increasingly being used as a complementary tool to histological findings in diagnosing cerebral glioma. The relative TBV_{max} derived from MR perfusion has high accuracy in differentiating cerebral glioma in adults as shown in chapter 4. This study showed an extended gain of $rTBV_{max}$ in predicting overall survival and tumour progression for all glioma grades, high grade glioma, and glioblastoma multiforme in specific. There was the intention of particularly looking for the survival of GBM patients due to the potential clinical concern stemming from the poor outcome and shorter survival time of this grade.

In this study we used the Kaplan–Meier curve to compare the potential prognostic value of the histological WHO grade and the MR perfusion derived hyperaemia grade for overall and time to progression in patients with cerebral glioma. It was shown that both overall survival and time to progression survival curves were well separated for low hyperaemia, moderate and severe hyperaemia based on the three-tier radiological classification. In contrast, the WHO histological grading failed to make a clear distinction between diffuse glioma and anaplastic glioma. This is the first study to compare graphically overall survival and time to progression within groups of patients with different glioma grades. Most previous studies have included one or two cerebral glioma grades and one study (Hirai et al., 2008) compared grades III and IV based on MR perfusion parameters. They reported $rTBV_{max}$ and histological diagnosis as independent 2-year survival predictors. Only three studies (Blankenberg et al., 1995; Law et al., 2008; Bisdas et al., 2009)

included three grades of cerebral glioma in which either overall survival or time to progression were studied. Among those three studies, one study (Law et al., 2008) compared time to progression between low grade gliomas and glioblastoma multiforme or high grade glioma. The other two studies recruited only a small population size of cerebral glioma and did not assess $rTBV_{max}$ (Blankenberg et al., 1995) or did not adjust for other variables (Bisdas et al., 2009).

The Kaplan–Meier survival function was used to assess the prognostic value of $rTBV_{max}$ within patients with glioblastoma multiforme. The median value of $rTBV_{max}$ was not useful as a cut-off in predicting survival and time to progression. A few studies have assessed the prognostic value of influential factors within glioblastoma multiforme such as age (Nwokedi et al., 2002; Chang and Barker 2nd, 2005; Mineo et al., 2007), tumour resection (Hung and Howng, 2003; Stark et al., 2007; Flynn et al., 2008; Ma et al., 2009), performance status (Hung and Howng, 2003; Gorlia et al., 2008; Ma et al., 2009), and treatment with Temozolomide (Mineo et al., 2007; Gorlia et al., 2008; Ma et al., 2009), which have been reported to be predictors of survival. Only one study (Oh et al., 2004), with a small sample size of GBM, assessed $rCBV_{max}$ in predicting survival and showed no significance in using a $rCBV_{max}$ threshold value of 1.3. Our study is in line with what has been reported, that $rTBV_{max}$ was not predictive within glioblastoma multiforme patients.

In this study, $rTBV_{max}$ was assessed in combination with other factors. The initial results using both the three-tier radiological and the WHO histological classification showed that a large percentage (83%) of events were

detected in patients of severe hyperaemia (high $rTBV_{max}$) and GBM. A large percentage (75%) of events were also detected among patients who are more than 52 years old. The effect of other factors such as performance status, steroid treatment, and genetic phenotype, initially appeared significant in some groups. In fact these factors were presented in a large percentage of live and dead patients. This is as a result of the fact that a large number of recruited patients were unevenly distributed within the variables' subgroups.

When assessing the prognostic factors in predicting survival and time to progression for all glioma grades, it was found that $rTBV_{max}$ and age were independent predictors of survival and tumour progression. Histological grade and treatment were independent predictors for overall survival but not for time to progression, while performance status was an independent predictor of tumour progression. Interestingly, steroid intake was shown to be associated with a decrease in survival time, which is attributed to the fact that steroids are mostly prescribed to high grade glioma patients. Our finding that the maximum $rTBV$ predicts survival in all glioma grades is in line with previous studies (Law et al., 2008; Bisdas et al., 2009). The exception to that is Bisdas (2009) who reported a $rCBV_{max}$ threshold value of 4.2 in predicting tumour progression. Relative TBV_{max} demonstrated independence in predicting survival which is in line with other imaging modalities such as single photon emission computed tomography (SPECT). The SPECT, using the amino acid analog [iodo-L-a-methyltyrosine], is an independent survival predictor when adjusted for age and histological grading (Weber et al., 2001). The authors only assessed the prognostic value of SPECT among the two main glioma grades (high versus low grade).

Again assessing the prognostic value of co-variate was performed within high grade glioma patients which revealed that $rTBV_{max}$, performance status, and age were predictors of survival and tumour progression. Interestingly, patients with severe hyperaemia (high $rTBV_{max}$) who had a performance status <30 demonstrated a shorter survival by about 11-fold, compared to those with moderate hyperaemia. This study for the subgroups of patients with high grade glioma was comparable to a previously reported study (Hirai et al., 2008) using a lower threshold value (2.3) of $rTBV_{max}$. $rTBV_{max}$, age, and performance status as survival predictors were found comparable to our study in predicting survival; however, that study did not elicit any significance in gender and surgical resection.

Further assessment was performed only for GBM patients to determine variables which might contribute to survival and tumour progression. Our findings showed that relative TBV_{max} failed to predict survival in GBM patients, which is in line with a previous study (Crawford et al., 2009) but is discrepant with others who found a significant association (Saraswathy et al., 2009; Mangla et al., 2010). However, Mangla et al. (2010) assessed the changes in cerebral blood volume after treatment with Temozolomide and radiotherapy and Saraswathy et al. (2009) reported that a 3-fold increase in CBV compared to white matter was associated with poor outcomes. Age was an independent predictor of survival and tumour progression in GBM patients, which is in line with several studies (Barker et al., 1996; Carson et al., 2007; Hung and Howng, 2003; Ma et al., 2009; Mineo et al., 2007) but disagrees with a few studies (Shinoda et al., 2001; Mangla et al., 2010). GBM patients who had not received treatment are at higher risk (hazard ratio=

6) with their survival shortened by 6-fold compared to those who received treatment including Temozolomide, whereas those who have received either or both chemotherapy and radiotherapy showed a trend towards significance. The findings in this study were in agreement with a previous study (Mineo et al., 2007). Others have found a significant association between conventional treatment and survival (Barker et al., 1996; Allahdini et al., 2010; Carson et al., 2007; Ma et al., 2009; Stark et al., 2007). We did not find any association between gender, steroid intake, and surgical resection, which in part is in agreement with previous studies (Barker et al., 1996; Carson et al., 2007; Chang and Barker 2nd, 2005), whereas others have found surgical resection significantly associated with improved survival (Ma et al., 2009; Mineo et al., 2007; Mangla et al., 2010). Age and performance status were independent predictors for tumour progression in the current study, which is in agreement with other studies (Li et al., 2009; Levin et al., 2000) albeit steroid intake was not assessed previously to the best of our knowledge. On the other hand, treatment, surgical resection, and gender did not demonstrate any significant association with tumour progression, which is partially in line with previous studies (Levin et al., 2000; Young et al., 2011).

Advanced MRI techniques and parameters have been assessed in survival prediction by a few studies. K^{trans} , vascular permeability factor, was assessed in recurrent glioblastoma multiforme patients who received anti-vascular endothelial growth factor (Sorensen et al., 2009). The reduction in K^{trans} was significantly associated with prolonged survival and progression free survival but other demographic and clinical factors were not considered in the analysis. Moreover, the apparent diffusion coefficient (ADC) as a diffusion MRI

bio-marker has been reported by several studies to be an independent survival predictor (Murakami et al., 2007; Yamasaki et al., 2010; Saksena et al., 2010). ADC predicts tumour progression in recurrent glioblastoma patients treated with anti-angiogenic therapy (Pope et al., 2009).

The methylated status of GBM is predictive of better outcomes in response to Temozolomide treatment (Hegi et al., 2004; Carrillo et al., 2012). The radiological features of the glioblastomas were under investigation by others to assess their predictive value. Ring enhancement of the tumour was associated with unmethylated MGMT status, indicating less sensitivity of the tumour to chemotherapy (Drabycz et al., 2010). Furthermore, methylated GBM without oedema had a longer survival than unmethylated or methylated tumours with oedema (Carrillo et al., 2012). Isocitrate dehydrogenase (IDH1) mutation in glioblastoma is reported as a survival predictor and is associated with longer survival (Dubbink et al., 2009; Carrillo et al., 2012). Interestingly, imaging features such as non-contrast enhanced are highly correlated with IDH1 mutation. The diffusion parameter, ADC ratios, and WHO histological grade were significantly higher in MGMT methylation versus unmethylated group of high grade gliomas (Moon et al., 2011).

The main limitation of this study was the different treatment regime applied to patients with the same glioma grades, which may reflect survival prediction. It is not known whether patients with a short survival time are so because of not receiving treatment or due to the effect of other influential factors such as low performance status or clinical deterioration. The second limitation was the small sample size and small number of events which did not permit assessing confidently more factors at one time. The third limitation

was that about half of the potential participants ($n = 56$) were histologically diagnosed based on surgical biopsy. The chance of sampling error and under-grading may arise when picking tissue of less malignant tumours in those with high grade glioma. The fourth limitation is that one parameter of MR perfusion was assessed and other functional imaging parameters such as cerebral blood flow and vascular permeability were not considered in the survival analysis.

6.5 Conclusion

The current method of predicting survival and tumour progression is based on the histological WHO grading system; however, it is limited by sampling error and under-grading. We implemented a Three-tier radiological classification derived from MR perfusion to predict survival in patients with cerebral glioma. The radiological classification was able to identify patients with intermediate hyperaemia as clearly separable from those with mild and severe hyperaemia. A Cox regression for survival and tumour progression demonstrated that radiological classification is an independent predictor of glioma patients with intermediate and severe hyperaemia. It would be of interest in the future to assess the baseline $rTBV_{max}$ value and the changes after treatment to monitor tumour response or progression in patients with cerebral glioma.

Chapter 7

Assessing the Technical and Biological Factors that may Affect TBV Measurements

7.1 Introduction

It is known that microvascular proliferation, along with an increase in mitotic activity and nuclear atypia, is one of the histological markers of tumour aggressiveness adopted in the WHO histological grading for cerebral gliomas (Scheithauer, 2008). An increase in cerebral blood volume can be measured non-invasively with MR perfusion techniques. A systematic review of the literature, with pooled data, (Chapter 2) found cerebral blood volume-derived T_2^* MR perfusion possessing a high sensitivity (95.6%) but a low specificity (75.5%) in differentiating high from low grade gliomas. But in the present study, we achieved a comparable sensitivity (95%) and a higher specificity (95%) than previously published in differentiating between high and low grade gliomas. Tumour heterogeneity produces variations in CBV values, most likely in high grade glioma, wherein the signal intensity may range from 3 to 7 above the baseline images (Provenzale et al., 2006). Another probable cause of this variation in signal intensity may be the biological effect in which differences may occur between individuals of the same glioma grade subjected to the same technical settings (Roberts et al., 2000).

In addition, technical factors such as dose and concentration of the contrast agent, rate of injection, type of contrast, pre-loading contrast dose, echo time, and flip angle, may affect the changes in MR signal and lead to variation within the same grade (Tofts, 2003). The biological factors which may contribute to CBV variation are age, phenotypes, and steroid intake at time of MRI scanning; the effects of these will be assessed in this chapter. There was little technical variation in this retrospective dataset subjected to stan-

standardized MR scanning clinical protocol. For example, one protocol variation consisted of giving a pre-loading dose of contrast to a subset of the patients, while other scanning protocols were applied equally to potential participants in this study. A literature review showed that steroids lead to a decrease in blood–brain barrier and decreased tumour perfusion (Kotsarini et al., 2010); however, it is not clear whether the administration of steroids may specifically change the blood volume. Accordingly, steroid intake and other factors such as a pre-load contrast dose and phenotype will be assessed for their influence on cerebral blood volume changes. The aim is to identify certain technical and biological factors that may affect CBV measurements. The hypothesis is based on the knowledge that a pre-loading dose and steroids lower CBV, while glioma with an oligodendroglial cell line has an elevated CBV.

7.2 Methods

7.2.1 Patient criteria and clinical data

The patient criteria and data are described in Appendix F and Chapter 3. The demographic and clinical data for the two subgroups are given in Table 7.1. Two groups were created to compare the accuracy between DSC- T_2^* MR perfusion with and without a pre-load contrast dose. The first group comprised 43 patients with different glioma grades receiving a pre-load contrast before DSC- T_2^* MR perfusion. The second group comprised the same number of patients and were matched for grade, steroid intake, and phenotype, but underwent DSC- T_2^* MR perfusion without a pre-load dose.

Variable	First group (Pre-load dose) ($n = 43$)	Second group (without pre-load dose) ($n = 43$)
Age (Mean \pm SD)	53.5 \pm 15.6	55.6 \pm 15.8
Gender (Male/Female)	23/20	30/13
rTBV _{max} (overall mean)	11.55 \pm 6.6	11.80 \pm 6.3
Biopsy	19	23
Debulking	24	20
No treatment	10	11
Partial treatment	12	18
Full treatment	21	14
Performance status		
90–100	8	10
70–90	26	20
50–70	6	10
30–50	3	2
10–30	0	1

Table 7.1: Comparison of demographic and clinical data between the two groups (1) Patients receiving DSC- $T2^*$ MR perfusion with pre-load dose contrast (2) Patients receiving DSC- $T2^*$ MR perfusion without pre-load dose contrast

7.2.2 Statistical analysis

SPSS (17.0) was used to perform the statistical analysis. The difference in means of $rTBV_{max}$ per each group and grade were evaluated using the Mann–Whitney test. The correlation between the DSC- T_2^* perfusion techniques was assessed with Spearman's correlation coefficient and is presented in a scatter plot graph. Pearson's Chi square was used to assess the distribution of patients in number, percentage, means, and standard deviation per each factor and grade. To identify the effect from biological and clinical factors, analysis of covariance (ANOVA) was used to test the null hypothesis that the means of the groups per each factor were equal. The analysis was corrected using the Bonferroni procedure for single and combined factors. A p value <0.05 was considered significant throughout the analysis.

7.3 Results

7.3.1 Correlation of different MR perfusion techniques

The means and standard deviations of $rTBV_{max}$ derived from DSC- T_2^* MR perfusion, with and without pre-load contrast, showed no significant difference per each glioma grade (Table 7.2). Figure 7.1 illustrates the goodness-of-fit between the two techniques in a scatter plot with a value of 0.62.

MR techniques	DSC- T_2^* without pre-load dose	DSC- T_2^* with pre-load dose	p value
	Mean \pm SD		
LGG	4.26 \pm 1.49	4.20 \pm 1.17	0.895
AG	8.6 \pm 2.90	7.36 \pm 2.79	0.565
GBM	15.14 \pm 5.33	15.08 \pm 5.68	0.917

Table 7.2: Mean values of $rTBV_{max}$ of different glioma grades were measured per each technique. Non-parametric Mann–Whitney test of independent samples found no differences between the techniques per each grade.

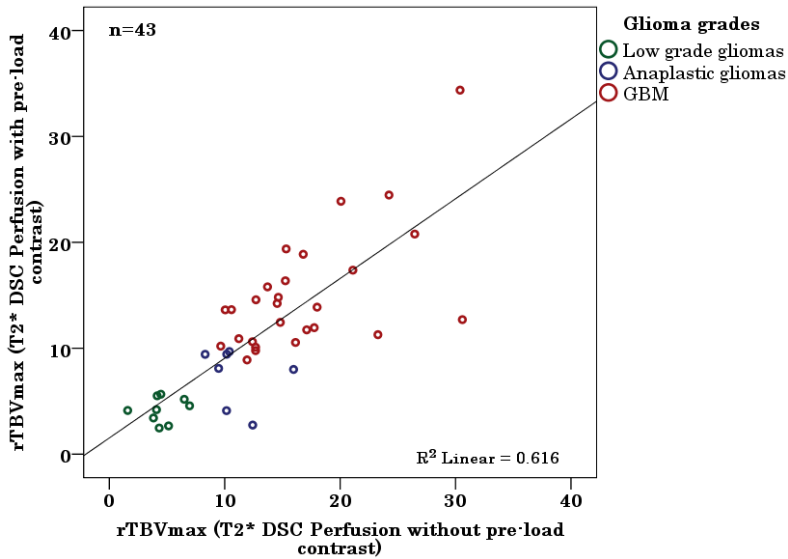


Figure 7.1: Scatter plots of the correlations between the relative tumour blood volume values obtained from T_2^* DSC-MR perfusion with and without pre-load dose. The correlation was assessed for two groups matched for tumour grade, steroid and phenotype. The best fit was determined by the coefficient of determination (R^2) between the two techniques.

7.3.2 Assessment of the potential effect of biological and clinical factors on changes in $rTBV_{max}$

Table 7.3 uses Pearson’s Chi square to illustrate the distribution in number and percentage of glioma patients per each tested factor. The means and

standard deviations were obtained from pairwise comparisons for the groups of steroid, pre-load dose, and phenotype, for each glioma grade (Table 7.4).

Factors		LGG	AG	GBM
Receiving steroids	yes	16 (41%)	18 (75%)	54 (90%)
	No	23 (59%)	6 (25%)	6 (10%)
Pre-load dose	Yes	9 (23%)	7 (29%)	27 (45%)
	No	30 (77%)	17 (71%)	33 (55%)
Cell line	Astrocytoma	28 (72%)	18 (75%)	59 (98%)
	Mixed cell type	11 (28%)	6 (25%)	1 (2%)

Table 7.3: Pearson Chi square for the distribution of patients within each factor

Factors		LGG	AG	GBM
		Mean \pm SD		
Receiving steroids	Yes	4.79 \pm 1.3	9.04 \pm 3.7	15.25 \pm 5.4
	No	4.77 \pm 3.7	9.77 \pm 3.3	18.00 \pm 6.0
Pre-load dose	Yes	4.20 \pm 1.2	7.36 \pm 2.8	15.08 \pm 5.7
	No	4.95 \pm 3.2	9.99 \pm 3.5	15.88 \pm 5.4
Cell line	Astrocytoma	4.59 \pm 3.3	8.48 \pm 3.1	15.50 \pm 5.5
	Mixed cell type	5.26 \pm 1.3	11.46 \pm 4.0	17.1

Table 7.4: The means and standard deviations of $rTBV_{max}$ among the groups were compared per each group and grade

Steroid intake, administration of a pre-load contrast dose, and phenotype, were assessed for their possible effect on changes in $rTBV_{max}$. An analysis of variance was performed to test for differences in means between the steroid, pre-load contrast dose, and phenotype groups. The main effect of the tested factors for their influence on the changes of $rTBV_{max}$ derived from MR perfusion was adjusted to the tumour grades. The three groups of patients based on steroids (Table 7.5), pre-load contrast dose (Table 7.6)

and phenotype (Table 7.7) found no differences between subjects per each group, with p values of 0.139, 0.140, and 0.411, respectively. All three factors were adjusted to grade because most patients with high grade gliomas receive steroids as part of their treatment. On the other hand, patients with low grade glioma or anaplastic glioma were assigned, based on their histological grade, to either of both astrocytoma and oligodendrogliomas, while patients with glioblastoma multiforme were assigned to astrocytoma, except for one patient, based on the old WHO classification. The F ratios of the between-groups mean squared to the within-groups mean squared are close to unity, indicating that the sample variances were characteristic of a normal population. The null hypothesis of no difference between groups was retained, which means the all cases in each group are equal. The second step in the analysis is to test if there is an interaction effect between those factors on $rTBV_{max}$ variation (Table 7.8). It is worth noting that during the assessment of either the separate effect of each factor or in combination with other factors, the Bonferroni procedure was performed, which adjusts the observed significance level to the number of comparisons used. Table 7.8 shows that the pairwise interactions between all factors were not significant and that even combining two or three factors does not result in a difference between the groups. As mentioned before, all assessments were adjusted by histological grade, which shows that it is the only significant factor in all interactions. The F ratio was very small for each factor and for each possible interactions except that of the grade. It is to be concluded that the means of $rTBV_{max}$ were equal within each group categorised by steroids, pre-load contrast, and cell line.

Test of between-subjects effect (rTVB _{max} dependent variable)						
Source	Sum of Squares	df	Mean Square	<i>F</i>	Sig.	Partial Eta Squared
Corrected Model	3039.91	5	607.98	28.6	.000	.550
Intercept	7318.26	1	7318.26	343.7	.000	.746
Steroids	47.14	1	47.14	2.2	.139	.019
Grade	2006.02	2	1003.01	47.1	.000	.446
Steroid*Grade	57.05	2	28.53	1.3	.266	.022
Error	2490.99	117	21.29			
Total	20353.29	123				
Corrected Total	5530.91	122				

Table 7.5: Analysis of variance of the effect of steroids on rTVB_{max} showed no difference between subjects and the difference is mainly attributed to the difference in grades

Test of between-subjects effect (rTVB _{max} dependent variable)						
Source	Sum of Squares	df	Mean Square	<i>F</i>	Sig.	Partial Eta Squared
Corrected Model	3010.15	5	602.0	27.9	.000	.544
Intercept	8057.48	1	8057.5	373.9	.000	.762
Pre-load dose	47.50	1	47.5	2.2	.140	.018
Grade	2541.84	2	1270.9	58.9	.000	.502
Pre-load dose*Grade	8.66	2	4.3	.20	.818	.003
Error	2520.76	117	21.6			
Total	20353.29	123				
Corrected Total	5530.91	122				

Table 7.6: Analysis of variance of effect of pre-load dose of contrast showed rTVB_{max} is the same across groups with different MR techniques

Test of between-subjects effect (rTBV _{max} dependent variable)						
Source	Sum of Squares	df	Mean Square	<i>F</i>	Sig.	Partial Eta Squared
Corrected Model	2986.71	5	597.3	27.5	.000	.540
Intercept	2824.46	1	2824.5	129.9	.000	.526
cell line	14.80	1	14.8	.68	.411	.006
Grade	609.17	2	304.6	14.0	.000	.193
cell line*Grade	9.23	2	4.6	.212	.809	.004
Error	2544.19	117	21.8			
Total	20353.29	123				
Corrected Total	5530.91	122				

Table 7.7: Analysis of variance of the effect of phenotype showed rTBV_{max} is not different across subjects

7.4 Discussion

The objective of this chapter was to assess the potential effect of certain factors on the rTBV_{max} obtained from DSC- T_2^* MR perfusion. The hypothesis is that there is no difference between the means of the different groups other than that attributed to the difference in tumour grade. Validating the robustness of the T_2^* MR perfusion technique was a suitable measure for a possible substitute of invasive histological diagnosis. Factors such as steroids, pre-load dose of contrast agent, and phenotype, adjusted for tumour grade, were assessed as potentially confounding factors that may contribute to rTBV_{max} variation. An analysis of variance (ANOVA) was used to test whether there is any difference within and between patient groups with regard to steroids, pre-load dose, and phenotype. The analysis was performed in two steps: the first step was to test each factor separately for its potential contribution to rTBV_{max} variation; the second step was to analyse the factors' interaction

Test of between-subjects effect (rTBV _{max} dependent variable)						
Source	Sum of Squares	df	Mean Square	<i>F</i>	Sig.	Partial Eta Squared
Corrected Model	3110	17	183	7.9	.000	.562
Intercept	2628	1	2629	114.0	.000	.521
Steroid	4.49	1	4.5	.20	.660	.002
Pre-load dose	8.82	1	8.8	.38	.538	.004
cell line	5.15	1	5.2	.22	.637	.002
Grade	647.8	2	324	14.1	.000	.211
Steroid*Pre-load dose	.17	1	.17	.01	.933	.000
Steroid*cell line	.29	1	.29	.01	.911	.000
Steroid*Grade	24.9	2	12.5	.54	.584	.010
Pre-load dose*cell line	.12	1	.12	.01	.942	.000
Pre-load dose*Grade	1.87	2	.93	.04	.961	.001
cell line*Grade	.86	2	.43	.02	.982	.000
Steroid*Pre-load dose*cell line	5.81	1	5.8	.25	.617	.002
Steroid*Pre-load dose*Grade	.68	1	.68	.03	.864	.000
Steroid*cell line*Grade	1.50	1	1.5	.07	.799	.001
Pre-load dose*cell line*Grade	.00	0				.000
Steroid*Pre-load dose*cell line*Grade	.00	0				.000
Total	20353	123				
Corrected Total	5531	122				

Table 7.8: Two-way analysis of variance of the interacting factors was adjusted for grades and corrected by Bonferroni procedures

to assess the combined effect of all included factors. As it was expected to have variation due to glioma grades, all the statistical analyses were grade-adjusted.

Steroids have been used for the treatment of intracranial tumours due to their quick and beneficial effect on reducing brain oedema and relieving symptoms. A total of 88 out of 123 patients received steroids as part of the treatment protocol (Table 7.3). A large percentage (86%) of patients with high grade glioma received steroids while fewer low grade glioma patients (41%) did. Comparing the means of the two groups using ANOVA revealed no statistical significance ($p = 0.139$), which indicates that the $rTBV_{max}$ of patients who have received steroids did not differ from those who had not. The F ratio was about 2, which is close to the population variance ($F = 1$), so the group variances are not different from the population variances. When examining the changes in $rTBV_{max}$ for each tumour grade, patients with diffuse astrocytoma showed no change in means between the two groups while a lower mean was found for glioblastoma patients who received steroids ($p = 0.246$). Our result was in line with a previous study (Bastin et al., 2006) conducted on glioblastoma multiforme patients who were treated for three days with steroids and showed no difference in cerebral blood volume before and after treatment. In contrast, cerebral blood volume was significantly decreased in peri-tumoural gray matter assessed by dynamic MR imaging (Ostergaard et al., 1999) and in tumoural area using a PET study (Leenders et al., 1985).

Contrast leak into the extravascular space is often present in brain tumours as a result of a breach in the blood–brain barrier (Rosen et al., 1990).

During contrast injection, the leak of contrast leads to a shortening of the T_1 in tissue, which results in a high T_1 signal. The contrast leak into the extravascular space leads to a decrease in the T_2^* signal and hence underestimation of the $rTBV_{max}$ value (Hu et al., 2010). Pre-load injection of contrast prior to dynamic susceptibility MR imaging is one of the methods that may saturate the brain tissue and minimize this effect. The effect of a pre-load dose of contrast was assessed in pairwise groups to evaluate its effect on changes in $rTBV_{max}$. The hypothesis is that injection of pre-load contrast results in a decrease in $rTBV_{max}$. In this study we performed ANOVA test of means to compare the effect of a pre-load dose on two different groups treated differently in regard to the pre-load dose. A minimal decrease in the means of $rTBV_{max}$ in patients with a pre-load dose of contrast was noted, but this did not reach statistical significance ($p = 0.140$). Our result is in line with a previously published study (Paulson and Schmainda, 2008) which showed no significant difference in relative cerebral blood volume between patients with and without pre-loading dose of contrast. The small changes that appear in patients with a pre-load dose could be attributed to the small flip angle (7°) used in this study, which reduced the sensitivity to the T_1 effect. Testing the effect of the small flip angle was not possible as patients were retrospectively studied and the scanning protocol was basically set for clinical workup. Other reasons for the reduced sensitivity to a T_1 leak are the post-processing gamma fitting algorithm and the correction for contrast re-circulation. Indeed, the dynamic MR perfusion technique in this study was based on hot spot localization within the tumour area that did not necessarily match the enhancement areas of the tumour.

A total of 18 out of 123 patients were diagnosed as having oligodendroglioma or oligoastrocytoma. Only one patient with glioblastoma was diagnosed with the cell type of oligoastrocytoma based on the new WHO classification. In this study, we compared the means of patients with astrocytoma cell type to that of oligodendroglioma and oligoastrocytoma and found no difference ($p = 0.411$) between the two groups. The sample variance did not differ from the population variance as the F ratio was closer to unity. The non-significant elevation of $rTBV_{max}$ in patients of oligodendroglioma and oligoastrocytoma in this study is in agreement with a previous study (Lev et al., 2004) while contradictory to others (Bian et al., 2009; Cha et al., 2005).

Finally, the combined effect of those factors was assessed to evaluate any synergistic effect. Yet the interaction of the factors was not significant and only the grade showed statistical significance. To our knowledge, building a model to test the variance in $rTBV_{max}$ between groups for these factors had not yet been performed to demonstrate the robustness of MR derived-cerebral blood volume.

One of the limitations of this study is that other factors such as tumour size, presence of necrosis, and the site of the tumour were not studied to assess whether they potentially affect variation in $rTBV_{max}$. Tumour size has been reported as a survival predictor (Fujii et al., 2010; Schomas et al., 2009a), while others did not find any statistical significance (Mangla et al., 2010; Back et al., 2007). The presence of necrosis was reported as a survival predictor in (van den Bent et al., 2009; Ekici et al., 2011), while others found contradictory findings (Idbaih et al., 2011). Tumour location was reported by

others as a significant survival predictor (Idbaih et al., 2011) and in one study showed a trend (Barri et al., 2005) whereas contradictory survival findings had been reported earlier (Yamada et al., 1993). However, treatment choice was greatly affected by the location of the tumour: parietal lobe tumours were more likely to receive radiation therapy and less likely to receive surgical resection (Claus and Black, 2006).

7.5 Conclusion

In the present study, the potential effect of steroids, pre-load contrast dose, and phenotype, was assessed on $rTBV_{max}$ derived from T_2^* MR perfusion. Univariate analysis showed no difference in $rTBV_{max}$ between the groups of steroid, pre-load contrast, and phenotype, which is indicative of the robustness of $rTBV_{max}$ as a perfusion parameter in assessing gliomas. The current limitations associated with histological diagnosis with consequent brain tissue damage, neurological symptoms, bleeding, and tumour inaccessibility, could be overcome in the future with an MR perfusion technique.

Chapter 8

General conclusions and future outlook

8.1 Conclusions

The current project was that of assessing the diagnostic accuracy of T_2^* -DSC and T_1 -DCE MR perfusion in grading cerebral gliomas in adults. Furthermore, the prognostic value of this technique in predicting survival and tumour progression was assessed in conjunction with other variables.

Chapter 1 presented the background about the prevalence of cerebral glioma and a historical review of the implementation of the WHO histological diagnosis for cerebral gliomas and their limitations. We also highlighted the limitations associated with conventional MR imaging in grading gliomas. An overview of the literature about MR perfusion parameters in grading and predicting survival was performed, and their techniques and limitation were explored. This includes the use of absolute and relative CBV in glioma grading and the methods used in reducing the T_1 signal effect. In that chapter, non-MRI techniques, such as CT perfusion and radioisotope scanning, for grading gliomas were discussed. The accuracy of these is generally lower than MR perfusion, in addition, they expose patients to the hazards of radiation. In terms of predictive value, MR perfusion imaging is a plausible method for prediction of survival and tumour progression and for monitoring treatment response. Nevertheless, a few limitations were encountered by the previous techniques, either in grading gliomas or in survival prediction. These limitations were mainly due to the small sample sizes involved, the MR parameters used, or the post-processing methodology. The next chapters dealt with the current knowledge gap and the variation in accuracy in the previous studies.

Chapter 2 carried out a systematic review of the previous literature. The aim was to identify studies assessing the diagnostic value of MR perfusion, specifically the $rCBV_{max}$ parameter, in differentiating between high and low grade gliomas. The included studies were subjected to qualitative and quantitative analysis. QUADAS criteria were used to assess the quality of these studies. A quantitative analysis was performed on a subgroup of 20 studies that had the same MR sequence and magnetic field strength (1.5 T). That systematic review revealed a homogeneity among the studies with pooled sensitivity of 93% and pooled specificity of 75%. However, differences in the threshold values among the studies is salient, which may lead to a variability of the accuracies obtained. In addition, those studies included brain tumours of different nature from gliomas, which may have resulted in inaccuracies in defining the appropriate threshold value. The final conclusion from the systematic review was that there was a difference in accuracy among the studies either because of chance or the technical settings of the MR parameters.

In Chapter 3, we provided the methods used in my thesis. The study was approved by the research ethical committee (Appendix D) and the clinical audit service (Appendix E). The initial recruitment from both routes was 205 patients. The final recruited glioma patients numbered 123, after excluding patients with post-operative or post-treatment MR perfusion scans, patients without histological diagnosis, patients with a wide gap (>18 months) between histological diagnosis and MR perfusion scan, and patients who underwent MR perfusion scan at 1.5 T. The MR imaging was performed as part of their clinical work up protocol using 3 T field strength. $DSC-T_2^*$

MR perfusion was performed after gadolinium contrast injection to assess the degree of change in signal intensity. A subset of patients ($n = 43$) underwent, in addition to DSC- T_2^* , DCE- T_1 MR perfusion wherein 25% of the total dose of contrast was received in this analysis. Post-processing was performed to generate CBV maps using Java Image software (www.xinapse.com). The technique used in this study is different from that which had been previously published; this is partly to be attributed to the clinical setting of a low flip angle and echo time and partly due to truncation in the signal intensity time curve to avoid counting any contrast recirculation or leakage. Multiple ROIs were drawn over the most hyperemic areas (hot spot) in the tumour. The highest value among the means of hot spots was considered and normalized to that of the averaged value obtained from normal white matter. The normalized value was considered as representative of the tumour and used in the final analysis to assess both the diagnostic and prognostic value of MR perfusion. The histological diagnosis was used as the standard reference to assess the diagnostic accuracy of the MR perfusion parameter in question.

Chapter 4 assessed the diagnostic accuracy of T_2^* -DSC MR Perfusion at 3 T in grading cerebral gliomas against histological diagnosis. Intra-rater and inter-rater reliability tests showed substantial agreement within and between raters' observations. The first recruited group of patients ($n = 50$) was used as a training set to generate, based on optimising the accuracy separately for each glioma grade, the threshold value to be used subsequently. These threshold values obtained were then assessed for reproducibility on the test set ($n = 73$). The accuracy in differentiation between high and low grade glioma and between diffuse astrocytoma and anaplastic glioma were the same

in the training and test sets. Our threshold values are different from those which had been previously published, for two reasons: the technical MR parameters included a short echo time (TE) and low flip angle (7°), and the post-processing technique. In this thesis, we obtained high accuracy in differentiating between glioblastoma and anaplastic glioma. This separation is important clinically, as the treatment plan and survival differ between the two glioma grades. Only two studies had attempted such separation: one yielding low accuracy (Lu et al., 2008) and the other (Park et al., 2009) obtaining comparable accuracy of 86% albeit without validation. The results of our study need to be validated in a multi-centre study as the threshold values depend mainly on our local MR perfusion settings and post-processing technique.

Chapter 5 aimed at evaluating the diagnostic accuracy of T_1 -DCE MR Perfusion based on turbo field echo. A subset ($n = 43$) of cerebral glioma patients underwent T_1 MR perfusion as part of their clinical workup. These patients received 25% of the total calculated dose of gadolinium per body weight. Ten slices with 45 repeats were performed for each patient. Java Image software (www.xinapse.com) was used for post-processing to produce T_1 CBV maps. The diagnostic accuracy of T_1 -DCE MR perfusion was compared to that of T_2^* -DSC MR Perfusion. It showed high accuracy in differentiating between high and low grade glioma; diffuse glioma and anaplastic glioma; and between glioblastoma and anaplastic glioma.

Chapter 6 assessed the prognostic value of the relative tumour blood volume derived from MR perfusion in predicting overall survival and tumour progression. The $rTBV_{max}$ value was categorized based on the optimal

diagnostic accuracy threshold into three hyperaemic groups: mild, moderate, and severe hyperaemia. The prognostic value of this MR perfusion parameter was assessed against the WHO histological grading system in addition to other known variables such as age, type of treatment, performance status, steroid intake, phenotype, and surgical procedure. Fifty-three patients died in our cohort study during the follow up period from August 2006 to January 2010, of which 90% were among the high grade gliomas. The Kaplan–Meier survival curves illustrated a better separation between diffuse astrocytoma and anaplastic glioma compared to that of the WHO histological diagnosis. A Cox regression model showed that radiological classification is an independent predictor of survival and tumour progression. Patients with moderate or severe hyperaemia had short survival and their tumour progressed in a shorter time compared to patients who had mild hyperaemia. The WHO histological diagnosis failed to predict overall survival and tumour progression in grade 3 glioma patients.

Chapter 7 discussed the probable confounders that may affect the variation of tumour blood volume derived from T_2^* -DSC MR perfusion. We tested the hypothesis that a pre-loading dose of contrast agent or steroid intake lowers TBV and the oligodendrogliotic component tumour cell has an elevated TBV. Each confounder (variable) is created in a pairwise group. Statistical analysis was performed using analysis of variance to test the difference in means per each variable. A subset of glioma patients ($n = 43$) underwent a pre-load dose before T_2^* -DSC MR perfusion (first group). A similar numbered group matched for grade, steroid intake, and phenotype, was created and compared to the first group. Goodness-of-fit between the two groups

was 0.62. The three tested confounders were adjusted to histological grade and corrected by Bonferroni procedures. All the variables were not significant between the groups except for histological grade. In this test of a few variables, we conclude that the changes in $rTBV_{max}$ values are to be ascribed only to the difference in histological grade and that the assumed variables have no effect.

8.2 Clinical impact

WHO histological grading based on surgical debulking or stereotactic biopsy carries significant risk of mortality and morbidity. Major complications (6%) such as intra-cerebral haemorrhage, which may pass to hemiparesis and death (Teixeira et al., 2009; Dammers et al., 2010; Shastri-Hurst et al., 2006; Jackson et al., 2001). Other centres have reported complication rates ranging between 3% and 20%, including intracerebral haemorrhage, sub-arachnoid haemorrhage, deep venous thrombosis, wound infection, hydrocephalus, and infarct (Coffey et al., 1988; Vecht et al., 1990; Kreth et al., 1993; Bernstein and Parrent, 1994; Kelly and Hunt, 1994; Bernstein, 2001). Moreover, there is a chance of 10% sampling error was reported in clinical practice (Shastri-Hurst et al., 2006).

Recently there has been a move towards using advanced MRI techniques which provide information on the tissue micro-environment to characterise brain tumours. The tumour growth showed correlation with an increase in blood flow and volume derived from perfusion MR (Cha et al., 2002). Previous studies showed $rCBV_{max}$ is correlated with the histological grading and

with an increased vascularity of the tumour (Aronen et al., 1994; Sugahara et al., 1998; Knopp et al., 1999; Cha et al., 2002).

Accurate grading of different glioma grades is important clinically because survival and treatment plans differ especially for the differentiation among high glioma grades (Louis et al., 2007). Only two studies (Lu et al., 2008; Park et al., 2009), have attempted to distinguish between the two tumour grades but demonstrated low accuracy or unvalidated data. In this study, we demonstrated high sensitivity (98%) where only one GBM in this cohort study was falsely classified as anaplastic glioma. On the other side, more anaplastic glioma cases were falsely classified as GBM but some of them presented later with clinical deterioration and short survival time. In addition, the survival analysis has shown that the radiological classification used in the study is a robust and able to discriminate patients with intermediate hyperaemia, while histological diagnosis failed to separate between low grade and anaplastic glioma.

A subset sample ($n = 42$) of the cohort performed T_1 MR perfusion as part of new clinical MRI protocol. The worked out accuracy in this subset showed comparable sensitivity (97%) to that of T_2^* MR perfusion in distinguishing between low and high grade gliomas. Importantly, T_1 MR perfusion showed same accuracy compared to T_2^* MR perfusion in differentiation among high grade gliomas but with optimum specificity (100%). At the same analysis type, the test is able to define GBM with sensitivity of 93%. This sequence is less sensitive to susceptibility artefact and therefore would provide a better resolution than T_2^* MR perfusion images especially for infratentorial tumours and in assessing post-operative tumour bed (Roberts et al., 2000). In addi-

tion, T_1 MR perfusion images overcome the disadvantages associated with contrast leak and expected to be used in tumours with blood brain barrier disruption or absence such as Meningioma (Pauliah et al., 2007).

In survival analysis data showed a new 3-tier radiological classification based MR perfusion images. Importantly, this classification creates a well defined group of $rTBV_{max}$ intermediate hyperaemia and coincides with moderate period of overall survival when histological classification failed to segregate anaplastic glioma patients' group from low grade glioma. The significance of radiological classification proposed in this study is manifested again when assessing the hazard ratio and being compared to other variables including the histological grading system. Adding to the previous use of the radiological criteria in assessing tumour progression (Macdonald et al., 1990), tumour blood volume assessment can now be used in predicting survival and tumour progression independent of other clinical and demographic factors.

MR perfusion could be used in the future for several applications such as MR perfusion can be used as non-invasive tool for assessing treatment efficacy (Tomoi et al., 1999; Akella et al., 2004; Wenz et al., 1996), distinguishing tumour recurrence from post-radiation necrosis (Barajas, Jr. et al., 2009; Hu et al., 2009; Matsusue et al., 2010; Henry et al., 2000). Importantly, non-invasive assessment via MR perfusion highlights its clinical diagnostic utility which could be used during the follow-up period of low grade glioma patients to assess tumour progression (Law et al., 2006b). In my opinion, by knowing the value of $rTBV_{max}$ during the follow-up period, the surgical decision based on the risk-to-benefit analysis can be judged appropriately. Unfortunately, the aim of this study was not inclusive of such analysis as only pre-operative

and pre-treatment scans were included in a single time point.

In this study we showed comparable high accuracy, using histological grading as standard reference, in both the training and test data in differentiating high from low grade glioma and anaplastic glioma from low grade glioma. Moreover, we showed a high sensitivity in differentiating glioblastoma from anaplastic glioma. The study showed an extended gain of $rTBV_{max}$ -based radiological classification in predicting overall survival and tumour progression for all glioma grades, high grade glioma. Our study did not demonstrate any significance in predicting survival among glioblastoma patients

8.3 Future outlook

The present research and systematic review defined preliminary answers to the questions of whether MRI perfusion, specifically relative cerebral blood volume, is a diagnostic tool in differentiating between high and low grade gliomas. However, to combat the limitations arising in the systematic review, diverse web sources should be included such as the EMBASE and Cochrane library database, in addition to PubMed, to assure the involvement of a diversity of related scientific papers and abstracts.

The diagnostic value of $rTBV_{max}$ MR perfusion derived from both T_2^* -DSC and T_1 -DCE is promising; however, the generalizability of these findings need to be proven in a multi-centre study.

Molecular genetic findings in gliomas are now being applied to refine the WHO histological grading (Reifenberger and Wesseling, 2010). A further

development in application of this approach would be to integrate imaging and molecular findings in an attempt to achieve better survival prediction.

Appendix A

Research Protocol

A.1 Study objectives and purpose

A.1.1 Purpose

The aim of this research is to assess the accuracy of multimodality MRI techniques in characterising and classifying brain tumours.

A.1.2 Primary objective

The predictive value of multimodality MRI for (i) glioma grading and (ii) tumour classification (gliomatous, non-gliomatous primary and secondary brain tumours) will be assessed against histopathological findings as the standard reference. Their diagnostic accuracy will be compared with that achieved by conventional MRI. As histopathological grading may be flawed by tissue sampling error, the value of multimodal MR in predicting the biological aggressiveness of tumours will be assessed against clinical and radiological outcomes. Lastly, we will assess whether multimodality imaging can predict outcomes within a histologically uniform grade by performing a survival analysis in patients with histologically defined Glioblastoma.

This prospective study involves the analysis of scans and tissue that will have been obtained for clinical patient management only. We will not perform any additional research scanning or tissue sampling for research purposes, nor will there be any influence on the standard of care. The research entails solely (i) the refined and systematic analysis of clinical imaging data, (ii) comparison of the findings with clinical data and histology, as well as (iii) additional biological tissue tests on existing samples. All histological samples

that we will use will have been acquired for clinical assessment and treatment purposes only. Hence the study carries no risk for the participants.

A.1.3 Secondary objectives

Measure the survival rate and find if there is any correlation between the different cut-off values derived from advanced MR imaging and the survival rate (the expected period of living after the diagnosis) in relation to tumour types and grades.

A.2 Study design

A.2.1 Study configuration

Participants: About 150–200 patients who are newly diagnosed with brain lesion and aged 18 years and above. Magnetic resonance images and histological findings will be subjected to data analysis. Participants who have no contraindications to MRI scanning will be able to complete the consent process and proceed to scanning.

Methods: All patients will already be undergoing conventional MRI and perfusion, diffusion, and MR spectroscopy scanning as part of their routine clinical investigations prior to biopsy or other neurosurgical treatment. Thus patients will only have to attend for the scan requested by their neurosurgeon, and will not have to have any additional scans, appointments, or hospital admissions. Furthermore, they will not be subjected to any additional scanning sequences for research purposes. All patients will have the same op-

portunity to have conventional MRI scans primarily as part of their clinical care. Patients with MRI findings of having brain lesions will be required to have additional multimodality MRI techniques as part of their clinical care, while other patients with normal brain findings will be dismissed, as usually happens within routine clinical care. There is no sub-grouping or classification of patients, as we won't recruit normal healthy volunteers. Consecutive patients will be recruited and subjected to image data analysis. The whole process, which includes different scanning techniques, won't take more than one hour and one clinical visit, which will require the intravenous injection of a contrast material at the time of scanning, something which is part of clinical care. The time allocated for the data analysis does not affect the time of scanning or the patient's stay in the hospital, as the data will be analysed off-line with a specially encrypted workstation.

As part of identifying the accuracy of these new multimodality techniques in diagnosing or excluding brain lesions, the data obtained from the participants' scans will be analysed using specialised analysis software on a computer station. All imaging data will be stored electronically after being anonymously transformed into a secure computer system within the Academic Radiology department.

The ability of this data to predict tumour type and grade (as defined by subsequent histopathological examination of biopsy tissue) will be evaluated and compared to conventional MRI. By defining the degree of tumour aggressiveness and whether the tumour is in its early or late stage, treatment planning can be made.

A.2.2 Study management

Part of assessing scientific quality is through weekly meetings within the department of Academic Radiology. Adding to that, the outcome of this research will be published either in a national and /or international journal, and displayed at an academic conference related to neuroradiology. Furthermore, both an external and internal peer reviewer will be asked to contribute through a formal critical appraisal.

A.2.3 Duration of the study and participant involvement

The potential participants are those newly diagnosed and confirmed as having brain tumours. The normal management scheme will comprise conventional and multimodality magnetic resonance imaging followed by surgical intervention as treatment and for histopathological diagnosis. This research study will not interfere with the management scheme in any way. It does not require extra time or extra scanning sequences; the patients' data will only be used for finding out the efficacy of the multimodality MRI in diagnosing the brain tumours.

A.2.4 End of the Study

The part of the study involving data collection will be ended once the target number (about 200) of potential participants is achieved. However, the data collected will be used for about two years.

A.2.5 Selection and withdrawal of participants

Recruitment

Potential patients will be identified (I) via documentation of the neuro-oncology in Multi-disciplinary Team (MDT) meeting that contains information on multimodality MRI, (II) by checking the clinical request forms for multimodality MR scans, and (III) by asking clinical colleagues to inform the named researchers when patients report on multimodality MRI. The potential participants are those newly diagnosed and proved to have brain lesions by using all of clinical diagnosis, MRI data, and histological findings.

Patients will be approached at any given time and once in which patients will be asked to read the information pack. Different ways will be followed to approach the potential participants: First, the vast majority of potential participants are in-patients who are under the care of the clinical team. Our approach for those patients will be at any time after they have been informed from their clinical team that they have brain lesion. The approach will occur once a member of the clinical care team asks the patient if he or she is willing to take part in the study and if so the patients will be contacted by one of our researchers. Second, out-patients could only be approached during their follow-up visit to one of the clinical care departments (i.e., neurosurgery, neurology, or neuro-oncology) after they were proved to have a brain lesion. In this case, the patient will be asked by a member of the clinical team taking care of him or her for his/her willingness to meet with one of our researchers. In either of these two approaches, one of our named researchers will have a brief introduction in which the aim of the study will be explained and

then the patient will be asked if they are happy to participate. Time will be given to the patients to read the information sheet and they will have the opportunity to ask questions and sign the consent form if they are interested in taking part. The consent form will allow the research team to access their MR data and histopathological specimens and associated details.

Participation in the study is voluntary and the participant has the right to withdraw from the study at any time and without giving a reason. This will not affect the standard of care that the patients receive.

Inclusion criteria

- Adult patients who are proved to have a brain lesion and are aged 18 years or older - Due to undergo MRI for tumour evaluation prior to biopsy or other neurosurgical treatment - Patients of different sexes, ethnic origins, religions, and those with a physical disability or a low literacy level are included in the study if they presented with brain lesions and agree to take part.

Exclusion criteria

- History of previous brain surgery or brain radiotherapy - Those unable to complete the consent process - Those with implanted devices that are magnetic incompatible, such as intra-orbital metallic foreign bodies, pacemakers, or implantable defibrillators.

Expected duration of participant participation

Study participants will be participating in the study for one visit which is within the normal caring services; however, their data will be used for a

longer period. The participant will not be asked to revisit the hospital for research purposes.

Participant withdrawal

The consent is primarily being taken to allow the researchers to use the imaging data for further study. Given the poor prognosis that many brain tumours have, it is possible that some of the participants will lose capacity or die in the months following the MRI scan while the data is still being analysed. It is assumed in the consent process that participants will be giving permission for the imaging data to be used for analysis regardless of clinical outcome, unless they specifically request that their data is withdrawn from the study. As stated in the consent form and information sheet, participants are free to withdraw from the study at any time without giving any reason and without their medical care being affected; however, their data will be used in the analysis unless they ask us not to do so. Withdrawn participants will be replaced during the period of the study until the required number of participants is achieved.

Informed consent

A short interview will be taken by one of our trained researcher (Prof. Dorothee Auer, Dr. Muftah Manita) during which the aim of the study and its methods will be explained and the information sheet will be handed out to the participant. Written informed consent will be obtained by one of the co-investigators after the potential participant has had an opportunity to read the information sheet and invitation letter and been given the op-

portunity to ask questions. All participants will provide written informed consent. The consent form will be signed and dated by the participant before they enter the study. The investigator will answer any questions that the participant has concerning study participation. Informed consent will be collected from each participant before their data will be analysed. One copy of this will be kept by the participant, one will be kept by the investigator, and a third will be retained in the patients hospital records. Should there be any subsequent amendment to the final protocol which might affect a participants participation in the study, continuing consent will be obtained using an amended consent form which will be signed by the participant.

A.2.6 Study regimen

The study involves evaluation data obtained from participants when MRI scanning is performed and during their clinical visit. Potential patients with brain tumours and who are above 18 years of age are involved if they agree to take part in the study. Patients of different sexes, ethnic origins, religions, and those with a physical disability or a low literacy level are welcomed to participate. There are some exclusion criteria related essentially to the incompatibility with the MR magnetic field. For example, patients with a cardiac defibrillator or an intra-orbital metallic foreign body are excluded. Also, patients with previous brain surgery and radiotherapy will be excluded as the study involves newly diagnosed brain lesions. The exclusion criteria usually are set out from the clinical side and the research study will not intervene with the clinical scheme.

A.3 Statistics

A.3.1 Methods

Group differences between various tumour types and grades will be tested using standard statistical approaches in a multivariate framework where appropriate. Both techniques are standardized to histopathological findings for calculating sensitivity, specificity, positive and negative predictive values, in addition to calculating other measurable diagnostic parameters. Positive and negative predictive values will be computed as well as receiver operating characteristic (ROC) curves. Survival analysis will be done by Kaplan–Meier tests and univariate and multivariate regression analyses for selected predictors.

It is anticipated that the results of this research will be presented at national and international research conferences, and the findings published in international journals of neuroimaging, cancer, and neurosurgery.

For each individual sub-study, formal sample size estimations will be performed. Based on the results from the retrospective audit, we are confident of being able to recruit sufficient numbers to assess the diagnostic accuracy and predictive power of rCBV for glioma grading. The sub-study requiring the largest sample is the survival analysis, especially for the intended multivariate regression. Practically, we cannot change the length of the study, and we therefore aim at recruiting consecutively, aiming for about 100 patients with glioblastoma, which is the expected number based on the frequency of multimodality and expected acceptance rate as per our previous experience. The final included number of glioblastomas will then determine the num-

ber of regressors we will be able to enter into the survival prediction model. We will then use a combination of prior knowledge and univariate testing to select the most promising indicators.

The histology of all participating studies will be systematically reviewed by one of the consultant neuropathologists. For subgroups of patients, biological studies will be performed including the assessment of hypoxia markers and MGMT (O6-methyl-guanine-DNA methyltransferase) promoter methylation status. Standard procedures within pathology will be followed for tissue handling and all biological investigations will be performed according to established protocols.

A.3.2 Sample size and justification

The aim is to get a large sample size with a powerful statistical study. Further sub-groupings of the total number, according to types of tumour, will be created and will result in a smaller number for each tumour type if a sufficient number has not been undertaken from the start. In analysing the survival rate for the different tumour grades, and especially for the multivariate regression, a large number of participants is encouraged. A powerful statistical result is guaranteed with a large sample of participants, and also to minimize the standard error. The sample size can be increased to validate our results in promoting the statistical significance of the advanced technique used.

A.4 Adverse events

The occurrence of an adverse event as a result of participation within this study is not expected and no adverse event data will be collected.

A.5 Ethical and regulatory aspects

The research involves the analysis of data which has been acquired for clinical purposes. The ethical issues therefore concern data storage and keeping tissue samples for the study purposes.

Written formal consent will be taken from potential participants after full explanation of the aim of the study and the participants will be given sufficient time to read the information sheet and have an opportunity to ask questions and sign if they are happy to participate. Furthermore, the participants are free to withdraw from the study at any time of the study. Patients' data will be kept anonymised and any personal information will be deleted and every participant will be given a code number so they won't be identified. As the research will employ a high standard of data management performed within the confines of the data protection act, and as informed consent for data storage and retention will be sought in all cases, we do not anticipate there being any ethical conflict.

The research does NOT involve taking new tissue samples. In contrast, only tissue samples that had been taken as part of clinical care for diagnostic purposes will be used for research after the clinical diagnosis has been established. The histological investigations are performed within the pathology

department as part of routine clinical tissue diagnosis and tumour grading; nevertheless, the research team will re-examine the specimen for the benefit of the research in a refined and more systematic fashion including novel biological assays such as the MGMT promoter methylation and hypoxia markers. In conducting the study, there will thus be no extra tissue specimen taken, but we plan to re-examine tissue samples that had previously been taken for routine tissue diagnosis if the participants agree for us to do so. The research handling of those tissue specimens will be in accordance with the Human Tissue Act, only anonymous specimens will be investigated. The participants have the right to withdraw from this agreement at any time and their tissue samples will be immediately destroyed should the participants so wish.

A.5.1 Ethics committee and regulatory approvals

The study will not be initiated before the protocol, consent forms, and participant and GP information sheets have received approval / favourable opinion from the Research Ethics Committee (REC) and from the respective National Health Service (NHS) Research and Development department. Should a protocol amendment be made that requires REC approval, the changes in the protocol will not be instituted until the amendment and revised informed consent forms and participant and GP information sheets (if appropriate) have been reviewed and received approval / favourable opinion from the REC and Research and Development departments. A protocol amendment intended to eliminate an apparent immediate hazard to participants may be imple-

mented immediately provided that the REC are notified as soon as possible and an approval is requested. Minor protocol amendments only for logistical or administrative changes may be implemented immediately, and the REC will be informed.

The study will be conducted in accordance with the ethical principles that have their origin in the Declaration of Helsinki, 1996; the principles of Good Clinical Practice; and the Department of Health Research Governance Framework for Health and Social Care, 2005.

A.5.2 Informed consent and participant information

The consent form is designed according to REC guidance and the participation in the study is entirely voluntary and the participants have the right to withdraw from the study without giving reason and without affecting the quality of medical care. The original form will be retained in the study records, a first copy will be handed to the participant, and a second copy will be filed in the participants medical notes. The consent form will be signed by both the participant and one of the named researchers. Should the consent form be amended, new approval will be sought and the participants, if applicable, will be asked to sign the revised consent form. Potential participants should be informed of any changes which might happen in the design of the study.

A.5.3 Direct access to source data / documents

All source documents shall made be available at all times for review by the Chief Investigator, Sponsors designee, and inspection by relevant regulatory authorities.

A.5.4 Data protection

The study and data analysis will take place at the Academic Radiology department of the University of Nottingham and the Queen's Medical Centre. The study will be conducted by members of the research team and the data analysis will be analysed by the same team with statistical consultation if needed. In addition, the clinical team who are taking care of the participants will have access to the participants' data. The imaging data required for research purposes will be stored on DVDs kept within a locked office in the Department of Academic Radiology for about 10 years. The data will also be kept anonymised on the secure Academic Radiology computer system (which can only be accessed by authorised co-researchers from within the department) for up to 10 years. [The Data protection act states that personal data which are processed only for research purposes in compliance with the relevant conditions may, notwithstanding the fifth data protection principle, be kept indefinitely]. 33/3 (1998) part iv.

As the MRI scan is being performed for clinical purposes, the imaging data will also be stored in the Nottingham University Hospitals image storage network referred to as the Picture Archiving and Communication System (PACS) for an indefinite period. This data is not anonymised but can only

be accessed by authorised NHS staff (in accordance with Trust policy).

A.6 Quality assurance and audit

A.6.1 Insurance and indemnity

The usual diagnosing protocol is applied within the routine health care frame already designed, so the investigators won't interrupt the diagnosing scheme. In addition, the potential participants will not be scanned in sites other than the usual site organized for diagnosis and management. The University of Nottingham has taken out an insurance policy to provide indemnity in the event of a successful litigious claim for proven non-negligent harm.

A.6.2 Study data

The imaging data required for research purposes will be stored on DVDs kept within a locked office in the Department of Academic Radiology for about 10 years. The data will also be kept anonymised on the secure Academic Radiology computer system (which can only be accessed by authorised co-researchers from within the department) for up to 10 years. [The Data protection act states that personal data which are processed only for research purposes in compliance with the relevant conditions may, notwithstanding the fifth data protection principle, be kept indefinitely]. 33/3 (1998) part iv.

As the MRI scan is being performed for clinical purposes, the imaging data will also be stored in the Nottingham University Hospitals image storage network referred to as the Picture Archiving and Communication Sys-

tem (PACS) for an indefinite period. This data is not anonymised but can only be accessed by authorised NHS staff (in accordance with Trust policy). One part of assessing scientific quality is through weekly meeting within the department of Academic Radiology. Adding to that, the outcome of this research will be published either in national and/or international journals and displayed at academic conferences related to neuroradiology. Furthermore, both an external and internal peer reviewer will be asked to contribute through a formal critical appraisal. Professor Dorothee Auer (Academic Radiology, University of Nottingham) has control of keeping the data and acts as the custodian.

A.6.3 Record retention and archiving

In compliance with the ICH/GCP guidelines, regulations and in accordance with the University of Nottingham Research Code of Conduct, the Chief or local Principal Investigator will maintain all records and documents regarding the conduct of the study. These will be retained for at least seven years or for longer if required. If the responsible investigator is no longer able to maintain the study records, a second person will be nominated to take over this responsibility. The study documents held by the Chief Investigator on behalf of the Sponsor shall be finally archived at secure archive facilities at the University of Nottingham. This archive shall include all study databases and associated meta-data encryption codes.

A.6.4 Discontinuation of the trial by the sponsor

The Sponsor reserves the right to discontinue this study at any time for failure to meet expected enrolment goals, for safety or any other administrative reasons. The Sponsor shall take advice as appropriate in making this decision.

A.6.5 Statement of confidentiality

Individual participant's medical or personal information obtained as a result of this study are considered confidential and disclosure to third parties is prohibited with the exceptions noted above. Participant confidentiality will be further ensured by utilising identification code numbers to correspond to treatment data in the computer files.

Such medical information may be given to the participants medical team and all appropriate medical personnel responsible for the participants welfare.

Data generated as a result of this study will be available for inspection on request by the participating physicians, the University of Nottingham representatives, the REC, local research and development Departments, and the regulatory authorities.

A.7 Publication and dissemination policy

Results of this research will be retained within the department of Academic Radiology at the University of Nottingham. An overview of the results (that is not specific to any participant) will be supplied to participants on request.

In addition, the usual caring team will be notified of any relevant positive data that may lead in the future to re-designing the scanning protocol.

A.8 Study finances

A.8.1 Funding source

The MRI scanning will have no additional research costs, as the scan is already being performed on clinical grounds. The salary cost of the lead investigators is already covered. The computing equipment required for the data storage and analysis are already available within the Department of Academic Radiology. All other costs will be covered by divisional funds. We foresee an extra 15 minutes for histopathological re-assessment and case discussion (about 30 per case) and costs for biological studies such as MGMT methylation status assessment for a subgroup of patients will be required. The majority of this cost will be covered by supervision fees funded by the Libyan government for Dr. Manita, which have been allocated in part to the division of Academic Radiology.

A.8.2 Participant stipends and payments

Participants will not be paid to participate in the study as the study involves data analysis. The first and the follow-up visits are part of the clinical caring scheme.

Appendix B

Consent form



The University of
Nottingham

Study Number:

Patient Identification Number for this trial:

CONSENT FORM

Title of Project: The Prognostic Value of Multimodality MRI in Brain Tumours

Name of Researcher: Prof. Dorothee Auer

Please initial box

- | | | |
|---|---|--------------------------|
| 1 | I confirm that I have read and understand the information sheet dated 15th July 2008 (version 1.2) for the above study and have had the opportunity to ask questions. | <input type="checkbox"/> |
| 2 | I understand that my participation is voluntary and that I am free to withdraw at any time, without giving any reason, without my medical care or legal rights being affected. | <input type="checkbox"/> |
| 3 | I understand that as part of this research, sections of any of my medical notes, clinical diagnostic images and pathology samples will be looked at by research team members. I give permission for these individuals to have access to my records, diagnostic images and tissue samples for research purposes. | <input type="checkbox"/> |
| 4 | I agree for samples of my brain lesion to be stored and used in the biological research studies integrated into this study. | <input type="checkbox"/> |
| 5 | I agree to take part in the above study. | <input type="checkbox"/> |

Name of Patient

Date

Signature

Name of Person taking consent
(If different from researcher)

Date

Signature

Researcher

Date

Signature

Appendix C

Patient information sheet

What if something goes wrong?

Medical research is covered for mishaps in the same way as for patients undergoing treatment in the NHS, i.e. compensation is only available if negligence occurs. As the study involves data analysis with no clinical intervention, there is no risk to you by participation in this study. Regardless of this, if you wish to complain about any aspect of the way you have been approached or treated during the course of this study, the normal National Health Service complaints mechanisms may be available to you. The Patient Advice and Liaison Service (PALS) can be contacted for further assistance at QMC by calling 0800 1830204

Who has reviewed the study?

This study has been approved by the Leicestershire, Northamptonshire and Rutland Research Ethical Committee 1 and by the Development Department of the Queen's Medical centre, Nottingham.

Contact for further information

If you would like to discuss the study further or would like more information, please feel free to contact me:

Prof. Dorothee Auer
 Dept. of Academic Radiology,
 Queen's Medical Centre,
 Nottingham,
 NG7 2UH
 Tel: 0115 8231178
 Email:
 dorothee.auer@nottingham.ac.uk

Many thanks for taking the time to read this information and for considering participating in this study.



The prognostic value of multimodality MRI in brain tumours

You are being invited to take part in a research study. Before you decide it is important for you to understand why the research is being done and what it will involve. Please take time to read the following information carefully and discuss it with friends and relatives if you wish. Ask us if there is anything that is not clear or if you would like more information. Take time to decide whether or not you wish to take part.

Study Number: 08.H0406.102

What is the purpose of the study?

Our main aim is to enhance the diagnostic value of MRI scan. We will specifically investigate whether dedicated analysis of recently enhanced MRI scan offered added value for managing with brain lesion.

Why have I been chosen?

You have been chosen because your consultants considered a particular advanced MRI scan of clinical value for you to guide decisions about your further treatment plan.

Do I have to take part?

It is up to you to decide whether or not to take part. If you do decide to take part you will be given this information sheet to keep and be asked to sign a consent form, a copy of which you will get to keep. If you decide to take part you are still free to withdraw at any time and without giving a reason. This will not affect the standard of care you receive.

What is involved?

If you consent to participate, your brain scans, clinical data and tissue findings will be used for analysis. The data used for the research will ALL have been obtained for your clinical care.

Is there anything that means I should not take part?

I cannot think of any reason why you should not take part in the study as no risk is involved.

What are the possible risks of taking part?

There is no risk involved in this study.

What are the possible benefits of taking part?

Although there is no direct benefit to participants, future care may be improved.

Will my taking part in this study be kept confidential?

Yes. All information which is collected about you during the course of the research will be kept strictly confidential. Any information about you which leaves the hospital will have your name and address removed so that you cannot be recognised from it. With your permission the consultant neurosurgeons and other team members of the multi-disciplinary neuro-oncology team looking after you will be informed of your participation.

What will happen to the results of the research study?

The results of the study will be published in a medical journal specialising medical imaging. However, the result will takes over a year to become available after the end of the study. Of course, you will not be identified in any report or publication arising from this research.

Appendix D

Ethical Approval

Leicestershire, Northamptonshire & Rutland Research Ethics Committee 1

1 Standard Court
Park Row
Nottingham
NG1 6GN

Telephone: 0115 912 3344 ext 39428
Facsimile: 0115 9123300

30 July 2008

Professor Dorothee Auer
Professor of Radiology
University of Nottingham
Queen's Medical Centre
Academic Radiology department
Nottingham
NG7 2UH

Dear Professor Auer

Full title of study: **The prognostic value of multimodality MRI in brain tumours**
REC reference number: **08/H0406/102**

Thank you for your letter of 17 July 2008, responding to the Committee's request for further information on the above research [and submitting revised documentation](#), subject to the conditions specified below.

The further information was considered at the meeting of the Committee held on 30 July 2008. A list of the members who were present at the meeting is attached.

Confirmation of ethical opinion

On behalf of the Committee, I am pleased to confirm a favourable ethical opinion for the above research on the basis described in the application form, protocol and supporting documentation [as revised](#).

Ethical review of research sites

The Committee has designated this study as exempt from site-specific assessment (SSA). There is no requirement for [other] Local Research Ethics Committees to be informed or for site-specific assessment to be carried out at each site.

Conditions of the favourable opinion

The favourable opinion is subject to the following conditions being met prior to the start of the study.

Management permission or approval must be obtained from each host organisation prior to the start of the study at the site concerned.

Management permission at NHS sites ("R&D approval") should be obtained from the relevant care organisation(s) in accordance with NHS research governance arrangements. Guidance on applying for NHS permission is available in the Integrated Research Application System or at <http://www.rdforum.nhs.uk>.

Approved documents

The final list of documents reviewed and approved by the Committee is as follows:

<i>Document</i>	<i>Version</i>	<i>Date</i>
Application	AB/137187/1	30 April 2008
Investigator CV		18 May 2008
Protocol	1.2	15 July 2008
Letter from Sponsor		19 May 2008
Peer Review		11 April 2008
Participant Information Sheet	1.2	15 July 2008
Participant Consent Form	1.2	15 July 2008
Response to Request for Further Information		17 July 2008
Evidence of Insurance - Clinical Trials Legal Liability		13 August 2007
Evidence of Insurance - Employer's Liability		09 August 2007

Statement of compliance

The Committee is constituted in accordance with the Governance Arrangements for Research Ethics Committees (July 2001) and complies fully with the Standard Operating Procedures for Research Ethics Committees in the UK.

After ethical review

Now that you have completed the application process please visit the National Research Ethics Website > After Review

You are invited to give your view of the service that you have received from the National Research Ethics Service and the application procedure. If you wish to make your views known please use the feedback form available on the website.

The attached document "After ethical review – guidance for researchers" gives detailed guidance on reporting requirements for studies with a favourable opinion, including:

- Notifying substantial amendments
- Progress and safety reports
- Notifying the end of the study

The NRES website also provides guidance on these topics, which is updated in the light of changes in reporting requirements or procedures.

We would also like to inform you that we consult regularly with stakeholders to improve our service. If you would like to join our Reference Group please email referencegroup@nres.npsa.nhs.uk.

08/H0406/102**Please quote this number on all correspondence**

With the Committee's best wishes for the success of this project

Yours sincerely

Dr Carl Edwards / Miss Jeannie McKie
Chair / Committee Coordinator

Email: jeannie.mckie@nottspct.nhs.uk

Enclosures: "After ethical review – guidance for researchers" [SL- AR2](#)

Copy to: *Mr Paul Cartledge, University of Nottingham*
[R&D office for NHS care organisation at lead site](#) – NUH (via email)

Appendix E

Clinical Audit Approval

Clinical Audit Registration Form

Title Pre-op and post-op multimodal MR imaging of brain tumours **Project ID** 1272

Teleform Number: 0

Division: Medical 1 Medical 2 Surgical 1 Surgical 2
 Family health Clinical support Trust wide Interface audit

Directorate: 1 Radiology 2
 3 4

Priority: Priority C, Local & Other

Audit lead: Prof D Auer, Dr M Manita, **Designation:** Consultant **Campus:** City QM

If designation is 'Medical Student' has an honorary contract been signed off?:

Contact/bleep No: 55962/63900 **E-mail address:**

Keywords *Insert words (not in title) that will help identify the audit*

Background information *Including literature review and audit rationale*

Magnetic resonance (MR) imaging is the standard imaging method for the assessment of brain tumours. Multimodal MR imaging includes conventional MRI, which provides the anatomical detail of a tumour and its environment, as well as newer modes of MR imaging that provide physiological information about a tumour. Examples of MR modalities used in standard clinical practice include Perfusion MR imaging, Diffusion Weighted Imaging and MR Spectroscopy. A combination of these modes of imaging (multimodal imaging) allows a more accurate diagnosis to be made of the type of tumour in many cases (Aronen et al., 1994, Sugahara et al., 1998, Hartmann et al., 2003, Calli et al., 2006). The treatment and prognosis of brain tumours differs according to the type and grade (aggressiveness) of the tumour, thus differentiating between tumour types is critical. Currently, the gold standard to obtain a pathological diagnosis is the stereotactic biopsy, an invasive procedure that carries a small, but significant, risk of morbidity and mortality. A recent audit of stereotactic biopsies carried out in Nottingham for cases over 4 years showed an overall diagnostic success rate of 89.3% (Shastri-Hurst et al., 2006). Multimodal imaging does not yet replace stereotactic biopsy to definitively determine the histology and nature of a brain tumour, but may be useful to avoid the need for biopsies in some cases. This audit aims to assess whether the performance of multimodality MR imaging is to a standard sufficient to provide the information required for tumour type differentiation. **Methodology:** Retrospective audit spanning 3 to 4 years, including about 100 patients with brain masses who have had multimodal imaging. For each patient, multimodal imaging data from the MRI scanner / PACS system will be retrieved, anonymised and analysed to determine a diagnosis. These results will be compared to the tissue or best clinical diagnosis. Subset analysis will be included to determine if certain subsets of tumours are more accurately diagnosed. Aronen, H. J., Gazit, I. E., Louis, D. N., Buchbinder, B. R., Pardo, F. S., Weisskoff, R. M., Harsh, G. R., Cosgrove, G. R., Halpern, E. F., Hochberg, F. H. & Et Al. (1994) Cerebral blood volume maps of gliomas: comparison with tumor grade and histologic findings. *Radiology*, 191, 41-51. Calli, C., Kitis, O., Yuntun, N., Yurtseven, T., Islekel, S. & Akalin, T. (2006) Perfusion and diffusion MR imaging in enhancing malignant cerebral tumors. *Eur J Radiol*, 58, 394-403. Hartmann, M., Heiland, S., Harting, I., Tronnier, V. M., Sommer, C., Ludwig, R. & Sartor, K. (2003) Distinguishing of primary cerebral lymphoma from high-grade glioma with perfusion-weighted magnetic resonance imaging. *Neurosci Lett*, 338, 119-22. Shastri-Hurst, N., Tsegaye, M., Robson, D. K., Lowe, J. S. & Macarthur, D. C. (2006) Stereotactic brain biopsy: An audit of sampling reliability in a clinical case series. *Br J Neurosurg*, 20, 222-6. Sugahara, T., Korogi, Y., Kochi, M., Ikushima, I., Hirai, T., Okuda, T., Shigematsu, Y., Liang, L., Ge, Y., Ushio, Y. & Takahashi, M. (1998) Correlation of MR imaging-determined cerebral blood volume maps with histologic and angiographic determination of vascularity of gliomas. *AJR Am J Roentgenol*, 171, 1479-86.

Aims of the audit

- We aim to compare the accuracy of radiological diagnosis of multimodal imaging, since its inception in clinical practice in Nottingham, for specific types of brain tumours including lymphoma, glioma and metastases to a benchmark defined in the literature by a recent local audit of stereotactic biopsies (Shastri-Hurst et al., 2006).

Secondary aims:

- To evaluate the added value of multimodality MR imaging of patients with brain masses in order to maximise the benefit of new technology to patients and neurosurgeons.

Standards *Please specify specific standard and its source* Audit of stereotactic biopsies carried out in Nottingham for cases over 4 years - diagnostic success rate of 89.3% (Shastri-Hurst et al., 2006).

Is this a baseline audit to set new standards

Is this a re-audit?

Original audit ID

Is this a survey?

Priority links. Please tick all that apply CG Clinical indicators Childcare protection agency

NHSLA HCC Integrated care pathway Local guidance National audit NICE guideline NSF

Quality assurance Patient experience Royal college SBH Other link (Specify) Availability of neuros

Audit group membership (tick staff groups involved)		Biomedical scientist <input type="checkbox"/>	Clinical psychology <input type="checkbox"/>
Dietetics <input type="checkbox"/>	Medical <input checked="" type="checkbox"/>	Midwifery <input type="checkbox"/>	Nursing <input type="checkbox"/>
OT <input type="checkbox"/>	Pharmacy <input type="checkbox"/>	Physiotherapy <input type="checkbox"/>	
Radiography <input type="checkbox"/>	SLT <input type="checkbox"/>	Other specialist <input type="checkbox"/>	Specify <input type="text"/>
Methodology			
Retrospective <input checked="" type="checkbox"/>	Prospective <input type="checkbox"/>	Tick either or both as appropriate	
Study population/Sample size	<input type="text" value="100 patients"/>		
Number of casenotes required	<input type="text" value="0"/>	Hyperlink to casenote request form	
List below the proposed start/end dates of the audit. If unknown enter an estimate			
Start date	<input type="text" value="05/11/2008"/>	Is CAT support required for this audit	<input type="checkbox"/>
End date	<input type="text" value="05/11/2009"/>	Open Support Form	
Authorisation	Date authorised	CAT Authorisation	
<input type="text" value="Consultant"/>	<input type="text" value="05/11/2008"/>	<input type="text" value="Sillitoe, Fiona"/>	
Name authoriser	Signature of Authoriser	Audit Officer responsible	
<input type="text" value="Professor D Auer"/>	<input type="text"/>	<input type="text" value="Sillitoe, Fiona"/>	
Authoriser's Ext. No.	<input type="text"/>	E-mail address:	<input type="text"/>

Appendix F

Demographic and Clinical Data

Pt. No.	Age(Y)	Sex	Grade	Recruitment	Cell line	PS	rTBVmax (T ₂ *)	rTBVmax (T ₁)	Status	O.S (days)	T.P (days)	Surgery	Steroid	Treatment
1	60	M	2	Audit	A	90	5.13	N/A	Died	55	55	biopsy	Yes	2
2	63	M	4	Audit	A	40	11.94	6.96	Died	144	144	debulk	Yes	2
3	70	M	4	Research	A	80	16.8	N/A	Died	322	159	debulk	Yes	3
4	42	M	2	Audit	ODG	90	6.95	N/A	Alive	985	804	biopsy	No	2
5	27	F	2	Audit	A	80	4.14	N/A	Alive	596	589	biopsy	No	1
6	56	M	4	Research	A	80	10.55	4.27	Died	431	147	biopsy	Yes	3
7	72	F	4	Audit	A	40	10.62	7.84	Alive	35	35	biopsy	Yes	2
8	34	M	2	Audit	A	80	2.67	1.87	Alive	395	395	debulk	No	1
9	41	M	4	Research	A	60	17.75	N/A	Died	88	88	biopsy	No	1
10	52	M	4	Audit	A	90	16.13	N/A	Died	828	87	debulk	No	3
11	50	M	4	Audit	A	90	12.4	N/A	Died	503	177	debulk	Yes	3
12	28	F	3	Research	A	80	8.5	N/A	Alive	1203	930	debulk	Yes	2
13	49	F	3	Audit	A	80	8.73	N/A	Alive	456	189	debulk	Yes	2
14	38	M	2	Audit	A	90	4.57	4.56	Alive	301	276	debulk	No	3
15	74	M	4	Audit	A	60	13.63	8.38	Alive	12	12	debulk	Yes	3
16	55	M	4	Audit	A	20	10.04	N/A	Died	39	39	debulk	Yes	1
17	59	M	4	Audit	A	90	9.65	N/A	Died	152	55	biopsy	Yes	3
18	66	F	2	Audit	A	90	4.46	N/A	Alive	1228	232	biopsy	Yes	2
19	25	M	3	Audit	A	80	7	N/A	Alive	13	13	biopsy	No	1
20	59	M	3	Audit	A	80	10.4	N/A	Alive	29	29	biopsy	No	1
21	49	M	4	Audit	A	60	14.64	N/A	Died	54	54	debulk	No	3
22	59	M	4	Audit	A	40	10.2	8.41	Died	250	110	biopsy	Yes	3
23	72	F	4	Audit	A	80	18.88	8.54	Died	291	7	debulk	Yes	3
24	47	F	4	Research	A	90	10.1	8.37	Alive	117	117	debulk	Yes	3
25	40	F	2	Audit	A	80	3.82	N/A	Alive	738	738	debulk	No	1
26	41	M	2	Audit	A	90	1.59	N/A	Alive	1718	1718	debulk	No	1
27	58	F	4	Audit	A	80	19.38	14.09	Died	472	472	debulk	Yes	3
28	62	F	3	Audit	A	80	9.69	5.34	Died	330	330	biopsy	Yes	2
29	42	M	2	Research	A	80	4.08	N/A	Alive	1095	256	debulk	Yes	2
30	41	F	2	Audit	A	80	4.32	N/A	Alive	897	897	debulk	Yes	1
31	23	M	3	Audit	A	90	9.44	4	Alive	467	364	biopsy	Yes	3
32	58	M	3	Audit	ODG	80	13.26	N/A	Alive	1370	1081	debulk	Yes	1

Pt. No.	Age(Y)	Sex	Grade	Recruitment	Cell line	PS	rTBVmax (T ₂ *)	rTBVmax (T ₁)	Status	O.S (days)	T.P (days)	Surgery	Steroid	Treatment
33	63	M	4	Audit	A	20	26.46	N/A	Died	157	6	debulk	No	1
34	44	F	3	Audit	ODG	80	9.47	N/A	Alive	419	366	debulk	No	2
35	40	M	3	Audit	A	80	12.42	N/A	Died	884	884	debulk	Yes	3
36	83	M	4	Research	A	80	14.81	30.1	Died	32	32	debulk	Yes	1
37	50	F	2	Research	ODG	80	4.6	N/A	Alive	1103	391	debulk	No	1
38	51	F	2	Research	ODG	80	5.51	2.16	Died	823	477	biopsy	No	1
39	56	F	4	Research	A	90	13.88	13.66	Alive	492	134	biopsy	Yes	3
40	39	M	2	Research	ODG	90	5.66	2.81	Alive	621	145	debulk	No	1
41	74	M	4	Audit	A	80	11.74	8.36	Died	186	186	biopsy	Yes	2
42	53	M	4	Audit	A	60	20.78	15.65	Died	25	25	debulk	Yes	2
43	72	M	4	Research	A	80	18	N/A	Died	396	229	debulk	Yes	2
44	58	M	4	Research	A	90	14.58	15.73	Alive	368	104	debulk	Yes	3
45	45	M	3	Research	ODG	80	8.3	N/A	Alive	836	704	biopsy	Yes	1
46	52	F	4	Audit	A	80	11.28	10	Died	214	214	biopsy	Yes	3
47	31	F	3	Audit	A	90	15.96	N/A	Alive	1002	1002	debulk	No	1
48	67	M	4	Research	A	60	12.67	N/A	Died	513	313	biopsy	Yes	3
49	68	M	4	Research	A	40	15.32	N/A	Died	105	105	biopsy	Yes	2
50	38	M	2	Research	A	80	3.47	N/A	Alive	1512	1387	debulk	Yes	3
51	41	F	4	Audit	ODG	80	17.1	N/A	Alive	133	133	debulk	Yes	3
52	27	F	2	Research	A	90	5.32	N/A	Alive	665	665	debulk	No	1
53	32	M	3	Audit	ODG	90	10.15	N/A	Alive	2574	1835	biopsy	Yes	2
54	27	M	2	Audit	A	80	2.55	N/A	Alive	850	850	debulk	No	1
55	56	F	4	Audit	A	80	12.7	7.86	Died	222	122	biopsy	Yes	3
56	30	M	2	Research	A	80	3.42	2.97	Alive	583	366	debulk	No	1
57	59	M	3	Research	A	80	7.69	N/A	Alive	1416	1136	debulk	No	2
58	29	M	2	Research	A	90	3.32	N/A	Alive	665	665	debulk	Yes	1
59	72	M	3	Research	A	80	9.43	4.96	Died	174	116	biopsy	Yes	2
60	49	F	2	Research	A	60	6.14	N/A	Alive	561	561	biopsy	No	2
61	24	F	4	Audit	A	90	15.8	22.21	Died	196	196	debulk	Yes	3
62	54	M	4	Audit	A	80	12.7	N/A	Alive	223	69	debulk	Yes	3
63	36	M	4	Research	A	80	8.9	8.36	Alive	879	424	debulk	Yes	3
64	53	F	4	Research	A	80	23.88	10.66	Died	266	192	biopsy	Yes	3

Pt. No.	Age(Y)	Sex	Grade	Recruitment	Cell line	PS	rTBVmax (T ₂ *)	rTBVmax (T ₁)	Status	O.S (days)	T.P (days)	Surgery	Steroid	Treatment
65	28	F	2	Research	ODG	80	4.2	3.29	Alive	361	361	debulk	Yes	1
66	68	F	4	Audit	A	90	23.27	N/A	Died	219	219	debulk	No	2
67	56	M	3	Audit	A	80	4.11	3.76	Alive	1387	216	debulk	Yes	1
68	69	F	4	Research	A	40	30.59	N/A	Alive	16	16	debulk	Yes	2
69	37	F	4	Research	A	60	21.1	N/A	Died	1123	419	biopsy	Yes	2
70	52	F	4	Audit	A	80	13.7	N/A	Died	141	141	debulk	Yes	3
71	68	M	4	Audit	A	80	20.07	N/A	Died	53	53	debulk	Yes	2
72	47	F	4	Audit	A	60	9.78	11.6	Alive	14	14	debulk	No	2
73	72	F	2	Research	ODG	90	2.65	N/A	Alive	713	713	biopsy	No	2
74	61	F	4	Audit	A	80	10.9	4.9	Died	288	15	biopsy	Yes	2
75	73	M	4	Audit	A	60	11.93	N/A	Died	110	110	biopsy	Yes	2
76	60	M	2	Research	ODG	80	6.3	N/A	Alive	1099	1099	biopsy	Yes	2
77	60	M	3	Audit	A	80	8.04	N/A	Died	274	274	biopsy	Yes	3
78	63	F	4	Audit	A	60	12.67	N/A	Died	525	444	biopsy	Yes	3
79	64	M	4	Research	A	60	16.32	N/A	Died	374	374	debulk	Yes	2
80	73	F	4	Audit	A	80	14.81	N/A	Died	49	49	debulk	Yes	1
81	60	M	4	Audit	A	80	24.47	16.78	Alive	230	230	debulk	Yes	3
82	29	F	4	Audit	A	80	12.44	10.17	Alive	266	266	debulk	Yes	3
83	58	F	4	Audit	A	80	14.23	12.43	Died	133	133	debulk	Yes	3
84	59	M	4	Research	A	60	14.54	N/A	Died	373	109	biopsy	Yes	2
85	43	M	3	Research	A	80	8.1	5.23	Alive	30	30	biopsy	No	1
86	46	M	3	Research	A	80	2.75	2.41	Alive	225	225	debulk	Yes	2
87	47	F	2	Research	ODG	80	4.83	N/A	Alive	1321	520	debulk	Yes	2
88	73	F	2	Research	A	80	4.13	3.06	Alive	505	505	biopsy	Yes	1
89	38	F	4	Research	A	60	11.22	N/A	Alive	837	534	biopsy	Yes	3
90	26	F	2	Research	A	80	19.85	N/A	Alive	539	539	debulk	No	1
91	63	M	3	Audit	A	80	7.83	N/A	Alive	414	120	biopsy	Yes	1
92	63	M	4	Research	A	80	34.37	14.62	Died	154	124	debulk	Yes	3
93	40	F	2	Audit	ODG	90	6.49	N/A	Alive	1184	1184	debulk	Yes	1
94	53	F	4	Audit	A	60	13.64	16.42	Died	204	204	biopsy	Yes	2
95	62	M	4	Research	A	80	24.23	N/A	Died	498	405	debulk	Yes	3
96	34	M	4	Audit	A	80	15.25	N/A	Died	583	547	biopsy	Yes	1

Pt. No.	Age(V)	Sex	Grade	Recruitment	Cell line	PS	rTBVmax (T_2^*)	rTBVmax (T_1)	Status	O.S (days)	T.P (days)	Surgery	Steroid	Treatment
97	68	M	2	Audit	A	80	5.18	3.71	Died	520	346	biopsy	Yes	2
98	70	F	4	Audit	A	60	10.58	N/A	Died	270	270	biopsy	Yes	2
99	63	M	4	Audit	A	90	12.35	N/A	Died	300	300	biopsy	Yes	2
100	45	F	2	Research	A	80	2.41	N/A	Alive	378	378	debulk	Yes	1
101	29	M	2	Audit	A	90	6.81	N/A	Alive	697	697	biopsy	No	1
102	76	F	3	Audit	A	80	8	5.8	Alive	55	55	biopsy	Yes	3
103	59	F	3	Research	ODG	80	8.77	N/A	Alive	1169	1169	biopsy	Yes	2
104	18	F	2	Audit	A	80	3.5	N/A	Alive	1722	1507	biopsy	No	2
105	40	F	4	Research	A	80	26.94	N/A	Died	411	261	debulk	Yes	3
106	69	M	4	Audit	A	60	16.37	15.33	Died	70	70	debulk	Yes	2
107	24	M	3	Audit	ODG	80	18.79	N/A	Alive	433	685	biopsy	Yes	2
108	25	M	4	Audit	A	80	10	N/A	Alive	43	43	debulk	Yes	3
109	48	F	4	Audit	A	60	17.38	12.52	Alive	18	18	debulk	Yes	3
110	71	M	2	Audit	A	80	2.58	N/A	Died	1122	719	biopsy	No	1
111	76	F	4	Audit	A	60	10.88	N/A	Alive	15	15	debulk	Yes	3
112	29	F	2	Research	A	90	2.39	N/A	Alive	604	604	debulk	No	1
113	51	F	2	Audit	A	80	7.3	N/A	Died	177	177	debulk	Yes	1
114	78	M	4	Audit	A	90	13.28	N/A	Died	51	51	biopsy	Yes	1
115	50	M	2	Research	A	80	5.41	N/A	Alive	3768	3300	biopsy	Yes	3
116	48	M	2	Audit	ODG	80	6.44	N/A	Alive	3775	2620	biopsy	No	2
117	59	F	2	Research	A	80	1.91	N/A	Alive	1106	567	biopsy	No	2
118	69	M	4	Audit	A	60	10.81	N/A	Died	227	227	biopsy	Yes	2
119	42	M	2	Audit	ODG	80	4.24	N/A	Alive	1984	1984	debulk	No	1
120	29	M	2	Research	A	90	2.47	3.76	Alive	330	330	biopsy	No	1
121	53	M	3	Research	A	90	10.84	N/A	Alive	729	646	biopsy	Yes	2
122	73	M	2	Audit	A	90	5.65	N/A	Alive	474	293	biopsy	Yes	2
123	25	M	3	Research	A	80	3.69	N/A	Alive	760	673	debulk	Yes	2

Figure F.1: Demographic and clinical data of glioma patients, where; A means the cell line Astrocytoma; ODG, the cell line Oligodendroglioma or Oligoastrocytoma; PS, performance status; rTBV_{max} T_2^* and rTBV_{max} T_1 , the relative maximum tumour blood volume using, respectively, T_2^* and T_1 perfusion; O.S., overall survival; T.P., tumour progression and treatment, which was categorized into 1 (no treatment), 2 (Radiotherapy and/or Chemotherapy), and 3 (Radiotherapy and/or Chemotherapy plus Temozolomide).

Appendix G

Ethical Amendment

Leicestershire, Northamptonshire & Rutland Research Ethics Committee 1

The Old Chapel
Royal Standard Place
Nottingham
NG1 6FS

Tel: 0115 8839368
Fax: 0115 9123300

16 September 2010

Professor Dorothee Auer
Professor of Radiology
University of Nottingham
Queen's Medical Centre
Academic Radiology Department
Nottingham
NG7 2UH

Dear Professor Auer,

Study title: The prognostic value of multimodality MRI in brain tumours
REC reference: 08/H0406/102
Amendment number: 1
Amendment date: 09 September 2010

Thank you for your letter of 09 September 2010, notifying the Committee of the above amendment.

The Committee does not consider this to be a "substantial amendment" as defined in the Standard Operating Procedures for Research Ethics Committees. The amendment does not therefore require an ethical opinion from the Committee and may be implemented immediately, provided that it does not affect the approval for the research given by the R&D office for the relevant NHS care organisation.

Documents received

The documents received were as follows:

Document	Version	Date	
Investigator CV: Additional investigator		10 September 2010	
Notification of a Minor Amendment - additional member of research team	1	09 September 2010	

Statement of compliance

The Committee is constituted in accordance with the Governance Arrangements for Research Ethics Committees (July 2001) and complies fully with the Standard Operating Procedures for Research Ethics Committees in the UK.

08/H0406/102:

Please quote this number on all correspondence

Yours sincerely,

Miss Susie Cornick-Willis
Committee Co-ordinator

E-mail: susie.cornick-willis@nottspct.nhs.uk

Copy to: Mr Paul Cartledge – University of Nottingham

R&D office for NHS care organisation at lead site - NUH

Appendix H

QUADAS Items

	Items	Yes	No	Unclear
1	Was the spectrum of patients representative of the patients who will receive the test in practice?	()	()	()
2	Were selection criteria clearly described?	()	()	()
3	Is the reference standard likely to correctly classify the target condition?	()	()	()
4	Is the time period between reference standard and index test short enough to be reasonably sure that the target condition did not change between the two tests?	()	()	()
5	Did the whole sample or a random selection of the sample, receive verification using a reference standard of diagnosis?	()	()	()
6	Did patients receive the same reference standard regardless of the index test result?	()	()	()
7	Was the reference standard independent of the index test (i.e. the index test did not form part of the reference standard)?	()	()	()
8	Was the execution of the index test described in sufficient detail to permit replication of the test?	()	()	()
9	Was the execution of the reference standard described in sufficient detail to permit its replication?	()	()	()
10	Were the index test results interpreted without knowledge of the results of the reference standard?	()	()	()
11	Were the reference standard results interpreted without knowledge of the results of the index test?	()	()	()
12	Were the same clinical data available when test results were interpreted as would be available when the test is used in practice?	()	()	()
13	Were uninterpretable/ intermediate test results reported?	()	()	()
14	Were withdrawals from the study explained?	()	()	()

Table H.1: QUADAS Items

Bibliography

- N. J. Abbott, D. C. Chugani, G. Zaharchuk, B. R. Rosen, and E. H. Lo. Delivery of imaging agents into brain. *Adv Drug Deliv Rev*, 37(1-3):253–277, 1999.
- N. S. Akella, D. B. Twieg, T. Mikkelsen, F. H. Hochberg, S. Grossman, G. A. Cloud, and L. B. Nabors. Assessment of brain tumor angiogenesis inhibitors using perfusion magnetic resonance imaging: Quality and analysis results of a phase I trial. *J Magn Reson Imaging*, 20(6):913–22, 2004.
- F. Allahdini, A. Amirjamshidi, M. Reza-Zarei, and M. Abdollahi. Evaluating the prognostic factors effective on the outcome of patients with glioblastoma multiformis: Does maximal resection of the tumor lengthen the median survival? *World Neurosurg*, 73(2):128–34; discussion e16, Feb 2010. doi: 10.1016/j.wneu.2009.06.001. URL <http://dx.doi.org/10.1016/j.wneu.2009.06.001>.
- J. C. Anderson, B. C. McFarland, and C. L. Gladson. New molecular targets in angiogenic vessels of glioblastoma tumours. *Expert Rev Mol Med*, 10:e23, 2008.

- H. Aronen and J. Perki. Dynamic susceptibility contrast MRI of gliomas. *Neuroimaging Clin N Am*, 12(4):501–523, Nov 2002.
- H. J. Aronen, I. E. Gazit, D. N. Louis, B. R. Buchbinder, F. S. Pardo, R. M. Weisskoff, G. R. Harsh, G. R. Cosgrove, E. F. Halpern, and F. H. Hochberg, et al. Cerebral blood volume maps of gliomas: Comparison with tumor grade and histologic findings. *Radiology*, 191(1):41–51, 1994.
- H. J. Aronen, J. Glass, F. S. Pardo, J. W. Belliveau, M. L. Gruber, B. R. Buchbinder, I. E. Gazit, R. M. Linggood, A. J. Fischman, and B. R. Rosen. Echo-planar MR cerebral blood volume mapping of gliomas. Clinical utility. *Acta Radiol*, 36(5):520–528, Sep 1995.
- H. R. Arvinda, C. Kesavadas, P. S. Sarma, B. Thomas, V. V. Radhakrishnan, A. K. Gupta, T. R. Kapilamoorthy, and S. Nair. Glioma grading: Sensitivity, specificity, positive and negative predictive values of diffusion and perfusion imaging. *J Neurooncol*, 94(1):87–96, 2009.
- M. F. Back, E. L. Ang, W. H. Ng, S. J. See, C. C. Lim, S. P. Chan, and T. T. Yeo. Improved median survival for glioblastoma multiforme following introduction of adjuvant temozolomide chemotherapy. *Ann Acad Med Singapore*, 36(5):338–42, 2007.
- R. F. Barajas, Jr., J. S. Chang, M. R. Segal, A. T. Parsa, M. W. McDermott, M. S. Berger, and S. Cha. Differentiation of recurrent glioblastoma multiforme from radiation necrosis after external beam radiation therapy with dynamic susceptibility-weighted contrast-enhanced perfusion MR imaging. *Radiology*, 253(2):486–96, 2009.

- F. G. Barker, M. D. Prados, S. M. Chang, P. H. Gutin, K. R. Lamborn, D. A. Larson, M. K. Malec, M. W. McDermott, P. K. Sneed, W. M. Wara, and C. B. Wilson. Radiation response and survival time in patients with glioblastoma multiforme. *J Neurosurg*, 84(3):442–448, Mar 1996. doi: 10.3171/jns.1996.84.3.0442. URL <http://dx.doi.org/10.3171/jns.1996.84.3.0442>.
- M. Barri, C. Couprie, H. Dufour, D. Figarella-Branger, X. Muracciole, K. Hoang-Xuan, D. Braguer, P. M. Martin, J. C. Peragut, F. Grisoli, and O. Chinot. Temozolomide in combination with bcnu before and after radiotherapy in patients with inoperable newly diagnosed glioblastoma multiforme. *Ann Oncol*, 16(7):1177–1184, Jul 2005. doi: 10.1093/annonc/mdi225. URL <http://dx.doi.org/10.1093/annonc/mdi225>.
- M. E. Bastin, T. K. Carpenter, P. A. Armitage, S. Sinha, J. M. Wardlaw, and I. R. Whittle. Effects of dexamethasone on cerebral perfusion and water diffusion in patients with high-grade glioma. *AJNR Am J Neuroradiol*, 27(2):402–8, 2006.
- A. Batra, R. P. Tripathi, and A. K. Singh. Perfusion magnetic resonance imaging and magnetic resonance spectroscopy of cerebral gliomas showing imperceptible contrast enhancement on conventional magnetic resonance imaging. *Australas Radiol*, 48(3):324–32, 2004.
- G. S. Bauman, Y. Ino, K. Ueki, M. C. Zlatescu, B. J. Fisher, D. R. Macdonald, L. Stitt, D. N. Louis, and J. G. Cairncross. Allelic loss of chromo-

- some 1p and radiotherapy plus chemotherapy in patients with oligodendrogliomas. *Int J Radiat Oncol Biol Phys*, 48(3):825–30, 2000.
- A. Behin, K. Hoang-Xuan, A. F. Carpentier, and J. Y. Delattre. Primary brain tumours in adults. *Lancet*, 361(9354):323–31, 2003.
- M. Bernstein. Outpatient craniotomy for brain tumor: A pilot feasibility study in 46 patients. *Can J Neurol Sci*, 28(2):120–4, 2001.
- M. Bernstein and A. G. Parrent. Complications of CT-guided stereotactic biopsy of intra-axial brain lesions. *J Neurosurg*, 81(2):165–8, 1994.
- W. Bian, I. S. Khayal, J. M. Lupo, C. McGue, S. Vandenberg, K. R. Lamborn, S. M. Chang, S. Cha, and S. J. Nelson. Multiparametric characterization of grade 2 glioma subtypes using magnetic resonance spectroscopic, perfusion, and diffusion imaging. *Transl Oncol*, 2(4):271–80, 2009.
- S. Bisdas, M. Kirkpatrick, P. Giglio, C. Welsh, M. V. Spampinato, and Z. Rumboldt. Cerebral blood volume measurements by perfusion-weighted MR imaging in gliomas: Ready for prime time in predicting short-term outcome and recurrent disease? *AJNR Am J Neuroradiol*, 30(4):681–8, 2009.
- F. G. Blankenberg, R. L. Teplitz, W. Ellis, M. S. Salamat, B. H. Min, L. Hall, D. B. Boothroyd, I. M. Johnstone, and D. R. Enzmann. The influence of volumetric tumor doubling time, DNA ploidy, and histologic grade on the survival of patients with intracranial astrocytomas. *AJNR Am J Neuroradiol*, 16(5):1001–12, 1995.

- J. L. Boxerman, L. M. Hamberg, B. R. Rosen, and R. M. Weisskoff. MR contrast due to intravascular magnetic susceptibility perturbations. *Magn Reson Med*, 34(4):555–66, 1995.
- J. L. Boxerman, K. M. Schmainda, and R. M. Weisskoff. Relative cerebral blood volume maps corrected for contrast agent extravasation significantly correlate with glioma tumor grade, whereas uncorrected maps do not. *AJNR Am J Neuroradiol*, 27(4):859–67, 2006.
- G. Brasil Caseiras, O. Ciccarelli, D. R. Altmann, C. E. Benton, D. J. Tozer, P. S. Tofts, T. A. Yousry, J. Rees, A. D. Waldman, and H. R. Jager. Low-grade gliomas: Six-month tumor growth predicts patient outcome better than admission tumor volume, relative cerebral blood volume, and apparent diffusion coefficient. *Radiology*, 253(2):505–12, 2009.
- A. Brickman, A. Zahra, J. Muraskin, J. Steffener, C. Holland, C. Habeck, A. Borogovac, M. Ramos, T. Brown, I. Asllani, and Y. Stern. Reduction in cerebral blood flow in areas appearing as white matter hyperintensities on magnetic resonance imaging. *Psychiatry Res*, 172(2):117–120, May 2009. doi: 10.1016/j.psychresns.2008.11.006. URL <http://dx.doi.org/10.1016/j.psychresns.2008.11.006>.
- R. Bruening, R. H. Wu, T. A. Yousry, C. Berchtenbreiter, J. Weber, M. Peller, H. J. Steiger, and M. Reiser. Regional relative blood volume MR maps of meningiomas before and after partial embolization. *J Comput Assist Tomogr*, 22(1):104–10, 1998.
- N. Bulakbasi, M. Kocaoglu, A. Farzaliyev, C. Tayfun, T. Ucoz, and I. So-

- muncu. Assessment of diagnostic accuracy of perfusion MR imaging in primary and metastatic solitary malignant brain tumors. *AJNR Am J Neuroradiol*, 26(9):2187–99, 2005.
- J. G. Cairncross, K. Ueki, M. C. Zlatescu, D. K. Lisle, D. M. Finkelstein, R. R. Hammond, J. S. Silver, P. C. Stark, D. R. Macdonald, Y. Ino, D. A. Ramsay, and D. N. Louis. Specific genetic predictors of chemotherapeutic response and survival in patients with anaplastic oligodendrogliomas. *J Natl Cancer Inst*, 90(19):1473–9, 1998.
- C. Calli, O. Kitis, N. Yuntun, T. Yurtseven, S. Islekel, and T. Akalin. Perfusion and diffusion MR imaging in enhancing malignant cerebral tumors. *Eur J Radiol*, 58(3):394–403, 2006.
- V. Callot, D. Galanaud, D. Figarella-Branger, Y. Lefur, P. Metellus, F. Nicoli, and P. Cozzone. Correlations between MR and endothelial hyperplasia in low-grade gliomas. *J Magn Reson Imaging*, 26(1):52–60, 2007.
- Y. Cao, C. I. Tsien, Z. Shen, D. S. Tatro, R. Ten Haken, M. L. Kessler, T. L. Chenevert, and T. S. Lawrence. Use of magnetic resonance imaging to assess blood-brain/blood-glioma barrier opening during conformal radiotherapy. *J Clin Oncol*, 23(18):4127–36, 2005.
- Y. Cao, V. Nagesh, D. Hamstra, C. I. Tsien, B. D. Ross, T. L. Chenevert, L. Junck, and T. S. Lawrence. The extent and severity of vascular leakage as evidence of tumor aggressiveness in high-grade gliomas. *Cancer Res*, 66(17):8912–7, 2006.

- J. A. Carrillo, A. Lai, P. L. Nghiemphu, H. J. Kim, H. S. Phillips, S. Kharbanda, P. Moftakhar, S. Lalaezari, W. Yong, B. M. Ellingson, T. F. Cloughesy, and W. B. Pope. Relationship between tumor enhancement, edema, IDH1 mutational status, MGMT promoter methylation, and survival in glioblastoma. *AJNR Am J Neuroradiol*, Feb 2012. doi: 10.3174/ajnr.A2950. URL <http://dx.doi.org/10.3174/ajnr.A2950>.
- K. Carson, S. Grossman, J. Fisher, and E. Shaw. Prognostic factors for survival in adult patients with recurrent glioma enrolled onto the new approaches to brain tumor therapy CNS consortium phase I and II clinical trials. *J Clin Oncol*, 25(18):2601–2606, Jun 2007. doi: 10.1200/JCO.2006.08.1661. URL <http://dx.doi.org/10.1200/JCO.2006.08.1661>.
- G. B. Caseiras, J. S. Thornton, T. Yousry, C. Benton, J. Rees, A. D. Waldman, and H. R. Jager. Inclusion or exclusion of intratumoral vessels in relative cerebral blood volume characterization in low-grade gliomas: Does it make a difference? *AJNR Am J Neuroradiol*, 29(6):1140–1, 2008.
- I. Catalaa, R. Henry, W. P. Dillon, E. E. Graves, T. R. McKnight, Y. Lu, D. B. Vigneron, and S. J. Nelson. Perfusion, diffusion and spectroscopy values in newly diagnosed cerebral gliomas. *NMR Biomed*, 19(4):463–75, 2006.
- S. Cha, E. A. Knopp, G. Johnson, S. G. Wetzel, A. W. Litt, and D. Zagzag. Intracranial mass lesions: Dynamic contrast-enhanced susceptibility-weighted echo-planar perfusion MR imaging. *Radiology*, 223(1):11–29, 2002.

- S. Cha, T. Tihan, F. Crawford, N. J. Fischbein, S. Chang, A. Bollen, S. J. Nelson, M. Prados, M. S. Berger, and W. P. Dillon. Differentiation of low-grade oligodendrogliomas from low-grade astrocytomas by using quantitative blood-volume measurements derived from dynamic susceptibility contrast-enhanced MR imaging. *AJNR Am J Neuroradiol*, 26(2):266–73, 2005.
- S. Cha, L. Yang, G. Johnson, A. Lai, M. H. Chen, T. Tihan, M. Wendland, and W. P. Dillon. Comparison of microvascular permeability measurements, $K(\text{trans})$, determined with conventional steady-state T1-weighted and first-pass T2*-weighted MR imaging methods in gliomas and meningiomas. *AJNR Am J Neuroradiol*, 27(2):409–17, 2006.
- S. Cha, J. M. Lupo, M. H. Chen, K. R. Lamborn, M. W. McDermott, M. S. Berger, S. J. Nelson, and W. P. Dillon. Differentiation of glioblastoma multiforme and single brain metastasis by peak height and percentage of signal intensity recovery derived from dynamic susceptibility-weighted contrast-enhanced perfusion MR imaging. *AJNR Am J Neuroradiol*, 28(6):1078–84, 2007.
- M. Chamberlain and S. Johnston. High-dose methotrexate and rituximab with deferred radiotherapy for newly diagnosed primary B-cell CNS lymphoma. *Neuro Oncol*, 12(7):736–744, Jul 2010. doi: 10.1093/neuonc/noq011. URL <http://dx.doi.org/10.1093/neuonc/noq011>.
- E. F. Chang, A. Clark, R. L. Jensen, M. Bernstein, A. Guha, G. Carrabba, D. Mukhopadhyay, W. Kim, L. M. Liau, S. M. Chang, J. S. Smith, M. S.

- Berger, and M. W. McDermott. Multiinstitutional validation of the university of california at san francisco low-grade glioma prognostic scoring system. clinical article. *J Neurosurg*, 111(2):203–10, 2009.
- L. Chang, D. McBride, B. L. Miller, M. Cornford, R. A. Booth, S. D. Buchthal, T. M. Ernst, and D. Jenden. Localized in vivo 1h magnetic resonance spectroscopy and in vitro analyses of heterogeneous brain tumors. *J Neuroimaging*, 5(3):157–63, 1995.
- S. M. Chang and F. G. Barker 2nd. Marital status, treatment, and survival in patients with glioblastoma multiforme: A population based study. *Cancer*, 104(9):1975–84, 2005.
- C. Chaskis, T. Stadnik, A. Michotte, K. Van Rompaey, and J. D’Haens. Prognostic value of perfusion-weighted imaging in brain glioma: A prospective study. *Acta Neurochir (Wien)*, 148(3):277–85; discussion 285, 2006.
- I. C. Chiang, Y. T. Kuo, C. Y. Lu, K. W. Yeung, W. C. Lin, F. O. Sheu, and G. C. Liu. Distinction between high-grade gliomas and solitary metastases using peritumoral 3-t magnetic resonance spectroscopy, diffusion, and perfusion imagings. *Neuroradiology*, 46(8):619–27, 2004.
- S. K. Cho, D. G. Na, J. W. Ryoo, H. G. Roh, C. H. Moon, H. S. Byun, and J. H. Kim. Perfusion MR imaging: Clinical utility for the differential diagnosis of various brain tumors. *Korean J Radiol*, 3(3):171–9, 2002.
- K. L. Chow, Y. P. Gobin, T. Cloughesy, J. W. Sayre, J. P. Villablanca, and F. Vinuela. Prognostic factors in recurrent glioblastoma multiforme and

- anaplastic astrocytoma treated with selective intra-arterial chemotherapy. *AJNR Am J Neuroradiol*, 21(3):471–8, 2000.
- E. Claus and P. Black. Survival rates and patterns of care for patients diagnosed with supratentorial low-grade gliomas: Data from the SEER program, 1973–2001. *Cancer*, 106(6):1358–1363, Mar 2006. doi: 10.1002/cncr.21733. URL <http://dx.doi.org/10.1002/cncr.21733>.
- R. J. Coffey, L. D. Lunsford, and F. H. Taylor. Survival after stereotactic biopsy of malignant gliomas. *Neurosurgery*, 22(3):465–73, 1988.
- J. Concato, P. Peduzzi, T. R. Holford, and A. R. Feinstein. Importance of events per independent variable in proportional hazards analysis. I. Background, goals, and general strategy. *J Clin Epidemiol*, 48(12):1495–501, 1995.
- F. W. Crawford, I. S. Khayal, C. McGue, S. Saraswathy, A. Pirzkall, S. Cha, K. R. Lamborn, S. M. Chang, M. S. Berger, and S. J. Nelson. Relationship of pre-surgery metabolic and physiological MR imaging parameters to survival for patients with untreated gbm. *J Neurooncol*, 91(3):337–51, 2009.
- V. Crooks, S. Waller, T. Smith, and T. J. Hahn. The use of the Karnofsky Performance Scale in determining outcomes and risk in geriatric outpatients. *J Gerontol*, 46(4):M139–M144, Jul 1991.
- R. Dammers, J. Schouten, I. Haitzma, A. Vincent, J. Kros, and C. Dirven. Towards improving the safety and diagnostic yield of stereotactic

- biopsy in a single centre. *Acta Neurochir (Wien)*, 152(11):1915–1921, Nov 2010. doi: 10.1007/s00701-010-0752-0. URL <http://dx.doi.org/10.1007/s00701-010-0752-0>.
- N. Danchaivijitr, A. D. Waldman, D. J. Tozer, C. E. Benton, G. Brasil Casseiras, P. S. Tofts, J. H. Rees, and H. R. Jager. Low-grade gliomas: Do changes in rCBV measurements at longitudinal perfusion-weighted MR imaging predict malignant transformation? *Radiology*, 247(1):170–8, 2008.
- C. Daumas-Duport, B. Scheithauer, J. O’Fallon, and P. Kelly. Grading of astrocytomas. a simple and reproducible method. *Cancer*, 62(10):2152–65, 1988.
- F. G. Davis, B. J. McCarthy, and M. S. Berger. Centralized databases available for describing primary brain tumor incidence, survival, and treatment: Central Brain Tumor Registry of the United States; Surveillance, Epidemiology, and End Results; and National Cancer Data Base. *Neuro Oncol*, 1(3):205–11, 1999.
- J. M. Derlon, F. Chapon, M. H. Noel, S. Khouri, K. Benali, M. C. Petit-Taboue, J. P. Houtteville, M. H. Chajari, and G. Bouvard. Non-invasive grading of oligodendrogliomas: Correlation between in vivo metabolic pattern and histopathology. *Eur J Nucl Med*, 27(7):778–87, 2000.
- R. DerSimonian and N. Laird. Meta-analysis in clinical trials. *Control Clin Trials*, 7(3):177–88, 1986.
- W. L. Deville, F. Buntinx, L. M. Bouter, V. M. Montori, H. C. de Vet, D. A. van der Windt, and P. D. Bezemer. Conducting systematic reviews

- of diagnostic studies: Didactic guidelines. *BMC Med Res Methodol*, 2:9, 2002.
- F. Dhermain, G. Saliou, F. Parker, P. Page, K. Hoang-Xuan, C. Lacroix, E. Tournay, J. Bourhis, and D. Ducreux. Microvascular leakage and contrast enhancement as prognostic factors for recurrence in unfavorable low-grade gliomas. *J Neurooncol*, 2009.
- A. Di Costanzo, S. Pollice, F. Trojsi, G. M. Giannatempo, T. Popolizio, L. Canalis, M. Armillotta, A. Maggialetti, A. Carriero, G. Tedeschi, and T. Scarabino. Role of perfusion-weighted imaging at 3 Tesla in the assessment of malignancy of cerebral gliomas. *Radiol Med (Torino)*, 113(1):134–43, 2008.
- K. M. Donahue, H. G. Krouwer, S. D. Rand, A. P. Pathak, C. S. Marszalkowski, S. C. Censky, and R. W. Prost. Utility of simultaneously acquired gradient-echo and spin-echo cerebral blood volume and morphology maps in brain tumor patients. *Magn Reson Med*, 43(6):845–53, 2000.
- G. C. Doms, S. Hecht, M. Brant-Zawadzki, Y. Berthiaume, D. Norman, and T. H. Newton. Brain radiation lesions: MR imaging. *Radiology*, 158(1):149–155, Jan 1986.
- S. Drabycz, G. Roldn, P. de Robles, D. Adler, J. McIntyre, A. Magliocco, J. Cairncross, and J. Mitchell. An analysis of image texture, tumor location, and MGMT promoter methylation in glioblastoma using magnetic resonance imaging. *Neuroimage*, 49(2):1398–1405, Jan 2010. doi:

- 10.1016/j.neuroimage.2009.09.049. URL <http://dx.doi.org/10.1016/j.neuroimage.2009.09.049>.
- H. J. Dubbink, W. Taal, R. van Marion, J. M. Kros, I. van Heuvel, J. E. Bromberg, B. A. Zonnenberg, C. Zonnenberg, T. J. Postma, J. Gijtenbeek, W. Boogerd, F. H. Groenendijk, P. Smitt, W. Dinjens, and M. J. van den Bent. IDH1 mutations in low-grade astrocytomas predict survival but not response to temozolomide. *Neurology*, 73(21):1792–1795, Nov 2009. doi: 10.1212/WNL.0b013e3181c34ace. URL <http://dx.doi.org/10.1212/WNL.0b013e3181c34ace>.
- R. Durmaz, M. Vural, E. I?ildi, E. Co?an, E. Ozkara, C. Bal, E. Cifti, A. Arslanta?, Metin, and Atasoy. Efficacy of prognostic factors on survival in patients with low grade glioma. *Turk Neurosurg*, 18(4):336–344, Oct 2008.
- M. Ekici, T. Bulut, B. Tucer, and A. Kurtsoy. Analysis of the mortality probability of preoperative MRI features in malignant astrocytomas. *Turk Neurosurg*, 21(3):271–279, 2011. doi: 10.5137/1019-5149.JTN.3321-10.3. URL <http://dx.doi.org/10.5137/1019-5149.JTN.3321-10.3>.
- S. K. Ellika, R. Jain, S. C. Patel, L. Scarpace, L. R. Schultz, J. P. Rock, and T. Mikkelsen. Role of perfusion ct in glioma grading and comparison with conventional MR imaging features. *AJNR Am J Neuroradiol*, 28(10):1981–7, 2007.
- K. E. Emblem, B. Nedregard, T. Nome, P. Due-Tonnessen, J. K. Hald, D. Scheie, O. C. Borota, M. Cvancarova, and A. Bjornerud. Glioma grading

- by using histogram analysis of blood volume heterogeneity from mr-derived cerebral blood volume maps. *Radiology*, 247(3):808–17, 2008a.
- K. E. Emblem, D. Scheie, P. Due-Tonnessen, B. Nedregard, T. Nome, J. K. Hald, K. Beiske, T. R. Meling, and A. Bjornerud. Histogram analysis of MR imaging-derived cerebral blood volume maps: Combined glioma grading and identification of low-grade oligodendroglial subtypes. *AJNR Am J Neuroradiol*, 2008b.
- Herbert H Engelhard, Ana Stelea, and Arno Mundt. Oligodendroglioma and anaplastic oligodendroglioma: clinical features, treatment, and prognosis. *Surg Neurol*, 60(5):443–456, Nov 2003.
- M. Farhoudi, K. Mehrvar, N. Aslanabadi, K. Ghabili, N. Baghmishe, and F. Ilkhchoei. Doppler study of cerebral arteries in hypercholesterolemia. *Vasc Health Risk Manag*, 7:203–207, 2011. doi: 10.2147/VHRM.S18663. URL <http://dx.doi.org/10.2147/VHRM.S18663>.
- G. Filippini, C. Falcone, A. Boiardi, G. Broggi, M. Bruzzone, D. Caldiroli, R. Farina, M. Farinotti, L. Fariselli, G. Finocchiaro, S. Giombini, B. Pollo, M. Savoiaro, C. Solero, M. Valsecchi, and Brain Cancer Register of the Fondazione IRCCS (Istituto Ricovero e Cura a Carattere Scientifico) Istituto Neurologico Carlo Besta. Prognostic factors for survival in 676 consecutive patients with newly diagnosed primary glioblastoma. *Neuro Oncol*, 10(1):79–87, Feb 2008. doi: 10.1215/15228517-2007-038. URL <http://dx.doi.org/10.1215/15228517-2007-038>.
- J. R. Flynn, L. Wang, D. L. Gillespie, G. J. Stoddard, J. K. Reid, J. Owens,

- G. B. Ellsworth, K. L. Salzman, A. Y. Kinney, and R. L. Jensen. Hypoxia-regulated protein expression, patient characteristics, and preoperative imaging as predictors of survival in adults with glioblastoma multiforme. *Cancer*, 113(5):1032–42, 2008.
- O. Fujii, T. Soejima, Y. Kuwatsuka, A. Harada, Y. Ota, K. Tsujino, M. Sasaki, H. Kudo, M. Nishihara, and K. Taomoto. Supratentorial glioblastoma treated with radiotherapy: Use of the radiation therapy oncology group recursive partitioning analysis grouping for predicting survival. *Jpn J Clin Oncol*, 40(8):726–731, Aug 2010. doi: 10.1093/jjco/hyq051. URL <http://dx.doi.org/10.1093/jjco/hyq051>.
- F. H. Gilles, W. D. Brown, A. Leviton, C. J. Tavar, L. Adelman, L. B. Rorke, R. L. Davis, and T. E. Hedley-Whyte. Limitations of the world health organization classification of childhood supratentorial astrocytic tumors. children brain tumor consortium. *Cancer*, 88(6):1477–1483, Mar 2000.
- T. Gorlia, M. J. van den Bent, M. E. Hegi, R. O. Mirimanoff, M. Weller, J. G. Cairncross, E. Eisenhauer, K. Belanger, A. A. Brandes, A. Allgeier, D. Lacombe, and R. Stupp. Nomograms for predicting survival of patients with newly diagnosed glioblastoma: Prognostic factor analysis of EORTC and NCIC trial 26981-22981/CE.3. *Lancet Oncol*, 9(1):29–38, 2008.
- J. S. Guillaumo, A. Monjour, L. Taillandier, B. Devaux, P. Varlet, C. Haie-Meder, G. L. Defer, P. Maison, J. J. Mazon, P. Cornu, J. Y. Delattre, and Association des Neuro-Oncologues d’Expression Franaise (ANOCEF).

- Brainstem gliomas in adults: Prognostic factors and classification. *Brain*, 124(Pt 12):2528–2539, Dec 2001.
- B. Hakyemez, C. Erdogan, I. Ercan, N. Ergin, S. Uysal, and S. Atahan. High-grade and low-grade gliomas: Differentiation by using perfusion MR imaging. *Clin Radiol*, 60(4):493–502, 2005.
- B. Hakyemez, C. Erdogan, N. Bolca, N. Yildirim, G. Gokalp, and M. Parlak. Evaluation of different cerebral mass lesions by perfusion-weighted MR imaging. *J Magn Reson Imaging*, 24(4):817–24, 2006.
- W. A. Hall. The safety and efficacy of stereotactic biopsy for intracranial lesions. *Cancer*, 82(9):1749–55, 1998.
- T. Hara, N. Kosaka, N. Shinoura, and T. Kondo. Pet imaging of brain tumor with [methyl-11c]choline. *J Nucl Med*, 38(6):842–7, 1997.
- T. Hara, T. Kondo, and N. Kosaka. Use of 18f-choline and 11c-choline as contrast agents in positron emission tomography imaging-guided stereotactic biopsy sampling of gliomas. *J Neurosurg*, 99(3):474–9, 2003.
- M. Haris, R. K. Gupta, A. Singh, N. Husain, M. Husain, C. M. Pandey, C. Srivastava, S. Behari, and R. K. Rathore. Differentiation of infective from neoplastic brain lesions by dynamic contrast-enhanced MRI. *Neuroradiology*, 50(6):531–40, 2008.
- H. A. Haroon, T. F. Patankar, X. P. Zhu, K. L. Li, N. A. Thacker, M. J. Scott, and A. Jackson. Comparison of cerebral blood volume maps generated

- from t_2^* and t_1 weighted MRI data in intra-axial cerebral tumours. *Br J Radiol*, 80(951):161–8, 2007.
- M. Hartmann, S. Heiland, I. Harting, V. M. Tronnier, C. Sommer, R. Ludwig, and K. Sartor. Distinguishing of primary cerebral lymphoma from high-grade glioma with perfusion-weighted magnetic resonance imaging. *Neurosci Lett*, 338(2):119–22, 2003.
- M. Hegi, A.-C. Diserens, S. Godard, P.-Y. Dietrich, L. Regli, S. Ostermann, P. Otten, G. Van Melle, N. de Tribolet, and R. Stupp. Clinical trial substantiates the predictive value of O-6-methylguanine-dna methyltransferase promoter methylation in glioblastoma patients treated with temozolomide. *Clin Cancer Res*, 10(6):1871–1874, Mar 2004.
- R. G. Henry, D. B. Vigneron, N. J. Fischbein, P. E. Grant, M. R. Day, S. M. Noworolski, J. M. Star-Lack, L. L. Wald, W. P. Dillon, S. M. Chang, and S. J. Nelson. Comparison of relative cerebral blood volume and proton spectroscopy in patients with treated gliomas. *AJNR Am J Neuroradiol*, 21(2):357–66, 2000.
- T. Hirai, R. Murakami, H. Nakamura, M. Kitajima, H. Fukuoka, A. Sasao, M. Akter, Y. Hayashida, R. Toya, N. Oya, K. Awai, K. Iyama, J. I. Kuratsu, and Y. Yamashita. Prognostic value of perfusion MR imaging of high-grade astrocytomas: long-term follow-up study. *AJNR Am J Neuroradiol*, 29(8):1505–10, 2008.
- T. Homma, T. Fukushima, S. Vaccarella, Y. Yonekawa, P. L. Di Patre, S. Franceschi, and H. Ohgaki. Correlation among pathology, genotype,

- and patient outcomes in glioblastoma. *J Neuropathol Exp Neurol*, 65(9): 846–54, 2006.
- K. A. Hossman and M. Bloink. Blood flow and regulation of blood flow in experimental peritumoral edema. *Stroke*, 12(2):211–7, 1981.
- B. L. Hou, M. Bradbury, K. K. Peck, N. M. Petrovich, P. H. Gutin, and A. I. Holodny. Effect of brain tumor neovasculature defined by rcbv on bold fMRI, activation volume in the primary motor cortex. *Neuroimage*, 32(2): 489–97, 2006.
- L. S. Hu, L. C. Baxter, K. A. Smith, B. G. Feuerstein, J. P. Karis, J. M. Eschbacher, S. W. Coons, P. Nakaji, R. F. Yeh, J. Debbins, and J. E. Heiserman. Relative cerebral blood volume values to differentiate high-grade glioma recurrence from posttreatment radiation effect: Direct correlation between image-guided tissue histopathology and localized dynamic susceptibility-weighted contrast-enhanced perfusion MR imaging measurements. *AJNR Am J Neuroradiol*, 30(3):552–8, 2009.
- L. S. Hu, L. C. Baxter, D. S. Pinnaduwage, T. L. Paine, J. P. Karis, B. G. Feuerstein, K. M. Schmainda, A. C. Dueck, J. Debbins, K. A. Smith, P. Nakaji, J. M. Eschbacher, S. W. Coons, and J. E. Heiserman. Optimized preload leakage-correction methods to improve the diagnostic accuracy of dynamic susceptibility-weighted contrast-enhanced perfusion MR imaging in posttreatment gliomas. *AJNR Am J Neuroradiol*, 31(1):40–8, 2010.
- K. S. Hung and S. L. Howng. Prognostic significance of annexin vii expression in glioblastomas multiforme in humans. *J Neurosurg*, 99(5):886–92, 2003.

- A. Idbah, C. Dalmasso, M. Kouwenhoven, J. Jeuken, C. Carpentier, T. Gorlia, J. Kros, P. French, J. Teepen, P. Brot, O. Delattre, K. Mokhtari, M. Sanson, J.-Y. Delattre, M. van den Bent, and K. Hoang-Xuan. Genomic aberrations associated with outcome in anaplastic oligodendroglial tumors treated within the EORTC phase III trial 26951. *J Neurooncol*, 103(2):221–230, Jun 2011. doi: 10.1007/s11060-010-0380-9. URL <http://dx.doi.org/10.1007/s11060-010-0380-9>.
- G. Iida, K. Ogawa, S. Ishiuchi, I. Chiba, T. Watanabe, N. Katsuyama, Y. Yoshii, and S. Murayama. Clinical significance of thallium-201 SPECT after postoperative radiotherapy in patients with glioblastoma multiforme. *J Neurooncol*, 103(2):297–305, Jun 2011. doi: 10.1007/s11060-010-0373-8. URL <http://dx.doi.org/10.1007/s11060-010-0373-8>.
- C. Irwin, M. Hunn, G. Purdie, and D. Hamilton. Delay in radiotherapy shortens survival in patients with high grade glioma. *J Neurooncol*, 85(3):339–43, 2007.
- A. Jackson, A. Kassner, D. Annesley-Williams, H. Reid, X. P. Zhu, and K. L. Li. Abnormalities in the recirculation phase of contrast agent bolus passage in cerebral gliomas: Comparison with relative blood volume and tumor grade. *AJNR Am J Neuroradiol*, 23(1):7–14, 2002.
- R. J. Jackson, G. N. Fuller, D. Abi-Said, F. F. Lang, Z. L. Gokaslan, W. M. Shi, D. M. Wildrick, and R. Sawaya. Limitations of stereotactic biopsy in the initial management of gliomas. *Neuro Oncol*, 3(3):193–200, 2001.
- R. Jain, S. K. Ellika, L. Scarpace, L. R. Schultz, J. P. Rock, J. Gutierrez,

- S. C. Patel, J. Ewing, and T. Mikkelsen. Quantitative estimation of permeability surface-area product in astroglial brain tumors using perfusion ct and correlation with histopathologic grade. *AJNR Am J Neuroradiol*, 29(4):694–700, 2008.
- R. K. Jain. Normalization of tumor vasculature: An emerging concept in antiangiogenic therapy. *Science*, 307(5706):58–62, 2005.
- K. A. Jellinger and W. Paulus. Primary central nervous system lymphomas—an update. *J Cancer Res Clin Oncol*, 119(1):7–27, 1992.
- M. D. Jenkinson, D. G. Du Plessis, C. Walker, and T. S. Smith. Advanced MRI in the management of adult gliomas. *Br J Neurosurg*, 21(6):550–61, 2007.
- S. E. Kaba and A. P. Kyritsis. Recognition and management of gliomas. *Drugs*, 53(2):235–44, 1997.
- P. J. Kelly and C. Hunt. The limited value of cytoreductive surgery in elderly patients with malignant gliomas. *Neurosurgery*, 34(1):62–6; discussion 66–7, 1994.
- G. Kitange, A. Misra, M. Law, S. Passe, T. M. Kollmeyer, M. Maurer, K. Ballman, B. G. Feuerstein, and R. B. Jenkins. Chromosomal imbalances detected by array comparative genomic hybridization in human oligodendrogliomas and mixed oligoastrocytomas. *Genes Chromosomes Cancer*, 42(1):68–77, 2005.

- P. Kleihues and H. Ohgaki. Phenotype vs genotype in the evolution of astrocytic brain tumors. *Toxicol Pathol*, 28(1):164–70, 2000.
- P. Kleihues and L. H. Sobin. World health organization classification of tumors. *Cancer*, 88(12):2887, 2000.
- P. Kleihues, P. C. Burger, and B. W. Scheithauer. The new who classification of brain tumours. *Brain Pathol*, 3(3):255–268, Jul 1993.
- P. Kleihues, F. Soylemezoglu, B. Schauble, B. W. Scheithauer, and P. C. Burger. Histopathology, classification, and grading of gliomas. *Glia*, 15(3):211–21, 1995.
- E. A. Knopp, S. Cha, G. Johnson, A. Mazumdar, J. G. Golfinos, D. Zagzag, D. C. Miller, P. J. Kelly, and II Kricheff. Glial neoplasms: Dynamic contrast-enhanced T2*-weighted MR imaging. *Radiology*, 211(3):791–8, 1999.
- M. Kocher, P. Frommolt, S. K. Borberg, U. Ruhl, M. Steingraber, M. Niewald, S. Staar, M. Stuschke, G. Becker, A. R. Fishedick, K. Herfarth, H. Grauthoff, and R. P. Muller. Randomized study of postoperative radiotherapy and simultaneous temozolomide without adjuvant chemotherapy for glioblastoma. *Strahlenther Onkol*, 184(11):572–9, 2008.
- V. Kornienko. *Diagnostic Neuroradiology*. Springer, Berlin, 2008.
- C. Kotsarini, P. D. Griffiths, I. D. Wilkinson, and N. Hoggard. A systematic review of the literature on the effects of dexamethasone on the brain from

- in vivo human-based studies: Implications for physiological brain imaging of patients with intracranial tumors. *Neurosurgery*, 67(6):1799–815; discussion 1815, 2010.
- T. N. Kreisl, L. Kim, K. Moore, P. Duic, C. Royce, I. Stroud, N. Garren, M. Mackey, J. A. Butman, K. Camphausen, J. Park, P. S. Albert, and H. A. Fine. Phase ii trial of single-agent bevacizumab followed by bevacizumab plus irinotecan at tumor progression in recurrent glioblastoma. *J Clin Oncol*, 27(5):740–5, 2009.
- F. W. Kreth, P. C. Warnke, R. Scheremet, and C. B. Ostertag. Surgical resection and radiation therapy versus biopsy and radiation therapy in the treatment of glioblastoma multiforme. *J Neurosurg*, 78(5):762–6, 1993.
- K. Lamborn, W. Yung, S. Chang, P. Wen, T. Cloughesy, L. DeAngelis, H. Robins, F. Lieberman, H. Fine, K. Fink, L. Junck, L. Abrey, M. Gilbert, M. Mehta, J. Kuhn, K. Aldape, J. Hibberts, P. Peterson, M. Prados, and North American Brain Tumor Consortium. Progression-free survival: An important end point in evaluating therapy for recurrent high-grade gliomas. *Neuro Oncol*, 10(2):162–170, Apr 2008.
- J. R. Landis and G. G. Koch. The measurement of observer agreement for categorical data. *Biometrics*, 33(1):159–74, 1977.
- H. B. Larsson, F. Courivaud, E. Rostrup, and A. E. Hansen. Measurement of brain perfusion, blood volume, and blood–brain barrier permeability, using dynamic contrast-enhanced T(1)-weighted MRI at 3 Tesla. *Magn Reson Med*, 62(5):1270–81, 2009.

- M. Law, S. Cha, E. A. Knopp, G. Johnson, J. Arnett, and A. W. Litt. High-grade gliomas and solitary metastases: Differentiation by using perfusion and proton spectroscopic MR imaging. *Radiology*, 222(3):715–21, 2002.
- M. Law, S. Yang, H. Wang, J. S. Babb, G. Johnson, S. Cha, E. A. Knopp, and D. Zagzag. Glioma grading: Sensitivity, specificity, and predictive values of perfusion MR imaging and proton MR spectroscopic imaging compared with conventional MR imaging. *AJNR Am J Neuroradiol*, 24(10):1989–98, 2003.
- M. Law, K. Kazmi, S. Wetzel, E. Wang, C. Iacob, D. Zagzag, J. G. Golfinos, and G. Johnson. Dynamic susceptibility contrast-enhanced perfusion and conventional MR imaging findings for adult patients with cerebral primitive neuroectodermal tumors. *AJNR Am J Neuroradiol*, 25(6):997–1005, 2004a.
- M. Law, S. Yang, J. S. Babb, E. A. Knopp, J. G. Golfinos, D. Zagzag, and G. Johnson. Comparison of cerebral blood volume and vascular permeability from dynamic susceptibility contrast-enhanced perfusion MR imaging with glioma grade. *AJNR Am J Neuroradiol*, 25(5):746–55, 2004b.
- M. Law, S. Oh, J. S. Babb, E. Wang, M. Inglese, D. Zagzag, E. A. Knopp, and G. Johnson. Low-grade gliomas: Dynamic susceptibility-weighted contrast-enhanced perfusion MR imaging—prediction of patient clinical response. *Radiology*, 238(2):658–67, 2006a.
- M. Law, S. Oh, G. Johnson, J. S. Babb, D. Zagzag, J. Golfinos, and P. J. Kelly. Perfusion magnetic resonance imaging predicts patient outcome as

- an adjunct to histopathology: A second reference standard in the surgical and nonsurgical treatment of low-grade gliomas. *Neurosurgery*, 58(6):1099–107; discussion 1099–107, 2006b.
- M. Law, R. Young, J. Babb, M. Rad, T. Sasaki, D. Zagzag, and G. Johnson. Comparing perfusion metrics obtained from a single compartment versus pharmacokinetic modeling methods using dynamic susceptibility contrast-enhanced perfusion MR imaging with glioma grade. *AJNR Am J Neuroradiol*, 27(9):1975–82, 2006c.
- M. Law, J. E. Brodsky, J. Babb, M. Rosenblum, D. C. Miller, D. Zagzag, M. L. Gruber, and G. Johnson. High cerebral blood volume in human gliomas predicts deletion of chromosome 1p: Preliminary results of molecular studies in gliomas with elevated perfusion. *J Magn Reson Imaging*, 25(6):1113–9, 2007a.
- M. Law, R. Young, J. Babb, E. Pollack, and G. Johnson. Histogram analysis versus region of interest analysis of dynamic susceptibility contrast perfusion MR imaging data in the grading of cerebral gliomas. *AJNR Am J Neuroradiol*, 28(4):761–6, 2007b.
- M. Law, R. J. Young, J. S. Babb, N. Peccerelli, S. Chheang, M. L. Gruber, D. C. Miller, J. G. Golfinos, D. Zagzag, and G. Johnson. Gliomas: Predicting time to progression or survival with cerebral blood volume measurements at dynamic susceptibility-weighted contrast-enhanced perfusion MR imaging. *Radiology*, 247(2):490–8, 2008.
- F. Le Jeune, F. Dubois, S. Blond, and M. Steinling. Sestamibi technetium-

- 99m brain single-photon emission computed tomography to identify recurrent glioma in adults: 201 studies. *J Neurooncol*, 77(2):177–183, Apr 2006. doi: 10.1007/s11060-005-9018-8. URL <http://dx.doi.org/10.1007/s11060-005-9018-8>.
- S. J. Lee, J. H. Kim, Y. M. Kim, G. K. Lee, E. J. Lee, I. S. Park, J. M. Jung, K. H. Kang, and T. Shin. Perfusion MR imaging in gliomas: Comparison with histologic tumor grade. *Korean J Radiol*, 2(1):1–7, 2001.
- K. L. Leenders, R. P. Beaney, D. J. Brooks, A. A. Lammertsma, J. D. Heather, and C. G. McKenzie. Dexamethasone treatment of brain tumor patients: Effects on regional cerebral blood flow, blood volume, and oxygen utilization. *Neurology*, 35(11):1610–6, 1985.
- K. L. Leenders, D. Perani, A. A. Lammertsma, J. D. Heather, P. Buckingham, M. J. Healy, J. M. Gibbs, R. J. Wise, J. Hatazawa, and S. Herold. Cerebral blood flow, blood volume and oxygen utilization. normal values and effect of age. *Brain*, 113 (Pt 1):27–47, Feb 1990.
- J. M. Legler, L. A. Ries, M. A. Smith, J. L. Warren, E. F. Heineman, R. S. Kaplan, and M. S. Linet. Cancer surveillance series [corrected]: Brain and other central nervous system cancers: Recent trends in incidence and mortality. *J Natl Cancer Inst*, 91(16):1382–90, 1999.
- D. W. Leung, G. Cachianes, W. J. Kuang, D. V. Goeddel, and N. Ferrara. Vascular endothelial growth factor is a secreted angiogenic mitogen. *Science*, 246(4935):1306–9, 1989.

- M. H. Lev and F. Hochberg. Perfusion magnetic resonance imaging to assess brain tumor responses to new therapies. *Cancer Control*, 5(2):115–123, 1998.
- M. H. Lev and B. R. Rosen. Clinical applications of intracranial perfusion MR imaging. *Neuroimaging Clin N Am*, 9(2):309–331, May 1999.
- M. H. Lev, Y. Ozsunar, J. W. Henson, A. A. Rasheed, G. D. Barest, G. R. th Harsh, M. M. Fitzek, E. A. Chiocca, J. D. Rabinov, A. N. Csavoy, B. R. Rosen, F. H. Hochberg, P. W. Schaefer, and R. G. Gonzalez. Glial tumor grading and outcome prediction using dynamic spin-echo MR susceptibility mapping compared with conventional contrast-enhanced MR: Confounding effect of elevated rCBV of oligodendrogliomas [corrected]. *AJNR Am J Neuroradiol*, 25(2):214–21, 2004.
- V. A. Levin, J. H. Uhm, K. A. Jaeckle, A. Choucair, P. J. Flynn, Yung WKA, M. D. Prados, J. M. Bruner, S. M. Chang, A. P. Kyritsis, M. J. Gleason, and K. R. Hess. Phase iii randomized study of postradiotherapy chemotherapy with alpha-difluoromethylornithine-procarbazine, n-(2-chloroethyl)-n'-cyclohexyl-n-nitrosurea, vincristine (dfmo-pcv) versus pcv for glioblastoma multiforme. *Clin Cancer Res*, 6(10):3878–3884, Oct 2000.
- K. L. Li, X. P. Zhu, D. R. Checkley, J. J L Tessier, V. F. Hillier, J. C. Waterton, and A. Jackson. Simultaneous mapping of blood volume and endothelial permeability surface area product in gliomas using iterative analysis of first-pass dynamic contrast enhanced MRI data. *Br J Radiol*, 76(901):39–50, Jan 2003.

- S. W. Li, X. G. Qiu, B. S. Chen, W. Zhang, H. Ren, Z. C. Wang, and T. Jiang. Prognostic factors influencing clinical outcomes of glioblastoma multiforme. *Chin Med J (Engl)*, 122(11):1245–9, 2009.
- B. Licata and S. Turazzi. Bleeding cerebral neoplasms with symptomatic hematoma. *J Neurosurg Sci*, 47(4):201–10; discussion 210, 2003.
- J. G. Lijmer, P. M. Bossuyt, and S. H. Heisterkamp. Exploring sources of heterogeneity in systematic reviews of diagnostic tests. *Stat Med*, 21(11):1525–37, 2002.
- G. Liu, G. Sobering, J. Duyn, and C. T. Moonen. A functional MRI technique combining principles of echo-shifting with a train of observations (presto). *Magn Reson Med*, 30(6):764–8, 1993.
- D. N. Louis, E. C. Holland, and J. G. Cairncross. Glioma classification: a molecular reappraisal. *Am J Pathol*, 159(3):779–786, Sep 2001. doi: 10.1016/S0002-9440(10)61750-6. URL [http://dx.doi.org/10.1016/S0002-9440\(10\)61750-6](http://dx.doi.org/10.1016/S0002-9440(10)61750-6).
- D. N. Louis, H. Ohgaki, O. D. Wiestler, W. K. Cavenee, P. C. Burger, A. Jouvett, B. W. Scheithauer, and P. Kleihues. The 2007 who classification of tumours of the central nervous system. *Acta Neuropathol*, 114(2):97–109, 2007.
- H. Lu, E. Pollack, R. Young, J. S. Babb, G. Johnson, D. Zagzag, R. Carson, J. H. Jensen, J. A. Helpert, and M. Law. Predicting grade of cerebral glioma using vascular-space occupancy MR imaging. *AJNR Am J Neuroradiol*, 29(2):373–8, 2008.

- L. Ludemann, W. Grieger, R. Wurm, M. Budzisch, B. Hamm, and C. Zimmer. Comparison of dynamic contrast-enhanced MRI with WHO tumor grading for gliomas. *Eur Radiol*, 11(7):1231–41, 2001.
- J. M. Lupo, S. Cha, S. M. Chang, and S. J. Nelson. Dynamic susceptibility-weighted perfusion imaging of high-grade gliomas: characterization of spatial heterogeneity. *AJNR Am J Neuroradiol*, 26(6):1446–54, 2005.
- J. M. Lupo, S. Cha, S. M. Chang, and S. J. Nelson. Analysis of metabolic indices in regions of abnormal perfusion in patients with high-grade glioma. *AJNR Am J Neuroradiol*, 28(8):1455–61, 2007.
- J. H. Ma, H. S. Kim, N-J. Rim, S-H. Kim, and K-G. Cho. Differentiation among glioblastoma multiforme, solitary metastatic tumor, and lymphoma using whole-tumor histogram analysis of the normalized cerebral blood volume in enhancing and perienhancing lesions. *AJNR Am J Neuroradiol*, 31(9):1699–1706, Oct 2010. doi: 10.3174/ajnr.A2161. URL <http://dx.doi.org/10.3174/ajnr.A2161>.
- X. Ma, Y. Lv, J. Liu, D. Wang, Q. Huang, X. Wang, G. Li, S. Xu, and X. Li. Survival analysis of 205 patients with glioblastoma multiforme: Clinical characteristics, treatment and prognosis in China. *J Clin Neurosci*, 16(12):1595–8, 2009.
- P. Macchiarini, G. Fontanini, M. J. Hardin, F. Squartini, and C. A. Angeletti. Relation of neovascularisation to metastasis of non-small-cell lung cancer. *Lancet*, 340(8812):145–146, Jul 1992.

- D. R. Macdonald, T. L. Cascino, S. C. Schold, Jr., and J. G. Cairncross. Response criteria for phase ii studies of supratentorial malignant glioma. *J Clin Oncol*, 8(7):1277–80, 1990.
- A. C. Maia, Jr., S. M. Malheiros, A. J. da Rocha, C. J. da Silva, A. A. Gabbai, F. A. Ferraz, and J. N. Stavale. MR cerebral blood volume maps correlated with vascular endothelial growth factor expression and tumor grade in nonenhancing gliomas. *AJNR Am J Neuroradiol*, 26(4):777–83, 2005.
- R. Mangla, G. Singh, D. Ziegelitz, M. T. Milano, D. N. Korones, J. Zhong, and S. E. Ekholm. Changes in relative cerebral blood volume 1 month after radiation-temozolomide therapy can help predict overall survival in patients with glioblastoma. *Radiology*, 256(2):575–84, 2010.
- E. Matsusue, J. R. Fink, J. K. Rockhill, T. Ogawa, and K. R. Maravilla. Distinction between glioma progression and post-radiation change by combined physiologic MR imaging. *Neuroradiology*, 52(4):297–306, 2010.
- Donald M. McDonald and Peter L. Choyke. Imaging of angiogenesis: from microscope to clinic. *Nat Med*, 9(6):713–725, Jun 2003. doi: 10.1038/nm0603-713. URL <http://dx.doi.org/10.1038/nm0603-713>.
- C. Ryan Miller, Christopher P Dunham, Bernd W Scheithauer, and Arie Perry. Significance of necrosis in grading of oligodendroglial neoplasms: a clinicopathologic and genetic study of newly diagnosed high-grade gliomas. *J Clin Oncol*, 24(34):5419–5426, Dec 2006. doi: 10.1200/JCO.2006.08.1497. URL <http://dx.doi.org/10.1200/JCO.2006.08.1497>.

- S. J. Mills, T. A. Patankar, H. A. Haroon, D. Baleriaux, R. Swindell, and A. Jackson. Do cerebral blood volume and contrast transfer coefficient predict prognosis in human glioma? *AJNR Am J Neuroradiol*, 27(4): 853–8, 2006.
- J. F. Mineo, A. Bordron, M. Baroncini, C. Ramirez, C. A. Maurage, S. Blond, and P. Dam-Hieu. Prognosis factors of survival time in patients with glioblastoma multiforme: A multivariate analysis of 340 patients. *Acta Neurochir (Wien)*, 149(3):245–52; discussion 252–3, 2007.
- D. Moher, A. Liberati, J. Tetzlaff, D. Altman, and P. R. I. S. M. A. Group. Preferred reporting items for systematic reviews and meta-analyses: the PRISMA statement. *J Clin Epidemiol*, 62(10):1006–1012, Oct 2009. doi: 10.1016/j.jclinepi.2009.06.005. URL <http://dx.doi.org/10.1016/j.jclinepi.2009.06.005>.
- W.-J. Moon, J. Choi, H. Roh, S. Lim, and Y.-C. Koh. Imaging parameters of high grade gliomas in relation to the MGMT promoter methylation status: The CT, diffusion tensor imaging, and perfusion MR imaging. *Neuroradiology*, Aug 2011. doi: 10.1007/s00234-011-0947-y. URL <http://dx.doi.org/10.1007/s00234-011-0947-y>.
- N. Morita, S. Wang, S. Chawla, H. Poptani, and E. Melhem. Dynamic susceptibility contrast perfusion weighted imaging in grading of nonenhancing astrocytomas. *J Magn Reson Imaging*, 32(4):803–808, Oct 2010. doi: 10.1002/jmri.22324. URL <http://dx.doi.org/10.1002/jmri.22324>.
- R. Murakami, T. Sugahara, H. Nakamura, T. Hirai, M. Kitajima,

- Y. Hayashida, Y. Baba, N. Oya, J. Kuratsu, and Y. Yamashita. Malignant supratentorial astrocytoma treated with postoperative radiation therapy: Prognostic value of pretreatment quantitative diffusion-weighted MR imaging. *Radiology*, 243(2):493–9, 2007.
- A. Murat, E. Migliavacca, S. F. Hussain, A. B. Heimberger, I. Desbaillets, M. F. Hamou, C. Ruegg, R. Stupp, M. Delorenzi, and M. E. Hegi. Modulation of angiogenic and inflammatory response in glioblastoma by hypoxia. *PLoS One*, 4(6):e5947, 2009.
- M. Nagy, D. Schulz-Ertner, M. Bischof, T. Welzel, H. Hof, J. Debus, and S. E. Combs. Long-term outcome of postoperative irradiation in patients with newly diagnosed WHO grade III anaplastic gliomas. *Tumori*, 95(3):317–24, 2009.
- E. C. Nwokedi, S. J. DiBiase, S. Jabbour, J. Herman, P. Amin, and L. S. Chin. Gamma knife stereotactic radiosurgery for patients with glioblastoma multiforme. *Neurosurgery*, 50(1):41–6; discussion 46–7, 2002.
- J. Oh, R. G. Henry, A. Pirzkall, Y. Lu, X. Li, I. Catalaa, S. Chang, W. P. Dillon, and S. J. Nelson. Survival analysis in patients with glioblastoma multiforme: Predictive value of choline-to-N-acetylaspartate index, apparent diffusion coefficient, and relative cerebral blood volume. *J Magn Reson Imaging*, 19(5):546–54, 2004.
- S. Ortega-Lozano, D. Martinez del Valle-Torres, M. Gomez-Ro, and J. Llamas-Elvira. Thallium-201 SPECT in brain gliomas: Quantitative assessment in differential diagnosis between tumor recurrence and ra-

- dionecrosis. *Clin Nucl Med*, 34(8):503–505, Aug 2009. doi: 10.1097/RLU.0b013e3181abb604. URL <http://dx.doi.org/10.1097/RLU.0b013e3181abb604>.
- L. Ostergaard, F. H. Hochberg, J. D. Rabinov, A. G. Sorensen, M. Lev, L. Kim, R. M. Weisskoff, R. G. Gonzalez, C. Gyldensted, and B. R. Rosen. Early changes measured by magnetic resonance imaging in cerebral blood flow, blood volume, and blood-brain barrier permeability following dexamethasone treatment in patients with brain tumors. *J Neurosurg*, 90(2):300–5, 1999.
- Scott D. Packard, Joseph B. Mandeville, Tomotsugu Ichikawa, Keiro Ikeda, Kinya Terada, Stephanie Niloff, E Antonio Chiocca, Bruce R. Rosen, and John J A. Marota. Functional response of tumor vasculature to paco2: determination of total and microvascular blood volume by mri. *Neoplasia*, 5(4):330–338, 2003. doi: NO_D0I. URL http://dx.doi.org/NO_D0I.
- A. R. Padhani. MRI for assessing antivasular cancer treatments. *Br J Radiol*, 76 Spec No 1:S60–80, 2003.
- M. V. Padma, S. Said, M. Jacobs, D. R. Hwang, K. Dunigan, M. Satter, B. Christian, J. Ruppert, T. Bernstein, G. Kraus, and J. C. Mantil. Prediction of pathology and survival by fdg pet in gliomas. *J Neurooncol*, 64(3):227–37, 2003.
- B. Palumbo, M. Lupattelli, G. P. Pelliccioli, P. Chiarini, T. O. Moschini, I. Palumbo, Donatella Siepi, P. Buoncristiani, M. Nardi, P. Giovenali, and R. Palumbo. Association of 99mtc-mibi brain spect and proton magnetic

- resonance spectroscopy (1h-mrs) to assess glioma recurrence after radiotherapy. *Q J Nucl Med Mol Imaging*, 50(1):88–93, Mar 2006.
- J. Park, T. Hodges, L. Arko, M. Shen, D. Iacono, A. McNabb, N. Bailey, T. Kreisl, F. Iwamoto, J. Sul, S. Auh, G. Park, H. Fine, and P. Black. Scale to predict survival after surgery for recurrent glioblastoma multiforme. *J Clin Oncol*, 28(24):3838–3843, Aug 2010a. doi: 10.1200/JCO.2010.30.0582. URL <http://dx.doi.org/10.1200/JCO.2010.30.0582>.
- M. J. Park, H. S. Kim, G. H. Jahng, C. W. Ryu, S. M. Park, and S. Y. Kim. Semiquantitative assessment of intratumoral susceptibility signals using non-contrast-enhanced high-field high-resolution susceptibility-weighted imaging in patients with gliomas: Comparison with MR perfusion imaging. *AJNR Am J Neuroradiol*, 30(7):1402–8, 2009.
- S. M. Park, H. S. Kim, G. H. Jahng, C. W. Ryu, and S. Y. Kim. Combination of high-resolution susceptibility-weighted imaging and the apparent diffusion coefficient: Added value to brain tumour imaging and clinical feasibility of non-contrast MRI at 3 T. *Br J Radiol*, 83(990):466–75, 2010b.
- M. Pauliah, V. Saxena, M. Haris, N. Husain, R. K. Rathore, and R. K. Gupta. Improved t(1)-weighted dynamic contrast-enhanced MRI to probe microvascularity and heterogeneity of human glioma. *Magn Reson Imaging*, 25(9):1292–9, 2007.
- E. S. Paulson and K. M. Schmainda. Comparison of dynamic susceptibility-weighted contrast-enhanced MR methods: Recommendations for measur-

- ing relative cerebral blood volume in brain tumors. *Radiology*, 249(2): 601–13, 2008.
- H. Pels, I. Schmidt-Wolf, A. Glasmacher, H. Schulz, A. Engert, V. Diehl, A. Zellner, G. Schackert, H. Reichmann, F. Kroschinsky, M. Vogt-Schaden, G. Egerer, U. Bode, C. Schaller, M. Deckert, R. Fimmers, C. Helmstaedter, A. Atasoy, T. Klockgether, and U. Schlegel. Primary central nervous system lymphoma: Results of a pilot and phase II study of systemic and intraventricular chemotherapy with deferred radiotherapy. *J Clin Oncol*, 21(24):4489–4495, Dec 2003. doi: 10.1200/JCO.2003.04.056. URL <http://dx.doi.org/10.1200/JCO.2003.04.056>.
- A. Perry, K. D. Aldape, D. H. George, and P. C. Burger. Small cell astrocytoma: An aggressive variant that is clinicopathologically and genetically distinct from anaplastic oligodendroglioma. *Cancer*, 101(10):2318–26, 2004.
- L. W. Pinto, M. B. Araujo, A. L. Vettore, L. Wernersbach, A. C. Leite, L. M. Chimelli, and F. A. Soares. Glioblastomas: Correlation between oligodendroglial components, genetic abnormalities, and prognosis. *Virchows Arch*, 452(5):481–90, 2008.
- W. B. Pope, J. Sayre, A. Perlina, J. P. Villablanca, P. S. Mischel, and T. F. Cloughesy. MR imaging correlates of survival in patients with high-grade gliomas. *AJNR Am J Neuroradiol*, 26(10):2466–74, 2005.
- W. B. Pope, H. J. Kim, J. Huo, J. Alger, M. S. Brown, D. Gjertson, V. Sai, J. R. Young, L. Tekchandani, T. Cloughesy, P. S. Mischel, A. Lai,

- P. Nghiemphu, S. Rahmanuddin, and J. Goldin. Recurrent glioblastoma multiforme: ADC histogram analysis predicts response to bevacizumab treatment. *Radiology*, 252(1):182–9, 2009.
- C. Preul, B. Kuhn, E. W. Lang, H. M. Mehdorn, M. Heller, and J. Link. Differentiation of cerebral tumors using multi-section echo planar MR perfusion imaging. *Eur J Radiol*, 48(3):244–51, 2003.
- M. Principi, M. Italiani, A. Guiducci, I. Aprile, M. Muti, G. Giulianelli, and P. Ottaviano. Perfusion MRI in the evaluation of the relationship between tumour growth, necrosis and angiogenesis in glioblastomas and grade 1 meningiomas. *Neuroradiology*, 45(4):205–211, 2003.
- J. M. Provenzale, G. R. Wang, T. Brenner, J. R. Petrella, and A. G. Sorensen. Comparison of permeability in high-grade and low-grade brain tumors using dynamic susceptibility contrast MR imaging. *AJR Am J Roentgenol*, 178(3):711–6, 2002.
- J. M. Provenzale, S. Mukundan, and M. Dewhirst. The role of blood-brain barrier permeability in brain tumor imaging and therapeutics. *AJR Am J Roentgenol*, 185(3):763–7, 2005.
- J. M. Provenzale, G. York, M. G. Moya, L. Parks, M. Choma, S. Kealey, P. Cole, and H. Serajuddin. Correlation of relative permeability and relative cerebral blood volume in high-grade cerebral neoplasms. *AJR Am J Roentgenol*, 187(4):1036–42, 2006.
- V. K. Puduvalli and R. Sawaya. Antiangiogenesis – therapeutic strategies

- and clinical implications for brain tumors. *J Neurooncol*, 50(1-2):189–200, 2000.
- J. H. Rees, J. G. Smirniotopoulos, R. V. Jones, and K. Wong. Glioblastoma multiforme: Radiologic–pathologic correlation. *Radiographics*, 16(6):1413–38; quiz 1462–3, 1996.
- G. Reifenberger and P. Wesseling. Molecular diagnostics of brain tumors. *Acta Neuropathol*, 120(5):549–551, Nov 2010. doi: 10.1007/s00401-010-0752-4. URL <http://dx.doi.org/10.1007/s00401-010-0752-4>.
- H. C. Roberts, T. P. Roberts, R. C. Brasch, and W. P. Dillon. Quantitative measurement of microvascular permeability in human brain tumors achieved using dynamic contrast-enhanced MR imaging: Correlation with histologic grade. *AJNR Am J Neuroradiol*, 21(5):891–9, 2000.
- N. Rollin, J. Guyotat, N. Streichenberger, J. Honnorat, V. A. Tran Minh, and F. Cotton. Clinical relevance of diffusion and perfusion magnetic resonance imaging in assessing intra-axial brain tumors. *Neuroradiology*, 48(3):150–9, 2006.
- Ilse Roodink, Maarten Franssen, Malou Zuidschewoude, Kiek Verrijp, Tom van der Donk, Jos Raats, and William Pj Leenders. Isolation of targeting nanobodies against co-opted tumor vasculature. *Lab Invest*, 90(1):61–67, Jan 2010. doi: 10.1038/labinvest.2009.107. URL <http://dx.doi.org/10.1038/labinvest.2009.107>.

- B. R. Rosen, J. W. Belliveau, J. M. Vevea, and T. J. Brady. Perfusion imaging with nMR contrast agents. *Magn Reson Med*, 14(2):249–65, 1990.
- B. R. Rosen, J. W. Belliveau, H. J. Aronen, D. Kennedy, B. R. Buchbinder, A. Fischman, M. Gruber, J. Glas, R. M. Weisskoff, and M. S. Cohen. Susceptibility contrast imaging of cerebral blood volume: Human experience. *Magn Reson Med*, 22(2):293–9; discussion 300–3, Dec 1991.
- C. M. Rutter and C. A. Gatsonis. A hierarchical regression approach to meta-analysis of diagnostic test accuracy evaluations. *Stat Med*, 20(19):2865–84, 2001.
- N. Sadeghi, I. Salmon, B. N. Tang, V. Denolin, M. Levivier, D. Wikler, S. Rorive, D. Baleriaux, T. Metens, and S. Goldman. Correlation between dynamic susceptibility contrast perfusion MRI, and methionine metabolism in brain gliomas: Preliminary results. *J Magn Reson Imaging*, 24(5):989–94, 2006.
- N. Sadeghi, I. Salmon, C. Decaestecker, M. Levivier, T. Metens, D. Wikler, V. Denolin, S. Rorive, N. Massager, D. Baleriaux, and S. Goldman. Stereotactic comparison among cerebral blood volume, methionine uptake, and histopathology in brain glioma. *AJNR Am J Neuroradiol*, 28(3):455–61, 2007.
- S. Saksena, R. Jain, J. Narang, L. Scarpace, L. Schultz, N. Lehman, D. Hearshen, S. Patel, and T. Mikkelsen. Predicting survival in glioblastomas using diffusion tensor imaging metrics. *J Magn Reson Imag-*

- ing*, 32(4):788–795, Oct 2010. doi: 10.1002/jmri.22304. URL <http://dx.doi.org/10.1002/jmri.22304>.
- S. Saraswathy, F. W. Crawford, K. R. Lamborn, A. Pirzkall, S. Chang, S. Cha, and S. J. Nelson. Evaluation of MR markers that predict survival in patients with newly diagnosed GBM prior to adjuvant therapy. *J Neurooncol*, 91(1):69–81, 2009.
- B. W. Scheithauer. Development of the WHO classification of tumors of the central nervous system: A historical perspective. *Brain Pathol*, 2008.
- K. M. Schmainda, S. D. Rand, A. M. Joseph, R. Lund, B. D. Ward, A. P. Pathak, J. L. Ulmer, M. A. Badruddoja, and H. G. Krouwer. Characterization of a first-pass gradient-echo spin-echo method to predict brain tumor grade and angiogenesis. *AJNR Am J Neuroradiol*, 25(9):1524–32, 2004.
- D. Schomas, N. Laack, R. Rao, F. Meyer, E. Shaw, B. O’Neill, C. Giannini, and P. Brown. Intracranial low-grade gliomas in adults: 30-year experience with long-term follow-up at Mayo Clinic. *Neuro Oncol*, 11(4):437–445, Aug 2009a. doi: 10.1215/15228517-2008-102. URL <http://dx.doi.org/10.1215/15228517-2008-102>.
- D. A. Schomas, N. N. Laack, and P. D. Brown. Low-grade gliomas in older patients: Long-term follow-up from Mayo Clinic. *Cancer*, 115(17):3969–78, 2009b.
- J. N. Scott, P. M. Brasher, R. J. Sevick, N. B. Rewcastle, and P. A. Forsyth.

- How often are nonenhancing supratentorial gliomas malignant? a population study. *Neurology*, 59(6):947–9, 2002.
- N. Shastri-Hurst, M. Tsegaye, D. K. Robson, J. S. Lowe, and D. C. Macarthur. Stereotactic brain biopsy: An audit of sampling reliability in a clinical case series. *Br J Neurosurg*, 20(4):222–6, 2006.
- J. H. Shin, H. K. Lee, B. D. Kwun, J. S. Kim, W. Kang, C. G. Choi, and D. C. Suh. Using relative cerebral blood flow and volume to evaluate the histopathologic grade of cerebral gliomas: Preliminary results. *AJR Am J Roentgenol*, 179(3):783–9, 2002.
- J. Shinoda, N. Sakai, S. Murase, H. Yano, T. Matsuhisa, and T. Funakoshi. Selection of eligible patients with supratentorial glioblastoma multiforme for gross total resection. *J Neurooncol*, 52(2):161–171, Apr 2001.
- T. Siegal, R. Rubinstein, T. Tzuk-Shina, and J. M. Gomori. Utility of relative cerebral blood volume mapping derived from perfusion magnetic resonance imaging in the routine follow up of brain tumors. *J Neurosurg*, 86(1):22–27, Jan 1997. doi: 10.3171/jns.1997.86.1.0022. URL <http://dx.doi.org/10.3171/jns.1997.86.1.0022>.
- S. Sinha, M. E. Bastin, J. M. Wardlaw, P. A. Armitage, and I. R. Whittle. Effects of dexamethasone on peritumoural oedematous brain: A DT-MRI study. *J Neurol Neurosurg Psychiatry*, 75(11):1632–5, 2004.
- A. G. Sorensen, T. T. Batchelor, W. T. Zhang, P. J. Chen, P. Yeo, M. Wang, D. Jennings, P. Y. Wen, J. Lahdenranta, M. Ancukiewicz, E. di Tomaso,

- D. G. Duda, and R. K. Jain. A "vascular normalization index" as potential mechanistic biomarker to predict survival after a single dose of cediranib in recurrent glioblastoma patients. *Cancer Res*, 69(13):5296–300, 2009.
- M. V. Spampinato, J. K. Smith, L. Kwock, M. Ewend, J. D. Grimme, D. L. Camacho, and M. Castillo. Cerebral blood volume measurements and proton MR spectroscopy in grading of oligodendroglial tumors. *AJR Am J Roentgenol*, 188(1):204–12, 2007.
- A. M. Stark, J. Hedderich, J. Held-Feindt, and H. M. Mehdorn. Glioblastoma—the consequences of advanced patient age on treatment and survival. *Neurosurg Rev*, 30(1):56–61; discussion 61–2, 2007.
- J. G. Strugar, G. R. Criscuolo, D. Rothbart, and W. N. Harrington. Vascular endothelial growth/permeability factor expression in human glioma specimens: correlation with vasogenic brain edema and tumor-associated cysts. *J Neurosurg*, 83(4):682–689, Oct 1995. doi: 10.3171/jns.1995.83.4.0682. URL <http://dx.doi.org/10.3171/jns.1995.83.4.0682>.
- R. Stupp, W. P. Mason, M. J. van den Bent, M. Weller, B. Fisher, M. J. Taphoorn, K. Belanger, A. A. Brandes, C. Marosi, U. Bogdahn, J. Curschmann, R. C. Janzer, S. K. Ludwin, T. Gorlia, A. Allgeier, D. Lacombe, J. G. Cairncross, E. Eisenhauer, and R. O. Mirimanoff. Radiotherapy plus concomitant and adjuvant temozolomide for glioblastoma. *N Engl J Med*, 352(10):987–96, 2005.
- R. Stupp, M. E. Hegi, W. P. Mason, M. J. van den Bent, M. J. Taphoorn, R. C. Janzer, S. K. Ludwin, A. Allgeier, B. Fisher, K. Belanger, P. Hau,

- A. A. Brandes, J. Gijtenbeek, C. Marosi, C. J. Vecht, K. Mokhtari, P. Wesseling, S. Villa, E. Eisenhauer, T. Gorlia, M. Weller, D. Lacombe, J. G. Cairncross, and R. O. Mirimanoff. Effects of radiotherapy with concomitant and adjuvant temozolomide versus radiotherapy alone on survival in glioblastoma in a randomised phase III study: 5-year analysis of the EORTC-NCIC trial. *Lancet Oncol*, 10(5):459–66, 2009.
- T. Sugahara, Y. Korogi, M. Kochi, I. Ikushima, T. Hirai, T. Okuda, Y. Shigematsu, L. Liang, Y. Ge, Y. Ushio, and M. Takahashi. Correlation of MR imaging-determined cerebral blood volume maps with histologic and angiographic determination of vascularity of gliomas. *AJR Am J Roentgenol*, 171(6):1479–86, 1998.
- T. Sugahara, Y. Korogi, Y. Shigematsu, L. Liang, K. Yoshizumi, M. Kitajima, and M. Takahashi. Value of dynamic susceptibility contrast magnetic resonance imaging in the evaluation of intracranial tumors. *Top Magn Reson Imaging*, 10(2):114–24, 1999.
- T. Sugahara, Y. Korogi, S. Tomiguchi, Y. Shigematsu, I. Ikushima, T. Kira, L. Liang, Y. Ushio, and M. Takahashi. Posttherapeutic intraaxial brain tumor: The value of perfusion-sensitive contrast-enhanced MR imaging for differentiating tumor recurrence from nonneoplastic contrast-enhancing tissue. *AJNR Am J Neuroradiol*, 21(5):901–9, 2000.
- T. Sugahara, Y. Korogi, M. Kochi, Y. Ushio, and M. Takahashi. Perfusion-sensitive MR imaging of gliomas: Comparison between gradient-echo and

- spin-echo echo-planar imaging techniques. *AJNR Am J Neuroradiol*, 22(7):1306–15, 2001.
- W. Taal, D. Brandsma, H. G. de Bruin, J. E. Bromberg, A. T. Swaak-Kragten, P. A. Smitt, C. A. van Es, and M. J. van den Bent. Incidence of early pseudo-progression in a cohort of malignant glioma patients treated with chemoradiation with temozolomide. *Cancer*, 113(2):405–10, 2008.
- M. Takasawa, P. Jones, J. Guadagno, S. Christensen, T. Fryer, S. Harding, J. Gillard, G. Williams, F. Aigbirhio, E. Warburton, L. stergaard, and J.-C. Baron. How reliable is perfusion MR in acute stroke? validation and determination of the penumbra threshold against quantitative PET. *Stroke*, 39(3):870–877, Mar 2008. doi: 10.1161/STROKEAHA.107.500090. URL <http://dx.doi.org/10.1161/STROKEAHA.107.500090>.
- A. Talacchi, S. Turazzi, F. Locatelli, F. Sala, A. Beltramello, F. Alessandrini, P. Manganotti, P. Lanteri, R. Gambin, M. Ganau, V. Tramontano, B. Santini, and M. Gerosa. Surgical treatment of high-grade gliomas in motor areas. the impact of different supportive technologies: A 171-patient series. *J Neurooncol*, 2010.
- M. Teixeira, E. Fonoff, M. Mandel, H. Alves, and S. Rosemberg. Stereotactic biopsies of brain lesions. *Arq Neuropsiquiatr*, 67(1):74–77, Mar 2009.
- J. Tie, D. Gunawardana, and M. Rosenthal. Differentiation of tumor recurrence from radiation necrosis in high-grade gliomas using 201Tl-SPECT. *J Clin Neurosci*, 15(12):1327–1334, Dec 2008. doi: 10.1016/j.jocn.2007.12.008. URL <http://dx.doi.org/10.1016/j.jocn.2007.12.008>.

- J. Tjuvajev, H. Uehara, R. Desai, B. Beattie, C. Matei, Y. Zhou, M. J. Kreek, J. Koutcher, and R. Blasberg. Corticotropin-releasing factor decreases vasogenic brain edema. *Cancer Res*, 56(6):1352–60, 1996.
- P. Tofts. *Quantitative MRI of the Brain: Measuring Changes Caused by Disease*. Wiley, Chichester, England, 1st edition, 2003.
- P. S. Tofts and A. G. Kermode. Measurement of the blood-brain barrier permeability and leakage space using dynamic MR imaging. 1. fundamental concepts. *Magn Reson Med*, 17(2):357–67, 1991.
- P. S. Tofts, G. Brix, D. L. Buckley, J. L. Evelhoch, E. Henderson, M. V. Knopp, H. B. Larsson, T. Y. Lee, N. A. Mayr, G. J. Parker, R. E. Port, J. Taylor, and R. M. Weisskoff. Estimating kinetic parameters from dynamic contrast-enhanced T(1)-weighted MRI of a diffusable tracer: Standardized quantities and symbols. *J Magn Reson Imaging*, 10(3):223–32, 1999.
- C. H. Toh, Y. L. Chen, T. C. Hsieh, S. M. Jung, H. F. Wong, and S. H. Ng. Glioblastoma multiforme with diffusion-weighted magnetic resonance imaging characteristics mimicking primary brain lymphoma. case report. *J Neurosurg*, 105(1):132–5, 2006.
- M. Tomoi, M. Maeda, M. Yoshida, H. Yamada, Y. Kawamura, N. Hayashi, Y. Ishii, and T. Kubota. Assessment of radiotherapeutic effect on brain tumors by dynamic susceptibility contrast MR imaging: A preliminary report. *Radiat Med*, 17(3):195–9, 1999.

- H. Uematsu, M. Maeda, N. Sadato, T. Matsuda, Y. Ishimori, Y. Koshimoto, H. Kimura, H. Yamada, Y. Kawamura, Y. Yonekura, and H. Itoh. Blood volume of gliomas determined by double-echo dynamic perfusion-weighted MR imaging: A preliminary study. *AJNR Am J Neuroradiol*, 22(10): 1915–9, 2001.
- M. Utriainen, M. Komu, V. Vuorinen, P. Lehtikainen, P. Sonninen, T. Kurki, T. Utriainen, A. Roivainen, H. Kalimo, and H. Minn. Evaluation of brain tumor metabolism with [11c]choline pet and 1h-mrs. *J Neurooncol*, 62(3): 329–338, May 2003.
- M. Valeriani, A. Ferretti, P. Franzese, and V. Tombolini. High-grade gliomas: Results in patients treated with adjuvant radiotherapy alone and with adjuvant radio-chemotherapy. *Anticancer Res*, 26(3B):2429–35, 2006.
- K. van Besien, C. Gisselbrecht, M. Pfreundschuh, and E. Zucca. Secondary lymphomas of the central nervous system: Risk, prophylaxis and treatment. *Leuk Lymphoma*, 49 Suppl 1:52–58, 2008. doi: 10.1080/10428190802311458. URL <http://dx.doi.org/10.1080/10428190802311458>.
- M. van den Bent, H. Dubbink, M. Sanson, C. van der Lee-Haarloo, M. Hegi, J. Jeuken, A. Ibdaih, A. Brandes, M. Taphoorn, M. Frenay, D. Lacombe, T. Gorlia, W. Dinjens, and J. Kros. MGMT promoter methylation is prognostic but not predictive for outcome to adjuvant PCV chemotherapy in anaplastic oligodendroglial tumors: A report from EORTC Brain Tumor Group Study 26951. *J Clin Oncol*, 27(35):5881–5886, Dec 2009. doi: 10.

- 1200/JCO.2009.24.1034. URL <http://dx.doi.org/10.1200/JCO.2009.24.1034>.
- M. J. van den Bent, H. J. Dubbink, Y. Marie, A. A. Brandes, M. J. Taphoorn, P. Wesseling, M. Frenay, C. C. Tijssen, D. Lacombe, A. Idhah, R. van Marion, J. M. Kros, W. N. Dinjens, T. Gorlia, and M. Sanson. Idh1 and idh2 mutations are prognostic but not predictive for outcome in anaplastic oligodendroglial tumors: A report of the european organization for research and treatment of cancer brain tumor group. *Clin Cancer Res*, 16(5):1597–604, 2010.
- P. van Gelderen, N. F. Ramsey, G. Liu, J. H. Duyn, J. A. Frank, D. R. Weinberger, and C. T. Moonen. Three-dimensional functional magnetic resonance imaging of human brain on a clinical 1.5-t scanner. *Proc Natl Acad Sci U S A*, 92(15):6906–6910, Jul 1995.
- C. J. Vecht, C. J. Avezaat, W. L. van Putten, W. M. Eijkenboom, and S. Z. Stefanko. The influence of the extent of surgery on the neurological function and survival in malignant glioma. a retrospective analysis in 243 patients. *J Neurol Neurosurg Psychiatry*, 53(6):466–71, 1990.
- M. Vos, J. Berkhof, O. Hoekstra, I. Bosma, E. Sizoo, J. Heimans, J. Reijneveld, E. Sanchez, F. Lagerwaard, J. Buter, D. Noske, and T. Postma. MRI and thallium-201 SPECT in the prediction of survival in glioma. *Neuroradiology*, Jul 2011. doi: 10.1007/s00234-011-0908-5. URL <http://dx.doi.org/10.1007/s00234-011-0908-5>.
- J. J. Vredenburgh, A. Desjardins, J. E. Herndon 2nd, J. Marcello, D. A.

- Reardon, J. A. Quinn, J. N. Rich, S. Sathornsumetee, S. Gururangan, J. Sampson, M. Wagner, L. Bailey, D. D. Bigner, A. H. Friedman, and H. S. Friedman. Bevacizumab plus irinotecan in recurrent glioblastoma multiforme. *J Clin Oncol*, 25(30):4722–9, 2007.
- C. Walker, D. G. du Plessis, D. Fildes, B. Haylock, D. Husband, M. D. Jenkinson, K. A. Joyce, J. Broome, K. Kopitski, J. Prosser, T. Smith, S. Vinjamuri, and P. C. Warnke. Correlation of molecular genetics with molecular and morphological imaging in gliomas with an oligodendroglial component. *Clin Cancer Res*, 10(21):7182–91, 2004.
- W. Weber, P. Bartenstein, M. W. Gross, D. Kinzel, H. Daschner, H. J. Feldmann, G. Reidel, S. I. Ziegler, C. Lumenta, M. Molls, and M. Schwaiger. Fluorine-18-fdg pet and iodine-123-imt spect in the evaluation of brain tumors. *J Nucl Med*, 38(5):802–8, 1997.
- W. A. Weber, S. Dick, G. Reidl, B. Dzewas, R. Busch, H. J. Feldmann, M. Molls, C. B. Lumenta, M. Schwaiger, and A. L. Grosu. Correlation between postoperative 3-[(123)i]iodo-l-alpha-methyltyrosine uptake and survival in patients with gliomas. *J Nucl Med*, 42(8):1144–50, 2001.
- N. Weidner, J. P. Semple, W. R. Welch, and J. Folkman. Tumor angiogenesis and metastasis—correlation in invasive breast carcinoma. *N Engl J Med*, 324(1):1–8, Jan 1991. doi: 10.1056/NEJM199101033240101. URL <http://dx.doi.org/10.1056/NEJM199101033240101>.
- S. Wemmert, R. Ketter, J. Rahnenfhrer, N. Beerenwinkel, M. Strowitzki, W. Feiden, C. Hartmann, T. Lengauer, F. Stockhammer, K. Zang,

- E. Meese, W.-I. Steudel, A. von Deimling, and S. Urbschat. Patients with high-grade gliomas harboring deletions of chromosomes 9p and 10q benefit from temozolomide treatment. *Neoplasia*, 7(10):883–893, Oct 2005.
- F. Wenz, K. Rempp, T. Hess, J. Debus, G. Brix, R. Engenhart, M. V. Knopp, G. van Kaick, and M. Wannemacher. Effect of radiation on blood volume in low-grade astrocytomas and normal brain tissue: Quantification with dynamic susceptibility contrast MR imaging. *AJR Am J Roentgenol*, 166(1):187–93, 1996.
- S. G. Wetzel, S. Cha, M. Law, G. Johnson, J. Golfinos, P. Lee, and P. K. Nelson. Preoperative assessment of intracranial tumors with perfusion mr and a volumetric interpolated examination: A comparative study with DSA. *AJNR Am J Neuroradiol*, 23(10):1767–74, 2002.
- P. Whiting, A. W. Rutjes, J. B. Reitsma, P. M. Bossuyt, and J. Kleijnen. The development of QUADAS: A tool for the quality assessment of studies of diagnostic accuracy included in systematic reviews. *BMC Med Res Methodol*, 3:25, 2003.
- R. G. Whitmore, J. Krejza, G. S. Kapoor, J. Huse, J. H. Woo, S. Bloom, J. Lopinto, R. L. Wolf, K. Judy, M. R. Rosenfeld, J. A. Biegel, E. R. Melhem, and D. M. O'Rourke. Prediction of oligodendroglial tumor subtype and grade using perfusion weighted magnetic resonance imaging. *J Neurosurg*, 107(3):600–9, 2007.
- F. Winkler, Y. Kienast, M. Fuhrmann, L. Von Baumgarten, S. Burgold, G. Mitteregger, H. Kretschmar, and J. Herms. Imaging glioma cell inva-

- sion in vivo reveals mechanisms of dissemination and peritumoral angiogenesis. *Glia*, 57(12):1306–15, 2009.
- Ronnie Wirestam, Oliver Thilmann, Linda Knutsson, Isabella M. Bjrkman-Burtscher, Elna-Marie Larsson, and Freddy Sthlberg. Comparison of quantitative dynamic susceptibility-contrast mri perfusion estimates obtained using different contrast-agent administration schemes at 3t. *Eur J Radiol*, 75(1):e86–e91, Jul 2010. doi: 10.1016/j.ejrad.2009.07.038. URL <http://dx.doi.org/10.1016/j.ejrad.2009.07.038>.
- S. Yamada, Y. Takai, K. Nemoto, Y. Ogawa, Y. Kakuto, A. Hoshi, and K. Sakamoto. Prognostic significance of ct scan in malignant glioma. *Tohoku J Exp Med*, 170(1):35–43, May 1993.
- F. Yamasaki, K. Sugiyama, M. Ohtaki, Y. Takeshima, N. Abe, Y. Akiyama, J. Takaba, V. Amatya, T. Saito, Y. Kajiwara, R. Hanaya, and K. Kurisu. Glioblastoma treated with postoperative radio-chemotherapy: Prognostic value of apparent diffusion coefficient at MR imaging. *Eur J Radiol*, 73(3):532–537, Mar 2010. doi: 10.1016/j.ejrad.2009.01.013. URL <http://dx.doi.org/10.1016/j.ejrad.2009.01.013>.
- D. Yang, Y. Korogi, T. Sugahara, M. Kitajima, Y. Shigematsu, L. Liang, Y. Ushio, and M. Takahashi. Cerebral gliomas: Prospective comparison of multivoxel 2D chemical-shift imaging proton MR spectroscopy, echoplanar perfusion and diffusion-weighted MRI. *Neuroradiology*, 44(8):656–66, 2002.
- Y. Yang, G. H. Glover, P. van Gelderen, A. C. Patel, V. S. Mattay, J. A. Frank, and J. H. Duyn. A comparison of fast MR scan techniques for

- cerebral activation studies at 1.5 Tesla. *Magn Reson Med*, 39(1):61–7, 1998.
- G. Young, E. Macklin, K. Setayesh, J. Lawson, P. Wen, A. Norden, J. Drapatz, and S. Kesari. Longitudinal MRI evidence for decreased survival among periventricular glioblastoma. *J Neurooncol*, 104(1):261–269, Aug 2011. doi: 10.1007/s11060-010-0477-1. URL <http://dx.doi.org/10.1007/s11060-010-0477-1>.
- J. Zamora, V. Abaira, A. Muriel, K. Khan, and A. Coomarasamy. Meta-DiSc: A software for meta-analysis of test accuracy data. *BMC Med Res Methodol*, 6:31, 2006.
- Y. Zhang, J. Wang, X. Wang, J. Zhang, J. Fang, and X. Jiang. Feasibility study of exploring a $t(1)$ -weighted dynamic contrast-enhanced MR approach for brain perfusion imaging. *J Magn Reson Imaging*, Feb 2012. doi: 10.1002/jmri.23570. URL <http://dx.doi.org/10.1002/jmri.23570>.
- P. Zonari, P. Baraldi, and G. Crisi. Multimodal MRI in the characterization of glial neoplasms: The combined role of single-voxel MR spectroscopy, diffusion imaging and echo-planar perfusion imaging. *Neuroradiology*, 49(10):795–803, 2007.